# Synthesis and Characterization of Hydrophilic-Hydrophobic Poly(Arylene Ether Sulfone) Random and Segmented Copolymers for Membrane Applications

**Ali Nebipasagil**

Dissertation submitted to the faculty of the Virginia Polytechnic Institute and State University in partial fulfillment of the requirements for the degree of

Doctor of Philosophy
In
Macromolecular Science and Engineering

James E. McGrath, Chair
Judy S. Riffle, Co-Chair
S. Richard Turner
Robert B. Moore
Eugene Joseph
Sue J. Mecham

12/8/2014
Blacksburg, Virginia

Keywords: poly(arylene ether sulfone), sulfonated poly(arylene ether sulfone), poly(ethylene oxide), copolymers, segmented polyurethanes, reverse osmosis membranes, gas separation membranes

**Synthesis and Characterization of Hydrophilic-Hydrophobic Poly(Arylene Ether Sulfone) Random and Segmented Copolymers for Membrane Applications**

**Ali Nebipasagil**

**Abstract**

Poly(arylene ether sulfone)s are high-performance engineering thermoplastics that have been investigated extensively over the past several decades due to their outstanding mechanical properties, high glass transition temperatures ($T_g$), solvent resistance and exceptional thermal, oxidative and hydrolytic stability. Their thermal and mechanical properties are highly suited to a variety of applications including membrane applications such as reverse osmosis, ultrafiltration, and gas separation. This dissertation covers structure-property-performance relationships of poly(arylene ether sulfone) and poly(ethylene oxide)-containing random and segmented copolymers for reverse osmosis and gas separation membranes.

The second chapter of this dissertation describes synthesis of disulfonated poly(arylene ether sulfone) random copolymers with oligomeric molecular weights that contain hydrophilic and hydrophobic segments for thin film composite (TFC) reverse osmosis membranes. These copolymers were synthesized and chemically modified to obtain novel crosslinkable poly(arylene ether sulfone) oligomers with acrylamide groups on both ends. The acrylamide-terminated oligomers were crosslinked with UV radiation in the presence of a multifunctional acrylate and a UV initiator. Transparent, dense films were obtained with high gel fractions. Mechanically robust TFC membranes were prepared from either aqueous or water-methanol solutions cast onto a commercial UDEL® foam support. This was the first example that utilized a water or alcohol solvent system and UV radiation to obtain reverse osmosis TFC membranes. The membranes were characterized with regard to composition, surface properties, and water

uptake. Water and salt transport properties were elucidated at the department of chemical engineering at the University of Texas at Austin.

The gas separation membranes presented in chapter three were poly(arylene ether sulfone) and poly(ethylene oxide) (PEO)-containing polyurethanes. Poly(arylene ether sulfone) copolymers with controlled molecular weights were synthesized and chemically modified to obtain poly(arylene ether sulfone) polyols with aliphatic hydroxyethyl terminal functionality. The hydroxyethyl-terminated oligomers and α,ω-hydroxy-terminated PEO were chain extended with a diisocyanate to obtain polyurethanes. Compositions with high poly(arylene ether sulfone) content relative to the hydrophilic PEO blocks were of interest due to their mechanical integrity. The membranes were characterized to analyze their compositions, thermal and mechanical properties, water uptake, and molecular weights. These membranes were also evaluated by collaborators at the University of Texas at Austin to explore single gas transport properties. The results showed that both polymer and transport properties closely related to PEO-content. The $CO_2/CH_4$ gas selectivity of our membranes were improved from 25 to 34 and the $CO_2/N_2$ gas selectivity nearly doubled from 25 to 46 by increasing PEO-content from 0 to 30 wt.% in polyurethanes.

Chapter four also focuses on polymers for gas separation membranes. Disulfonated poly(arylene ether sulfone) and poly(ethylene oxide)-containing polyurethanes were synthesized for potential applications as gas separation membranes. Disulfonated polyols containing 20 and 40 mole percent of disulfonated repeat units with controlled molecular weights were synthesized. Poly(arylene ether sulfone) polyols and α,ω-hydroxy-terminated poly(ethylene oxide) were subsequently chain extended with a diisocyanate to obtain polyurethanes. Thermal and

mechanical characterization revealed that the polyurethanes had a phase-mixed complex morphology.

**Acknowledgements**

I would like to express my sincere gratitude to my late advisor, Dr. James E. McGrath for giving me the opportunity to become his student, his continuous guidance, his wisdom, opportunities he provided and tremendous support from the first day I joined his group. It was an honor and a privilege to work under the guidance of such a distinguished scientist. I will always remember everything he passed on to me and will always be proud because I learned from him. My special thanks go to my current advisor Dr. Judy S. Riffle. She helped our group carry on and oversaw my transition and guided me through the end of my PhD studies after the untimely passing of Dr. McGrath. I would like to thank my committee Dr. S. Richard Turner, and Dr. Robert B. Moore, Dr. Eugene Joseph and Dr. Sue J. Mecham for their valuable time and their contributions, help and guidance throughout my time at Virginia Tech.

I also thank all my collaborators Jaesung Park, Euisoug Jang, and Dr. Benny D. Freeman from the University of Texas for their contributions to my work and for teaching me along the way. I need to thank Dr. Bruce Orler from Dr. Moore's groups for his help in my dissertation research. I especially thank Benjamin Sundell, Ozma Lane, Andrew Shaver, and Padmapriya Pisipati for their assistance with my research projects. I was very fortunate to work with brilliant people so I thank all my previous and present group members for their advice, discussions, and their suggestions. I also would like to thank the Macromolecules and Interfaces Institute staff members including Laurie Good, Cyndy Graham and Tammy Jo Hiner for helping me navigate through the graduate school requirements and for their help over the years.

I am forever grateful to my family. I would not have been where I am today without them. I especially thank my mother, nothing means more to me than making her proud. I

couldn’t realize my accomplishments without her. I can never pay her for sacrifices she made to allow me to pursue my life goals.

The author is grateful for the support of Dow Water & Process Solutions, Inc. and Bayer Material Science. This research was also supported by the U.S. National Science Foundation Partnerships for Innovation Accelerating Innovative Research (PFI-AIR, Grant #1237858) and Partnerships for Innovation (PFI) -Partnerships for Water Purification (Grant #0650277).

**Table of Contents**

Synthesis and Characterization of Hydrophilic-Hydrophobic Poly(Arylene Ether Sulfone) Random and Segmented Copolymers for Membrane Applications

## List of Figures

## List of Tables

## List of Equations

**Attributions**

**Chapter 2:**

Benjamin Sundell: This coauthor is from Virginia Tech in the department of Macromolecular Science and Engineering. Benjamin provided help in the preparation and the synthesis of the polymers presented in chapter 2

Euisong Jang: This coauthor is from University of Texas at Austin in the department of Chemical Engineering. Euisong provided help with water and salt transport experiments presented in chapter 2, these results are presented in table 2.4.

Ozma Lane: This coauthor is from the Virginia Tech in the department of Macromolecular Science and Engineering. Ozma preformed the AFM and SEM imaging of the polymers shown in this chapter. These images are shown in section 2.4.11, figures 2.6 and 2.7

Sue Mecham: This coauthor is from Virginia Tech in the department of Macromolecular Science and Engineering. Sue oversaw the project.

Benny Freeman: This coauthor is Professor of Chemical Engineering in the Chemical Engineering department at University of Texas at Austin. Prof. Freeman was Jaesung's advisor and oversaw the water and salt transport experiments.

James McGrath: This coauthor is Professor of Chemistry in the Chemistry department and Macromolecules and Interfaces Institute at Virginia Tech. Prof. McGrath was the author's advisor and oversaw the project.

**Chapter 3:**

Jaesung Park: This coauthor is from University of Texas at Austin in the department of Chemical Engineering. Jaesung provided help with the gas transport characterization presented in chapter 3.

Benjamin Sundell: This coauthor is from Virginia Tech in the department of Macromolecular Science and Engineering. Benjamin provided help in the hydrophilicity characterization of polymers presented in Chapter 3, Table 3.3

Sue Mecham: This coauthor is from Virginia Tech in the department of Macromolecular Science and Engineering. Sue oversaw and ran the SEC experiments of the polymers presented in Chapter 3. The molecular weights obtained from those experiments are shown in Figure 3.6

Benny Freeman: This coauthor is Professor of Chemical Engineering in the Chemical Engineering department at University of Texas at Austin. Prof. Freeman was Jaesung's advisor and oversaw the gas transport experiments.

Judy Riffle: This coauthor is Professor of Chemistry in the Chemistry department and Macromolecules and Interfaces Institute at Virginia Tech. Prof. Riffle was the author's co-advisor and oversaw the project.

James McGrath: This coauthor is Professor of Chemistry in the Chemistry department and Macromolecules and Interfaces Institute at Virginia Tech. Dr. McGrath was the author's advisor and oversaw the project.

**Chapter 4:**

Andrew Shaver: This coauthor is from Virginia Tech in the department of Macromolecular Science and Engineering. Andrew preformed the TGA experiments which are shown in Figure 4.6

Sue Mecham: This coauthor is from Virginia Tech in the department of Macromolecular Science and Engineering. Sue oversaw and ran the SEC experiments of the polymers presented in Chapter 4. The molecular weights obtained from those experiments are shown in Figure 4.4.

Judy Riffle: This coauthor is Professor of Chemistry in the Chemistry department and Macromolecules and Interfaces Institute at Virginia Tech. Prof. Riffle was the author's co-advisor and oversaw the project.

James McGrath: This coauthor is Professor of Chemistry in the Chemistry department and Macromolecules and Interfaces Institute at Virginia Tech. Dr. McGrath was the author's advisor and oversaw the project.

# 1. Introduction

## 1.1. Introduction to Poly(Arylene Ether Sulfone)s

Poly(arylene ether)s are well known engineering thermoplastics that were first successfully prepared in high molecular weight by R. N. Johnson in 1967 (Figure 1.1).[1] These versatile thermoplastics can be amorphous or semi-crystalline and they exhibit a variety of desirable properties. Poly(arylene ether sulfone)s (polysulfones) belong to the class of poly(arylene ethers) along with other variations such as poly(arylene ether ketone)s.

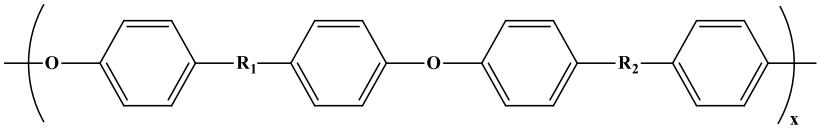


**Figure 1.1.** Poly(arylene ethers)

Polysulfones are high-performance engineering thermoplastics that have been investigated extensively over the past several decades due to their outstanding mechanical properties, high glass transition temperature ($T_g$), and exceptional thermal, oxidative and hydrolytic stability. Polysulfones' thermal and mechanical properties are highly suited to a variety of applications.[2,3] Figure 1.2 shows some of the commercial polysulfones available in the market.

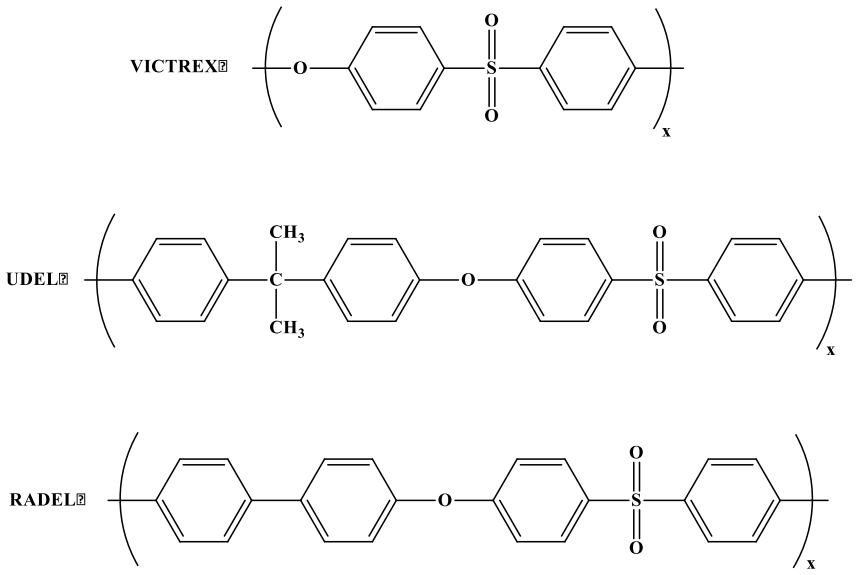


**Figure 1.2.** Commercial poly(arylene ether sulfone)s, http://www.solvay.com/, used under fair use, 2014

The high oxidation state of the sulfur combined with the resonance structure of the sulfone groups in the polymer repeat units result in excellent thermal and oxidative stability. These polymers can be melt-processed at temperatures beyond the degradation temperature of many consumer plastics. Polysulfones are melt-processible up to 400 ºC without any degradation.[4]

The glass transition temperatures of polysulfones varies between 180 and 260 °C (Table 1.1) and is affected by the presence of both stiff and flexible units in the polymer backbone. The high Tg's of polysulfones can be attributed to the strong inter and intra-molecular dipole-dipole interactions of the sulfone groups with the phenyl rings.[5,6] However, the presence of ether bonds introduces chain flexibility, and decreases strong inter-chain interactions which increase the conformational degrees of freedom.

**Table 1.1.** The glass transition temperatures of poly(arylene ether sulfone)s synthesized from 4,4'-dichlorodiphenylsulfone (DCDPS) and different biphenols.[2]

| | Glass Transition Temperature (°C) |
|---|---|
| 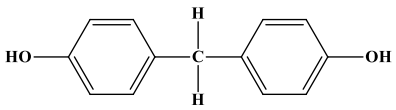 | 180 |
| 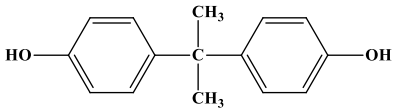 | 185 |
| 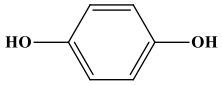 | 200 |
| 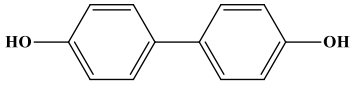 | 220 |
| 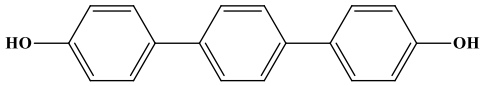 | 250 |
| 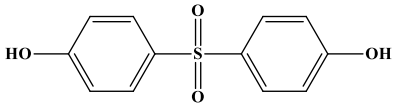 | 220 |
| 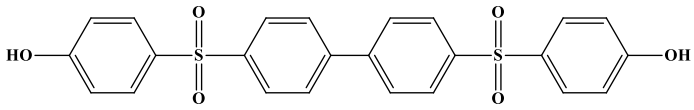 | 265 |

Polysulfones can tolerate prolonged exposure to temperatures from 150 to 190 ºC due to excellent thermal stability and their high Tg's

The presence of both rigid phenyl and flexible ether linkages in the polysulfone backbone structure results in tough, rigid, and ductile materials. Polysulfones display desirable mechanical properties such as high impact strength and creep resistance.[2] The high mechanical strength and

creep resistance of polysulfones has been attributed to segmental rotational motion of the backbone ether linkages which is responsible for the beta (β) transition at low temperatures.[5-7]

Polysulfones provide good solvent resistance to non-oxidizing acids, salts and aliphatic hydrocarbon solvents.[8-11] Moreover, polysulfones exhibit exceptional hydrolytic stability compared to other engineering plastics such as polycarbonates and polyesters.

Melt processibility and enhanced polymer properties including hydrolytic stability, solvent resistance and good mechanical properties have led to utilization of polysulfones in various sectors such as the medical, food service, automotive, membrane, electronics, and aerospace industries.[12] Bisphenol-A poly(arylene ether sulfone) has applications in membranes such as reverse osmosis, ultrafiltration, and gas separation.[13-16]

### 1.2. Synthesis of Polysulfones

Several synthetic routes have been developed to prepare polysulfones over the past several decades. This section discusses four different routes for polysulfone synthesis. The most commonly used nucleophilic aromatic substitution route will be discussed in greater detail.

#### *1.2.1. The Ullmann Reaction*

The Ullmann method utilizes non-activated aromatic halides in the reaction process (Figure 1.3).[17-20] This reaction takes place at high temperatures between an alkali metal salt of a phenol (phenolate) and an aromatic dihalide in the presence of a copper catalyst. The rate-determining step of this reaction is disassociation of the aryl halide bond. Therefore, the nature of the leaving group determines the reaction rate. The order of halide reactivity for the Ullmann reaction is I > Br > Cl >> F, opposite that of nucleophilic aromatic substitution reactions.

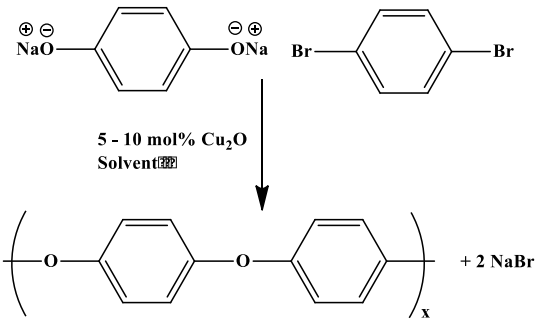


**Figure 1.3.** Representative reaction scheme for an Ullmann reaction

There are several reports of Ullmann syntheses producing high molecular weight poly(arylene ether)s in the literature.[19,21,22] The synthesis of p-bromo-sodium phenolate using cuprous chloride catalyst was reported in solvents such as nitrobenzene.[21] However, the reactions required a dry, oxygen-free reaction vessel to drive the reaction to higher conversion because oxygen causes a free radical side reaction which leads to branching and crosslinking. Jurek and others[19] also used Ullmann coupling reactions between bisphenols and dibromoarylene monomers to synthesize poly(arylene ether)s. They acknowledged a few drawbacks including difficulty in removal of copper salts, the need for specialty brominated monomers, and poor reproducibility.

### *1.2.2. Nickel Coupling Reaction*

Polysulfone synthesis using Ni-metal catalyzed coupling reactions have been reported. The nickel coupling synthetic route can utilize either activated (with electron withdrawing substituent) halides or non-activated (without electron withdrawing substituent) aromatic halides for preparing poly(arylene ether)s.[23-25] Nickel coupling employs a Ni catalyst to establish carbon-carbon bonds between the carbon atoms of aromatic halogens. Unlike Ullmann synthesis, this reaction proceeds at mild reaction temperatures (80 ºC) and utilizes either fluoro or chloro-halides.[26,27] In addition to Ni, Mn, Zn and Mg catalysts have been reported and such

polymerizations reach high conversions. These catalysts were only produce high molecular weight amorphous polymers that were soluble at reaction temperatures. The polymer product had to be soluble at reaction temperatures around 60 to 80 ºC to because the coupling polymerization reaction requires a homogeneous solution.[28]

### *1.2.3. Electrophilic Aromatic Substitution*

Electrophilic aromatic substitution is another alternative for polysulfone synthesis.[2] The reaction requires a strong Lewis acid ($AlCl_3$ or $BF_3$).[29,30] Figure 1.4 shows the electrophilic aromatic substitution reaction mechanism. In the first step, the reaction between the Lewis acid and a sulfonyl chloride yields a sulfonylium cation. Next, attack on the electrophilic sulfonylium cation by the benzene ring forms the intermediate. In the last step, the Lewis acid is restored when the intermediate loses a proton to reform the substituted aromatic ring and the by-product. The reaction of the aromatic ring with the electrophile determines the reaction rate since benzene is a poor electron donor. Electron donating substituents on the aromatic ring enhance the reaction rate whereas electron withdrawing groups reduce it.[29]

Electrophilic aromatic substitution can utilize self-condensing AB monomers that carry two types of functional groups, or two monomers with nucleophilic (AA) and electrophilic (BB) functional groups to synthesize polysulfones.

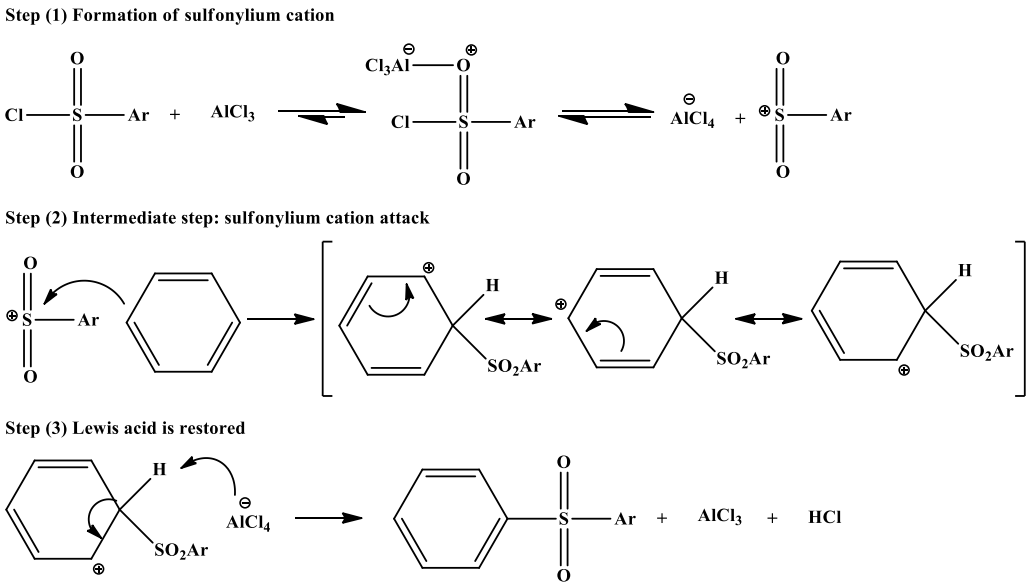


**Figure 1.4.** Representative scheme for electrophilic aromatic substitution reaction

### *1.2.4. Nucleophilic Aromatic Substitution*

The nucleophilic aromatic substitution reaction is the most common synthetic route to prepare polysulfones (Figure 1.5). This synthetic method was developed in the 1960s.[1] The nucleophilic aromatic substitution reaction occurs in two steps via an addition-elimination mechanism. The reaction takes place between an activated aromatic dihalide and a bisphenol in the presence of a base ($K_2CO_3$ or NaOH) in polar aprotic solvents such as N-methylpyrrolidone, dimethylacetamide, or dimethylsulfoxide.[1,3,18,31] The reaction rate depends on the electron withdrawing group of the dihalide monomer, the nature of the leaving group and, the nucleophilicity of the phenolate.

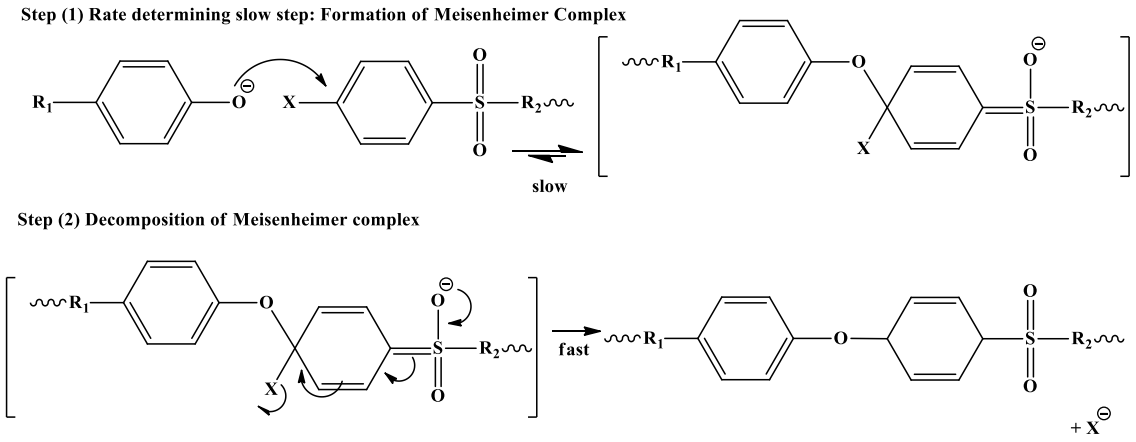


**Figure 1.5.** Representative reaction scheme for nucleophilic aromatic substitution

The attack of the nucleophilic phenoxide on the electron deficient aromatic carbon of the dihalide forms a Meisenheimer complex in the first step. This is the rate determining step of the reaction. The presence of the electron withdrawing group in the aromatic halides contributes as an activating group by making the carbon attached to the halide more electron deficient and increasing the reactivity.[32,33] Sulfones, ketones and phosphine oxides are the most commonly utilized electron withdrawing groups in poly(arylene ether) synthesis which yield poly(arylene ether sulfone), poly(arylene ether ketone) and poly(arylene ether phosphine oxide) respectively. Poly(phenylene sulfide)s are made commercially by nucleophilic aromatic substitution from sodium sulfide and dichlorobenzene. The range of nucleophiles participating in nucleophilic aromatic substitutions includes alkoxides, phenoxides, sulfides, fluoride ions and amines. The reaction rate increases with increasing nucleophilicity of the nucleophiles. The order of nucleophilicity is $ArS^-$ > RO- > $R_2NH$ > $ArO^-$ > $OH^-$ > $ArNH_2$ > $NH_3$ > $I^-$ > $Br^-$ > $Cl^-$ > $H_2O$ >ROH.[32,34] In general, nucleophilicity increases with increasing base strength.

In the second step the Meisenhimer complex decomposes and liberates the leaving group. The order of activity of leaving groups for nucleophilic aromatic substitution reaction is F > $NO_2$ > OTs > SOPh > Cl, Br, I > $N_3$ > $NR_3^+$ > OAr, OR, SR, $SO_2R$, $NH_2$ in the decreasing order .[35] In contrast to $SN_1$ or $SN_2$ mechanisms F is a better leaving group than I, Br, and Cl in nucleophilic aromatic substitution reaction. The rate limiting step is the formation of the Meisenhimer complex as opposed to breaking of the carbon-halide bond in other reactions. The reverse order F>Cl>Br>I is due to fluorine's strong electron withdrawing effect, which can best activate the aromatic halide towards nucleophilic substitution.[35]

Apart from these factors, many other factors like reaction temperature, solvent and the type of base influence the overall reaction. For example, the literature shows that reactions in dipolar aprotic solvents such as dimethylsulfoxide (DMSO), *N,N*-dimethylacetamide (DMAc), *N*-methyl-2-pyrrolidone (NMP), dimethylformamide (DMF) and sulfolane produce high molecular weight products.[36] The reaction rate is attributed to stabilization the Meisenheimer intermediate and enhancement of the active concentration of the attacking nucleophile in dipolar aprotic solvents.[37,38] Moreover, the activating groups play a key role in affecting the reaction rate. Activating groups in the ortho and para positions to the halogen leaving groups promote the nucleophilic aromatic substitution because the electron withdrawing activating groups strongly stabilize the Meisenheimer intermediate.

Earlier synthetic procedures for poly(arylene ether)s called for strong bases such as NaOH and KOH, and methods utilizing weaker bases such as $K_2CO_3$ were developed. The strong base approach was called the caustic process. During caustic process the protic contaminants such as alcohols, or moisture, could react with the polymer preventing the formation of a high molecular weight polymer.[39] Water can react with the aromatic halide resulting in unreactive polymer

endgroups or inactive monomer which upsets the stoichiometric balance. Therefore, the protic contaminants must be eliminated in polysulfone synthesis. The strong base is added in a stoichiometric amount to produce the bisphenoxide species and the by-product water must be azeotropically removed with solvents such as toluene or chlorobenzene[39] If excess strong base is charged to the reaction, the residual base can lead to hydrolysis of the dihalide, which alters the reaction stoichiometry and produces dead chain ends.[40,41]Excess strong base can also lead to ether-ether interchange and lower the degree of polymerization. Moreover, the alkali phenoxides are readily oxidized in air which also alters reaction stoichiometry, and thus the reaction must be purged with an inert gas to eliminate oxygen during the synthesis.

Utilization of a weak base eliminates the unwanted side reactions caused by the strong base.[42] The increased tolerance of excess base is a major advantage, but the reaction rate is slower with the weaker base. The slow reaction rates have been attributed to hydrogen bonding between phenate anions and phenol groups, the heterogeneity of $K_2CO_3$ and the presence of large amounts of azeotropic solvent. The poor solubility of the base in the polar protic solvents makes it necessary to use high temperatures to achieve high monomer conversion.[43]

The caustic process produces bisphenate from bisphenols, and they attack the activated aromatic halides. Although bisphenol A is soluble, some bisphenols such as biphenol or hydroquinone, are insoluble in bisphenate form, therefore they are not very applicable for high molecular weight copolymer synthesis via caustic process. McGrath *et al.* showed that weak bases initially produce only one phenate group per molecule, after this group reacts with the aromatic halides, the second phenol group can proceed and attack a different sulfone molecule.[42,44] Phenol terminated oligomers have enhanced solubility compared to the oligomers

produced by caustic process. Overall, weak base is a viable alternative to caustic process for polysulfone synthesis. [42,44,45]

### 1.3. Modification of Polysulfones for Membrane Applications

The previous section established that polysulfones have excellent thermal and oxidative stability, good mechanical properties, good processibility and exceptional hydrolytic stability. These properties qualify polysulfones as promising candidates for several industrial applications including water purification and gas separation membranes. Many studies have focused on modifications of polysulfones. The objective of modification consists of preparing polymers without sacrificing their excellent physical, chemical, and mechanical properties. The aromatic nature of the polysulfone backbone allows electrophilic and nucleophilic reactions. Many of the studies address incorporation of sulfonic acid groups onto the polysulfone backbones. Sulfonation is a versatile modification route to enhance physical properties such as hydrophilicity, water flux, and permeability.[46,47] There are two major ways to introduce sulfonic acid groups on polymers: (1) Post sulfonation of the polymer backbone and (2) direct copolymerization utilizing a sulfonated monomer.[47]

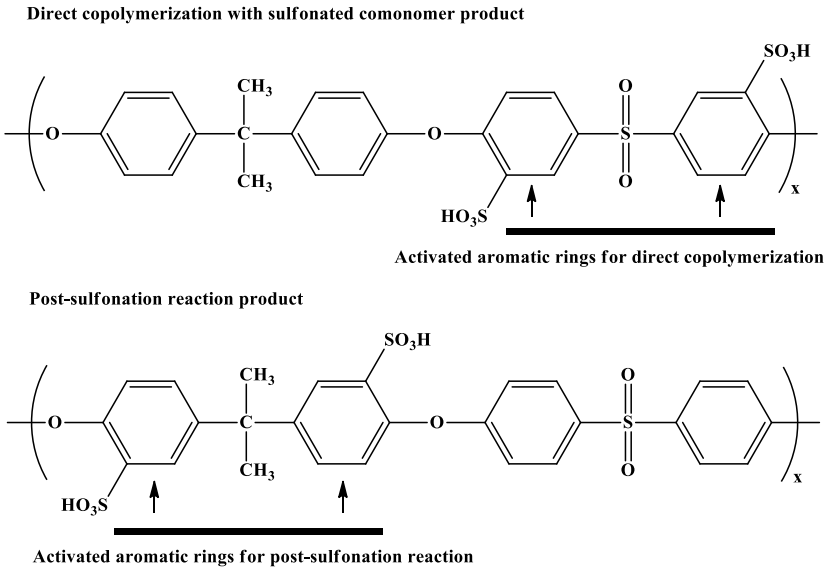


**Figure 1.6.** Comparison of polymer structures using post-sulfonation and direct polymerization

### *1.3.1. Post-Sulfonation of Polysulfones*

The post-sulfonation process has advantages such as convenient reactions and low cost yet there are several disadvantages which limit the application. Several articles in the literature reported the post sulfonation process leads to substitution of a sulfonic acid group on the electron deficient aromatic ring (Figure 1.6) and thus the post-sulfonated materials are thermally less stable relative to materials prepared in a direct-sulfonation route. Moreover, post-sulfonation lacks precise control of the degree of sulfonation, or the concentration and distribution of the sulfonic acid groups on the polymer chain.

Post-sulfonation of sulfone containing polymers is done using electrophilic aromatic substitution reactions (Figure 1.7). Generally, sulfonation via post-sulfonation takes place on the electron rich “activated” ring (biphenol or bisphenol ring) rather than the electron deficient “deactivated” ring (aromatic halide ring) in the polymer.

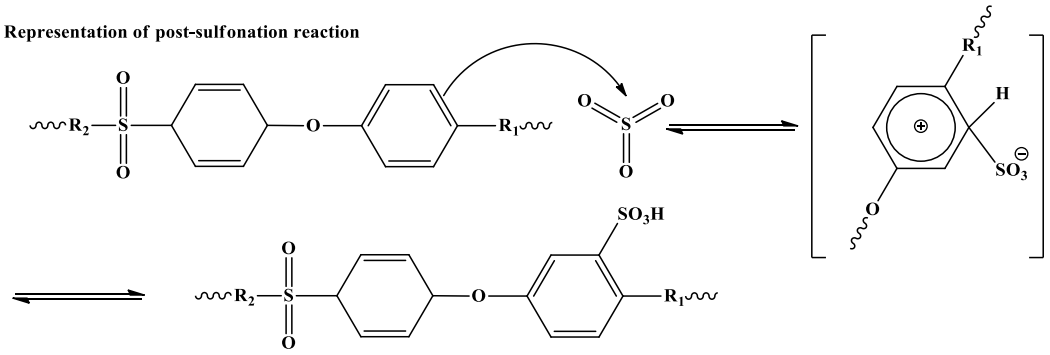


**Figure 1.7.** Representation of a post-sulfonation reaction of polysulfones

This facile reaction is attractive since it can produce sulfonated polysulfones from commercial aromatic polymers and a variety of sulfonation agents. Earlier efforts focused on utilizing chlorosulfonic acid.

In the early 1970's Quentin and coworkers reported sulfonation of commercial bisphenol A polysulfone with chlorosulfonic acid for reverse osmosis membrane applications.[48] They reported successful sulfonation of commercial polysulfones at various degrees of sulfonation at ambient temperature. Nevertheless, this route led to detrimental side reactions such as chain scission, branching and cross-linking of polysulfones. In the later years, several successful routes for post-sulfonation reactions utilizing chlorosulfonic acid, sulfuric acid, sulfur trioxide, chlorotrimethylsilane and acetyl sulfate followed Quentin's work.[49-53]

Concentrated sulfuric acid can sulfonate polysulfones attaching one sulfonic acid group to each repeat unit. The reaction time, temperature and acid concentration influence the degree of sulfonation and sulfonation reaction rate.[54,55] The degree of sulfonation can be between 30-100% depending on the sulfonation reaction time and the acid concentration.[56] A significant increase in water uptake of the sulfonated polymers correlates with higher degrees of sulfonation.[56]

Robeson and coworkers developed a sulfonation procedure using milder reaction conditions. Using sulfur trioxide and triethylphosphate complex as an alternative, milder sulfonation agent lead to diminishing and even elimination of possible side reactions.[52] However, it also resulted in slower reaction rates and diminished sulfonation efficiency. Similarly Johnson and colleagues showed that sulfur trioxide and triethylphosphate as the sulfonation agents eliminated crosslinking of the polysulfones.[51]

Another method to limit the occurrence of side reactions was to use trimethylsilyl chlorosulfonate as a protecting group during sulfonation of polysulfones. The sulfonation procedure utilized chlorosulfonic acid with trimethylchlorosilane in dichloroethane, this reaction lead to high degree of sulfonation which resulted in undesirable material properties.[57]

Kerres and others demonstrated sulfonation of UDEL by coupling lithium metalation of UDEL with SO2 sulfination and subsequent oxidation of the sulfinate moieties at low temperature.[58] This metalation-sulfination-oxidation route allowed sulfonic acids to be added to deactivated aromatic rings (Figure 1.6). However this approach proved to be difficult to control and reproduce.

### *1.3.2. Direct Copolymerization of Sulfonated Monomers*

A disadvantage of post-sulfonation of polysulfones is diminished chemical stability of the resultant polymer. The instability of the polymer can be attributed to the position of the sulfonic acid units in the polysulfone backbone. Generally, post-sulfonation takes place on the electron rich "activated" rings (biphenol or bisphenol ring) rather than the electron deficient "deactivated" rings (ring adjacent to a sulfone group) in the polymer. This sulfonation process decreases the electron density of the sulfonated ring and, as a result, makes the bond between the aromatic carbon and the ether oxygen more susceptible to hydrolysis.[59] The hydrolytic instability was one

motivation for developing an alternative route to synthesize sulfonated polysulfones in which the sulfonic acid groups are attached to the "deactivated" rings. Advantages of sulfonation on the deactivated rings include both better hydrolytic stability and higher acidity due to the presence of the electron-withdrawing sulfone group.

Two different methods yield sulfonic acid groups on the deactivated aromatic rings in the sulfonated polysulfone chain: (1) sulfination-oxidation,[58] and (2) the direct copolymerization of a modified monomer.[59-61] The metalation-sulfination-oxidation route has significant disadvantages such as chemically unstable products, difficulty in controlling the reaction, and reproducibility. Thus the latter method has gained focus over the past 30 years.

A few sources[51,59,62-65] have reported direct copolymerization using a nucleophilic aromatic substitution reaction with disulfonated monomers. Researchers disclosed that polysulfones produced with sulfonated monomers yield thermally, chemically, and mechanically enhanced stable polymers. They attribute the improved stability of the polymers to the position of the sulfonic acid moieties on the polysulfone repeat unit. Sulfonated polysulfones with the sulfonic acid groups attached to the more electron deficient deactivated ring are less susceptible to hydrolysis because the carbocation intermediate cannot be easily generated.[62] Furthermore, the direct copolymerization yields two sulfonic acid groups on the deactivated phenyl rings per repeat unit which leads to better control of degree of sulfonation, the concentration and the distribution of the sulfonic acid groups on polymer chain.[65]

Robeson and Matzner reported the first sulfonated polysulfone synthesis via direct copolymerization of a disulfonated monomer to obtain fire resistant polymers.[60] They demonstrated sulfonation of 4,4'-dichlorodiphenylsulfone (DCDPS) and synthesis of sulfonated polysulfone employing the sulfonated DCDPS as a comonomer.

Similarly, Ueda and others[61] reacted DCDPS with fuming sulfuric acid which yielded disulfonated DCDPS (SDCDPS). They also demonstrated synthesis of sulfonated polysulfone utilizing SDCDPS as a comonomer with bisphenol A and DCDPS to obtain a sulfonated polysulfone with a varying disulfonation degree as high as 30 mol %.

In the past fifteen years, McGrath and his colleagues contributed significantly to the synthetic route and characterization of both the disulfonated dichlorodiphenylsulfone (DCDPS) monomer[66] and disulfonated poly(arylene ether sulfone)s[67,68]. Unlike the procedure developed by Ueda and others, McGrath and colleagues developed a new single stage synthetic route to increase the purity and yield of the disulfonated monomer.[66] They reported a product yield of 80-90%, and this was significantly higher than previously reported.

In most cases researchers reported that recrystallization of the crude disulfonated monomer yield from an alcohol–water mixture was necessary to remove the impurities. The recrystallized monomer still retained some sodium chloride salt that could interfere with polymerization reaction. To solve this problem, investigations focused to accurately determine the purity and direct use of the crude SDCDPS. McGrath and others[66] were the first to demonstrate that high molecular weight disulfonated polysulfone from crude disulfonated monomer was possible. DCDPS can be completely converted to the disulfonated monomer with a single-step approach (Figure 1.8) and the crude SDCDPS monomer had an equal purity to recrystallized SDCDPS. The complete conversion of DCDPS to the SDCDPS required 1 to 3.3 reactant molar ratio of DCDPS to $SO_3$ at 110°C for 6 hours. Researchers developed a method using UV-Vis spectroscopy to accurately determine the amount of salt retained by the SDCDPS monomer. Charging the polymerization reaction with excess SDCDPS to compensate for the NaCl impurity allowed the synthesis of high molecular weight random disulfonated polysulfone copolymers.[66]

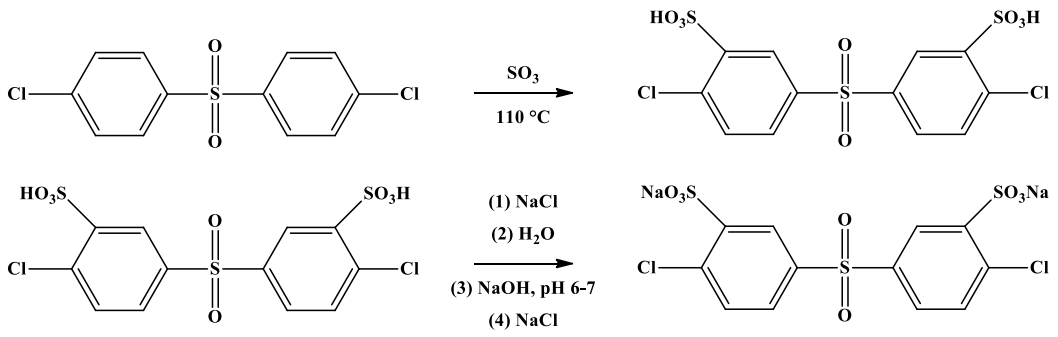


**Figure 1.8.** Direct sulfonation of DCDPS [66,69]

Along with many advantages, the random copolymers with ≥50% degree of sulfonation prepared by the direct copolymerization route exhibit excessive swelling and may become mechanically unstable. This behavior is attributed to the percolation threshold, and it is associated with phase inversion phenomenon between the hydrophilic and hydrophobic domains of the copolymers.[64]

### 1.4. Poly(Ethylene Oxide)

This section discusses polymerization of cyclic ethers with an emphasis on polymerization of ethylene oxide and its use in membrane separation technology.

Polyoxiranes are very well-known and useful polyethers with a wide range of applications. Polyoxiranes are an important component in production of cleaning agents (detergent and soap), cosmetic agents, lubricants, oil and gas well drilling muds, inks, metal working fluids, ceramics manufacturing, polyurethane flexible foams and elastomers, chemical intermediates for textile spin finishes, and many other industrial intermediates.

In 1878, Wurtz disclosed the earliest preparation of solid polyoxiranes. He described the polymerization of ethylene oxide (EO) in the presence of a catalytic amount of either an alkali metal hydroxide or zinc chloride.[70,71] Later in 1929, Staudinger and Schweitzer studied the

polymerization of EO utilizing various basic and acid catalysts. They synthesized high-molecular weight poly(ethylene oxide) (PEO) utilizing calcium, strontium, or zinc oxides as a catalyst and isolated the products depending on their molecular weights.[71,72] During the 1930s, low MW PEO (also known as poly(ethylene glycol) or PEG) became commercially available via utilization of base-initiated addition of EO to ethylene glycol. This new product found use in an array of applications such as pharmaceuticals, cosmetics, textile lubricants and detergents. In 1940, Flory investigated the mechanism of base-initiated polymerization of oxiranes and predicted a narrow, Poisson distribution of molecular weights.[73] Later efforts indicated calcium amides are effective in polymerizing EO to form high MW PEO.[74] In the 1950s, researchers attempted to polymerize substituted alkylene oxides to produce high MW polyoxiranes with controlled stereoregularity.[75] The earliest attempts on the coordination polymerization of an epoxide dates back to 1955. Pruitt and Baggett studied ferric chloride catalyzed polymerization of propylene oxide.[71,76]

PEO is a polyether with $(CH_2CH_2O)_n$ repeat units, and it is a crystalline, thermoplastic polymer. PEO is the most important representative of polyoxiranes due to having the simplest structure among water-soluble polymers. PEO is commercially available in a variety of molecular weights ranging from a few hundred to several million. PEO with any MW dissolves in water at room temperature. In contrast, polymers which closely resemble PEO such as polyacetal $[(CH_2O)_n]$, poly(trimethylene oxide) $[(CH_2CH_2CH_2O)_n]$, polyacetaldehyde $[(CH_3CHO)_n]$, and poly(propylene oxide) $[(CH_2CHCH_3O)_n]$ are water-insoluble.[71] Water solubility of PEO is attributed to balance hydrophilic-hydrophobic forces in the PEO repeat units. The latter dominates in the short PEO chains, thus their importance diminishes as the chain length increases. As a result of hydrophilic and hydrophobic competitive forces, the PEO is soluble in water and many organic solvents at temperatures below the boiling points of the

solvents. Due to its extraordinary solubility PEO exhibits unique binding, thickening, lubricity, water retention, and film formation properties.[77]

Three-, four-, five-, or higher-membered cyclic ethers carry significant ring strain (Table 1.2). The difference between the angles resulting from orbital overlap and the angles that ring size dictates account for the ring strain. Additionally the interactions of the atoms located in close proximity may contribute to ring strain. Cyclic ethers can form reactive intermediates that can polymerize to form polyethers. Cationic or acidic reagents can initiate the polymerization mechanisms for all cyclic ethers; however ethylene oxide (EO) is the only one that can be initiated by both anionic and cationic reagents. EO has an estimated strain energy of ~115 kJ $mol^{-1}$, which is the main driving force for ring-opening polymerization to PEO. The major ring-opening polymerization reactions of EO include anionic and coordinated polymerizations.[71,77]

**Table 1.2.** Rings strains of 3,4,5,6,8 membered cyclic ethers[78] Pell, A. S.; Pilcher, G., Measurements of heats of combustion by flame calorimetry. III. Ethylene oxide, trimethyl oxide, tetrahydrofuran, and tetrahydropyran. *Trans. Faraday Soc.* **1965,** 61, (Copyright (C) 2012 American Chemical Society (ACS). All Rights Reserved.), 71-77. Used with permission of Royal Society of Chemistry, 2014.

| Cyclic Ether | Atoms in the Ring | Ring Strain (kJ/mol) |
|---|---|---|
| Oxirane | 3 | 114 |
| Oxetane | 4 | 107 |
| Oxolane | 5 | 23 |
| Oxane | 6 | 5 |
| Oxocane | 8 | 42 |

Polymerizability in a thermodynamic sense is related to the Gibbs energy change ($\Delta G$) associated with conversion of a monomer into a polymer unit. The Gibbs energy of

polymerization is a function of enthalpy (ΔH) and entropy (ΔS) of polymerization (Equation 1.1). [79]

**Equation 1.1.**

$$\Delta G_P = \Delta H_P - T\Delta S_P$$

In the polymerization of heterocyclic monomers, the driving force for polymerization is provided by release of the strain of the ring upon its opening.[80,81] In the process of polymerization, many monomer molecules are incorporated into a polymer chain and thus entropy decreases. Although the entropy of polymerization depends on the ring size, −ΔS values for polymerization of cyclic ethers are typically not higher than 80 J/ °C x mol.[80,81] Thus, at ambient temperatures (300 K), the term –TΔS usually does not exceed 25 kJ /mol. This sets a borderline between polymerization that is practically irreversible and polymerization that proceeds reversibly because in order to make polymerization possible from the thermodynamic point of view (ΔG < 0), enthalpy (ΔH) must exceed the entropy term (TΔS). Thus, the thermodynamic polymerizability is governed by the enthalpy of polymerization that is closely related to the ring strain of the monomer.

Polymerization of highly strained three-and four-membered cyclic ethers is practically irreversible while polymerization of five-membered THF is a typical example of a reversible polymerization in which a significant amount of monomer remains in equilibrium with the polymer. Enthalpy of polymerization is mainly related (but not exclusively) to the ring strain.[78] Molecules of cyclic ethers, with the exception of EO, are not planar although the deviation from planarity in the four-and five-membered rings is small. The geometry of cyclic ethers governs the ring strain which relates to the number of atoms in the ring. The free electron pairs on the oxygen atoms also contribute to ring strain.

**Equation 1.2.**

$$K = 1/[M_e]$$

$[M_e]$ is the concentration of monomer at equilibrium and K is the equilibrium constant

**Equation 1.3.**

$$\Delta G^0 = \mathrm{RT} \ln K$$

**Equation 1.4.**

$$\mathrm{RT} \ln 1/[M_e] = \Delta H_P - T\Delta S_P$$

**Equation 1.5.**

$$\ln 1/[M_e] = \frac{\Delta H_P - T\Delta S_P}{RT}$$

Briefly from the thermodynamic point of view equation; (1) the equilibrium monomer concentration of cyclic ethers becomes larger as the ring strains becomes smaller. (2) The equilibrium monomer concentration increases with the increasing temperature. (3) For each initial monomer concentration of there is a temperature at that equilibrium monomer concentration and initial monomer concentration are equal therefore, at that temperature polymerization is not possible.

This temperature is denoted as a ceiling temperature for polymerization ($T_c$). For practical purposes, the value of $T_c$ is of interest because above this temperature the monomer will not polymerize under any conditions. The Gibbs energy of polymerization is strongly negative for the polymerization of strained three-and four-membered cyclic ethers. Therefore, polymerization is practically irreversible, which means that there are no thermodynamic barriers for reaching quantitative conversions even at low initial monomer concentration and higher temperatures. However, kinetic factors may inhibit quantitative conversion if a termination reaction takes place. In contrast, polymerizations of weakly strained cyclic ethers containing five or six atoms

in the ring are highly reversible, which means that there are thermodynamic limits on the ultimate conversion.

### *1.4.1. Anionic Ring Opening Polymerization Reaction*

Three-membered ring epoxides are the only cyclic ethers that can be polymerized by an anionic polymerization mechanism (Figure 1.9).

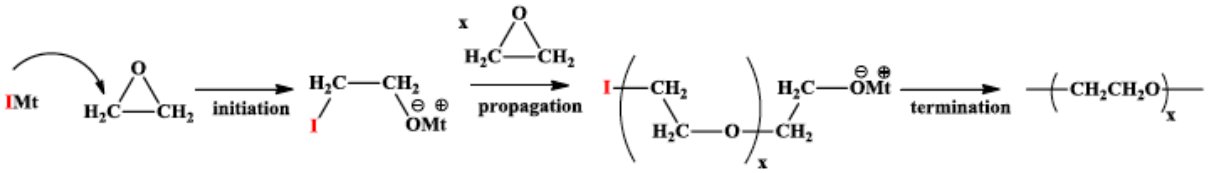


**Figure 1.9.** Representation of anionic ring opening polymerization of ethylene oxide

Initiation leads to the formation of an alkoxide ion with an associated metal counterion provided by the initiator. The alkoxide must be nucleophilic enough to attack another epoxide molecule and propagate.

Hydride, alkyl and aryl, hydroxide, alkoxide, and amide type alkali metal derivatives can be anionic polymerization initiators. Sodium or potassium are the most often used alkali metals.[82] Lithium-based initiators in hydrocarbon solvents generally yield alkoxide species that are unable to propagate the polymerization due to strong association following the initial monomer addition. Anionic polymerization of epoxides can proceed in polar aprotic solvents such as THF or DMSO, or simply without any solvent.

Several papers report studies on the anionic polymerization of EO in DMSO. The use of potassium tert-butoxide (t-BuOK) as initiator was reported to yield living PEO with molar masses controlled by the monomer to initiator ratio.[83-85] In the case of K and Cs salts, EO polymerization in DMSO proceeds almost exclusively by free ions.[85] In the case of a Na counter ion, both ion pairs and free ions contribute to the polymer propagation.[85] Researchers reported

that propagation rate constants in HMPA (at 40 °C) compared to DMSO (at 50 °C) were much higher. This large difference may be accounted for by an important stabilization of the free anion via polar interaction with DMSO.

Addition of complexing agents such as crown ethers, exceedingly increase the EO propagation rate in ether solvents. [86-88] They both reduce the aggregation of alkoxide propagating ends and increase the proportion of free ions.

### *1.4.2. Coordination Catalyst Ring Opening Polymerization Reaction*

Coordination organometallic polymerization catalysis can be considered as similar to anionic polymerization processes since epoxide ring opening involves a nucleophilic-like mechanism, which is assisted by monomer coordination on a metal atom of the catalytic system. In this preliminary coordination step ascribed to the Lewis acidity of the metal, the epoxide ring is activated for a nucleophilic attack, while the catalyst metal–counterion bond is weakened, increasing the nucleophilic character of the counterion. These systems can yield high-molar-mass polyethers. The possibility to synthesize stereoregular and crystalline optically active polyethers is also an important characteristic of these coordination processes.

In 1955 Pruitt and Baggett reported the first coordination epoxide polymerization based on an iron trichloride catalytic system.[76] Ever since, metal-based catalysts systems developed for epoxide polymerization the most extensively studied systems have been zinc or aluminum derivatives. Diethylzinc or trialkylaluminum associated to a ‘co-catalyst’ (water, alcohol, amine) that reacts with the alkyl metal to form in situ new metal derivatives also received attention.[89]

Trialkylaluminum and dialkylzinc when used alone yield very low epoxide conversions with long polymerization times.[90] Addition of water yields active metal oxides containing Mt–O–Mt

bonds, [91,92] which leads to a mixture of several polymer populations that are produced according to different mechanisms.[93]

Vandenberg and colleagues proposed a very complex coordination polymerization mechanism for the trialkylaluminum/water system.[94] According to the proposed bimetallic mechanism complexation of monomer with coordination catalyst results in partial electron transfer from the epoxide to the metal, causing the methylene carbon atom of the ring to become more prone to nucleophilic attack. Coordination also promotes an electron transfer between the two adjacent aluminum atoms coordinating two separate activated chains, which weakens the polymer– aluminum bond, increasing reactivity of the corresponding alkoxide moieties toward the electrophilic carbon of the neighboring epoxide.

Additives such as pyridine, tertiary amines, or acetylacetone have been used to modulate the metal acidity and improve the selectivity toward high-molar-mass polymers. As an example, the addition of acetylacetone as chelating agent to trialkylaluminum/water system increases the proportion of crystalline polymer. Similarly, addition of pyridine or tertiary amines decreases the amount the acid sites, leading to the same effect.[82,95,96] As a tradeoff, the crystalline polymer fraction is higher in those reactions however the overall polymerization rate is decreased.

Tsuruta and others explored diethylzinc/alcohol systems for the polymerization of epoxides. They identified several diethylzinc complexes as initiating species for the coordinated polymerization.[82,97]

Researchers discovered that diethylzinc/alcohol propylene oxide systems may lead to the formation of two polymer fractions: one essentially isotactic with high molar masses and a second one atactic with lower molar masses. The high molar masses, typically in the range of

100000 g/mol, result from a slow initiation. Ishimori [98] and Tsuruta [97] classified these systems as 'living-like' based on the continuous increase in molar mass with conversion.[82]

The metalloporphyrins of aluminum and zinc have quite different characteristics as epoxide polymerization catalysts.[82,99-104] The covalent nature of the aluminum–counter anion bonds suggests that polymerization occurs following a coordination process. Researchers hypothesize this due to the exclusive presence of regular head-to-tail connections [102]and tacticity that dependent on the porphyrin structure.[105]

Literature shows that the substituents on the phenyl groups affect the reactivity of the Al–halogen bond; polar groups lead to a very high initiation activity, whereas nonpolar substituents result in an opposite effect.

In contrast to conventional anionic polymerizations, in which epoxide insertion involves an inversion of the configuration at the carbon atom of the epoxide ring where cleaved, some porphyrin systems were shown to operate by a non-dissociative reaction mechanism, with retention of configuration at the carbon atom of the epoxide ring where cleaved.

Inoue and co-workers were the first to report the use of bulky Lewis acids as additives to aluminum porphyrin initiators to enhance the polymerization rate.[100] They attribute the coordination of the epoxide to the acidic aluminum center. Electron transfer from the oxygen to the metal makes the ring carbon atoms electron-deficient, favoring an attack by even weak nucleophilic species.[104] Due to the monomer activation, polymerization undergoes a drastic acceleration while keeping a good control of molar masses and distributions.[104]

### *1.4.3. Role of PEO in Separation Processes*

Poly(ethylene oxide)-containing polymers are used in many membranes today. For example, microporous poly(ethylene oxide)-block-polyamide (PEBAX®) membranes are used as fouling-

resistant ultrafiltration/nanofiltration membranes.[106] Similar poly(ethylene oxide)-block-polyamide multiblock copolymers are employed as gas separation membranes in olefin/alkane separations.[106] Another application that involves poly(ethylene oxide)-containing multiblock polymer membranes is pervaporation to separate ethanol from water.[106] The development of fouling-resistant membranes would improve the reliability, and simplify the desalination process. Today, despite intensive efforts, anti-fouling membranes are not available for desalination applications. These efforts on the other hand, established the relationship between polymer surface chemistry and the tendency of adhesion of biomolecules and microorganisms. Research demonstrated that hydrophilic surfaces containing only hydrogen-bond acceptor groups but not donor groups, and neutral surfaces resist bioadhesion.[107] Researchers hypothesized that these films can form a barrier with a thin layer of water on their surface, which hinders adhesion.[107-109] Moreover, surface roughness of thin film composites enables bioadhesion of substances on the membrane surface.[110] Literature suggests that PEO-containing surfaces among others meet the requirements for fouling resistance.[107,109] Briefly PEO-based membranes have potential to prevent membrane fouling, and they have the potential for application in next generation RO membranes.

McGrath, Lee and others, investigated blends of disulfonated poly(arylene ether sulfone) random copolymers with PEO oligomers for enhancing the water permeability of RO membranes.[111] They concluded that a strong ion-dipole interaction between the ionic sulfonate groups and PEO existed. This interaction resulted in "pseudo immobilization" of PEO chains which prevented the PEO from leaching out of the blended membranes. They demonstrated that introduction of PEO into disulfonated poly(arylene ether sulfone) random copolymers reduced the $T_g$'s of the blends due to the disruption of ionic crosslinking. $T_g$ can be tuned via PEO

segment molecular weight and PEO concentration in the disulfonated poly(arylene ether sulfone)-PEO blends . Researchers attributed this to plasticization due to an increase in free volume. Further investigation of the blends revealed that higher concentrations of PEO led to interconnected hydrophilic domains in which long PEO chains formed tortuous pathways. Researchers discovered that introducing PEO improved water permeability up to 200% in some cases.

The separation of acid gases such as carbon dioxide and hydrogen sulfide from mixtures of gases has considerable industrial importance (e.g. natural gas sweetening). $CO_2$ occurs as either a natural impurity or a by-product of industrial chemical processes and must be separated from gas mixtures. Natural gas streams contain impurities such as $C_2H_6$ and $CO_2$ along with $CH_4$. $C_2H_6$ is a commercially important petrochemical feed stock to be recovered and $CO_2$ has to be removed to meet natural gas pipeline specifications. This separation has been conducted via conventional methods such as chemical absorption with amine solutions, selective solvent (NMP) adsorption, and cryogenic distillation. However, these methods are capital and energy intensive and require complex equipment and maintenance.[112-114]

Conventional commercial membranes used for $CO_2$ separations rely on diffusivity selectivity.[115,116] In a heavy/light gas separation such as $CO_2$/separation from $H_2$, $N_2$ or $O_2$, diffusivity selective membranes yield low pressure light gas products due to the higher permeability of light gasses compared to $CO_2$.[116,117] At the end of the separation process the product must be re-pressurized which complicates the process and increases the production cost. Thus, to separate $CO_2$ from a light gas stream a highly $CO_2$ permeable membrane is desirable.

The membrane technology for $CO_2$ separations offers significant advantages with respect to energy requirements and maintenance. PEO-containing polymers have been been extensively

investigated as promising membrane material candidates to selectively permeate $CO_2$.[118-120] Freeman and colleagues investigated the relationship between structure and gas transport properties of PEO-based membranes.[121]

The tendency of PEO to crystallize limits its viability as a gas separation membrane. Crosslinking restricts the crystallization of PEO, and therefore crosslinked membrane designs consisting of UV-crosslinked low molecular weight PEO diacrylates are particularly of interest.[113,116,118,121,122] The presence of polar ether oxygens leads to dispersive interactions between PEO repeat units and $CO_2$ molecules. This interaction enhances solubility and thus the solubility selectivity of $CO_2$ in light gas streams.[115,121,123]

A variety of PEO-based diacrylates and monoacrylates in a variety of molar ratios were studied. Investigation of the effect of structure on $CO_2$ separation properties revealed that the PEO-rich crosslinking reagents with pendant mono- functional PEO acrylates of varying length yielded membranes with enhanced gas transport performance. The presence of flexible monoacrylates throughout the network increased the free volume leading to enhanced permeability. In some cases the permeability of $CO_2$ exceeded the permeability of control systems without the pendent PEO acrylates. The selectivity of the crosslinked systems remained high despite the well-established trade-off relationship between selectivity and permeability.

### 1.5. Polyurethane Synthesis

Polyurethanes are part of a very versatile group of materials that find uses in a wide range of applications, both domestic and industrial. Polyurethanes are widely used in many applications such as paints and lacquers, foam mattresses, medical implants, and industrial applications such as rollers, electrical encapsulation, engineering components, shoe soles, seals, and in the mining industry.[124]

In 1849, Wurtz discovered the formation of aliphatic isocyanates when he reacted organic sulfates with cyanates.[125] The first important commercial development was a result of the work of Professor Otto Bayer in 1937. He discovered how to make a polymer using diisocyanates employing polymerization techniques when working to develop a polymer fiber to compete with nylon.[125] In 1938, Rinke and colleagues succeeded in producing a low-viscosity melt that could be formed into fibers.[126] This led to the production of many different types of polyurethanes. Intensive research discovered that there were many modifications that could be made to the chemistry surrounding the urethane linkage. During the 1940s and early 1950s, DuPont and ICI developed castable polyurethanes.[124,126]

The rapid formation of high molecular weight urethane polymers from liquid monomers, which occurs even at ambient temperature, is a unique feature of the polyaddition process, yielding products that range from cross-linked networks to linear fibers and elastomers. The enormous versatility of the polyaddition process allowed the manufacture of many products for a wide variety of applications.

Polyurethanes contain carbamate groups (-NHCOO-), also referred to as urethane groups, in their backbone structure. They are formed by the reaction of a diisocyanate with a polyol, or with a combination of a polyol and a short-chain-diol extender. In the latter case, segmented block copolymers are generally produced. Polyols consist primarily of polyether-, polyester-, polycarbonate-, or polysiloxane-based oligomers with glass transition temperatures below room temperature and number average molecular weights (Mn) between few hundred to a few thousand g/mol. The conventional methods to synthesize segmented polyurethanes (Figure 1.10) include single-step “one-shot” and two-step “prepolymer” methods. In single step “one-shot” synthesis, all constituents react simultaneously. In the “prepolymer” method, the reaction of

excess isocyanate with α,ω-hydroxyl terminated polyol yields isocyanate-terminated pre-polymer which later reacts with chain extender to form a high molecular weight segmented polyurethane with alternating soft (SS) and hard segments(HS).[126]

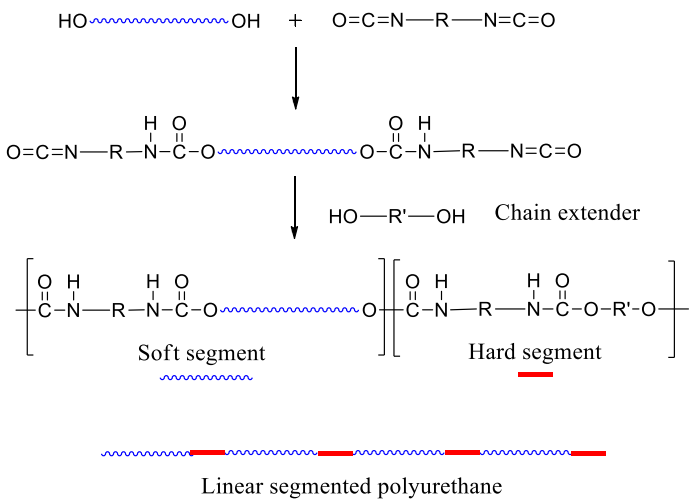


**Figure 1.10.** General representation of polyurethane synthesis

The factors that control the polyurethane characteristics include molecular structure (flexibility/rigidity), density, hydrophobicity/hydrophilicity and processing characteristics (e.g. thermoplastic or thermoset). Additionally some other general principles that dictate the structure-property relationship involve: (1) Molecular weight which influences some important polymer properties such as tensile strength, elongation, elasticity, and $T_g$, (2) intermolecular forces such as presence of hydrogen bonds, (3) stiffness of chain due to presence of aromatic rings or flexible ether bonds, and (4) crystallization which can influence solubility, elasticity, and tensile strength.[125]

These properties describe the individual contributions of each component, therefore to be able to understand the properties that manifest; one should understand the contribution of the each chemical component.

Isocyanate type, symmetry, and structure have a profound impact on the properties of polyurethanes. Figure 1.11 shows several different diisocyanates; aliphatic, cycloaliphatic, aromatic, diisocyanates used for polyurethane synthesis below.

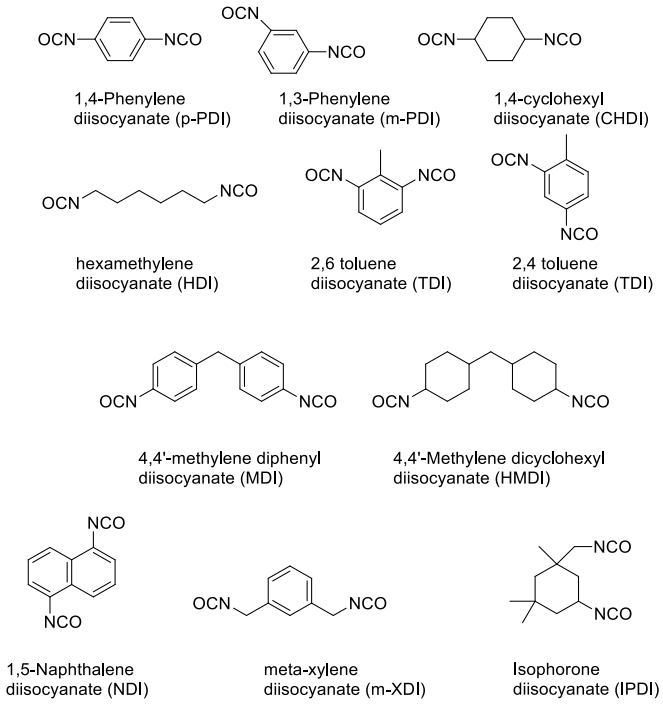


**Figure 1.11.** Structures of common isocyanates

Yilgor and others,[127] presented that the symmetry of diisocyanates influenced the degree of crystallinity of polyurethanes. These studies suggested that symmetric diisocyanates organized to form crystalline domains; however, the presence of non-symmetric diisocyanates in the PU backbone disrupted the degree of organization and inhibited the self-organization of HS domains. DMA analyses of different segmented PU with different diisocyanates indicated that the PU bearing symmetric diisocyanate units had higher transition temperatures and showed better mechanical properties over a wider range of temperatures than asymmetric diisocyanate SPU. AFM analysis of PU revealed that the surface morphology of symmetrical diisocyanate

containing samples showed phase separation whereas; the asymmetrical diisocyanate containing samples were featureless. SAXS and tensile testing methods also confirm that the symmetry of the diisocyanate affected the crystallinity of PU. All the symmetric polyurethanes that showed phase-separated surface morphologies in AFM also showed a first order interference peak in their SAXS profiles. SAXS data validated that SPU with symmetrical diisocyanates have higher degree of crystallinity than those with non-symmetrical diisocyanates.[127]

Commercial hydrophilic polyurethanes predominantly contain toluene diisocyanate (TDI) and methylene diphenyl diisocyanate (MDI) diisocyanates. The relative importance of these diisocyanates is due to a number of reasons. TDI was the first successful diisocyanate used to make PU and it remains important, mostly because TDI tend to yield soft more hydrophilic materials due to reduced crystallinity. Compared to TDI, MDI on the other hand can yield a tougher hard segment with a given polyol and the reaction rate is faster. The aromatic diisocyanates present some problems with respect to weathering, especially yellowing upon UV or heat exposure. Yellowing is typically seen as indicative of degradation and relates to the usefulness of the material. Alternative diisocyanates are available to eliminate yellowing. Methylene dicyclohexyl diisocyanate (HMDI) and isophrone diisocyanate (IPDI) are aliphatic counter parts of MDI and TDI respectively. Aliphatic isocyanates are less subject to yellowing.[128]

The polyol is the component that gives the chemical nature to the polyurethane for the most part. Hydrophilic polyurethanes comprise of mostly polyester and polyether type polyols. The polyester type polyols for hydrophilic polyurethanes consist of mostly adipic acid derivatives. Ethylene and propylene oxides compose most polyether polyols. The propylene oxide polyols are also hydrophobic, thus, ethylene oxide polyethers are the basis of the most hydrophilic

polyurethanes.[128] Oligomeric α,ω-hydroxy-terminated poly(ethylene oxide) also known as poly (ethylene glycol) (PEG), which has the general formula HO–($CH_2CH_2O$)$_n$–H, is a water soluble, hydrophilic polyol. This characteristic behavior seems to be due to a crucial balance of the hydrophobic forces exerted by the ethylene unit, –CH2–CH2–, with the hydrophilic interaction of the oxygen presented in the repeating unit.[77] The crystalline state PEG assumes a helical conformation. Moreover, the ether oxygen spacing provides a good structural fit for the hydrogen-bonding network in water. This extraordinary balance of hydrophobic-hydrophilic interaction balance and oxygen spacing also give PEG its $CO_2$-philic nature.[115]

The PEG-containing polyurethanes received interest for gas separation membrane applications. PEGs with different molecular weights (400 g/mol and 600 g/mol) were used during the syntheses. PEG600-containing polyurethanes had lower $T_g$ PEG400, which indicated a better phase separation morphology. Better phase-separation of PEG600-based polyurethane lead to a higher $CO_2$ permeability and $CO_2/N_2$ and $CO_2/CH_4$ selectivity than the PEO400-containing polyurethane's. It was hypothesized that $CO_2$ preferably diffused through the PEG segments. Although the diffusivity selectivity of $CO_2/N_2$ were similar, the solubility selectivity of PEG600-based polyurethanes were almost three times the PEG400-based polyurethanes The better phase-separated morphology lead to higher solubility selectivity.

Moreover, the following properties of PEG draw attention to PEG-containing polyurethanes due to several properties. PEG displays amphipathic behavior; it is soluble in water, and organic solvents. FDA approval allows low MW (1000–5000) PEG to be administered for internal consumption and it is non-toxic. PEG usually doesn't cause an immune response. PEG polyols can precipitate proteins and nucleic acids and can covalently couple with proteins. PEG can solubilize enzymes and bioactive substances in various organic aqueous media. Moreover, it can

alter pharmaceutical kinetics of various drugs; and most importantly PEG can be used in biological applications due to its human blood and tissue compatibility.[77] Therefore, hydrophilic polyurethanes containing PEG segments are the focus of much interest in biomedical and biotechnical applications. These types of polyurethanes find applications in wound care and treatment dressings, postsurgical dressings, artificial organs, permeability/diffusivity controlled release devices, and even unusual application such as in biological treatment of municipal waste.

## 1.6. Water Desalination and Gas Separation

### *1.6.1. Reverse Osmosis*

The UN World water development report in 2003 estimated that about 97.5% of the earth's water is located in seas and only about 2.5% is fresh water. Almost two thirds of the fresh water is locked in icecaps and under permanent snow cover. Precipitation is the main source of fresh water for human consumption and for ecosystems. This precipitation is taken up by plants and soil, evaporates into the atmosphere, and runs off to the sea via rivers, and to lakes and wetlands. The evaporated water supports forests, and other ecosystems. Annually humans withdraw 8% of the total annual renewable fresh water, and about 26% of annual precipitation and 54% of accessible runoff.[129] However traditional water resources are under stress due to growing demand. Today, the production of drinkable water has become a worldwide concern. For many countries, the projected population growth and demand exceed available water resources. Over 1 billion people are without clean drinking water and approximately 2.3 billion people (41% of the world population) live in regions with water shortages.[130,131]

The precise impact of climate change on water resources is uncertain. The United Nations World water development report states that precipitation will probably increase noticeably with a trend towards recurrent extreme weather conditions; it is likely that floods, droughts, mudslides,

and typhoons will increase.[129] Climate change certainly will impact the water quality. Recent estimates suggest that climate change will account for about 20% of the increase in global water scarcity.[129] Additional challenges related to global water scarcity are; (1) health concerns due to water-borne diseases, (2) protecting ecosystems, biodiversity and natural food sources (e.g. fish), (3) increasing rate of urbanization causes pollution diminishing water quality, (4) irrigation for securing food for a growing world population.[129]

The osmotic phenomenon was first observed by Abbe` Nollet in 1748.[132] In 1867 the first semi-permeable membrane was synthesized by Traube.[133] After that, several membrane systems were discovered. The first commercial reverse osmosis units were made available to the public in the mid-1960's and since then the growth of the reverse osmosis industry has become enormous.[134] If a semipermeable membrane separates a solution and a pure solvent, or two solutions of different concentrations, solvent flows from the less concentrated side to the more concentrated side to equalize the concentrations. This phenomenon is called "osmosis". If pressure is exerted against the solution, the rate of flow will reduce and with increasing pressure it will be totally stopped at one point. This equilibrium pressure is called the "osmotic pressure". Further increase in pressure on the solution side forces solvent to flow to the reverse side: from the solution side to the pure solvent side. This phenomenon is called "reverse osmosis".[135] Reverse osmosis has wide application in desalination which is a general term for the process of removing salt from water to produce fresh water (Figure 1.12).

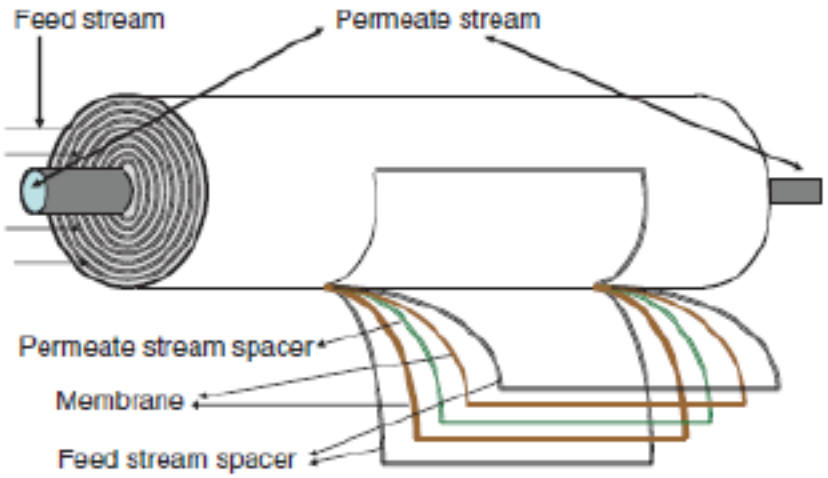


**Figure 1.12.** RO membrane module illustration[199] Robeson, L. M., 8.13 - Polymer Membranes. In *Polymer Science: A Comprehensive Reference*, Matyjaszewski, K.; Möller, M., Eds. Elsevier: Amsterdam, 2012; pp 325-347. Used with permission of Elsevier, 2014.

The RO membranes are comprised of layered, web-like structures. The membrane has a convoluted path through the module for water to reach the permeate side. RO membranes can reject the smallest contaminants such as monovalent ions.[130] Diffusion is the main transport mechanism through RO membranes since membranes have no open channels for water flow. The RO transport mechanism is called a "solution-diffusion mechanism".[130,137-140]

The solution-diffusion model suggests three distinct stages for water transport. The first stage involves the absorption of water onto the membrane surface. In the second step, water diffuses through the membrane with a water concentration gradient within the membrane. This concentration gradient across the membrane induces water diffusion from the high to the low side of the gradient which is the permeate side of the membrane. Finally water desorption takes place from the permeate surface of the membrane.

RO membrane function depends on the hydrostatic pressure exceeding the osmotic pressure of the solution. The pressure difference causes a concentration gradient due to the chemical

potential difference that drives the liquid across the membrane in the opposite direction to osmosis. Upon water transport, the solutes remain behind on the feed water side of the membrane. Some salt may transport depending on concentration and temperature. The following relationship describes the mass transport through RO membranes, where $N_A$ is water flux, L is the permeability coefficient, Δp is the pressure difference, and Δπ is the osmotic pressure difference.[130]

**Equation 1.6.**

$$N_A = L(\Delta p - \Delta \pi)$$

The osmotic pressure (π) depends on the solution concentration and the solution temperature. The relationship below describes the concentration and temperature dependence, where C is the ion concentration (molar), R is the gas constant, and T is the temperature.

**Equation 1.7.**

$$\pi = CRT$$

The membrane characteristics determine the permeability coefficient (L), where D is the water diffusivity, S is the water solubility, V is the water partial molar volume, R is the gas constant, T is the temperature, and l is the membrane thickness. [141,142]

**Equation 1.8.**

$$L = \frac{DSV}{RTl}$$

The osmotic pressure of seawater can be anywhere from 2300 to 3500 kPa.[143] Perry and Green showed the osmotic pressure, π, closely relates to the water recovery ($R_w$), and in order to surpass the osmotic pressure, feed pressures should range from 6000 to 8000 kPa.[143]

**Equation 1.9.**

$$\pi = \frac{1}{1 - R_w}$$

Recovery indicates RO efficiency. The ratio of permeate volumetric flow rate ($Q_P$) to the feed volumetric flow rate ($Q_F$) yields the overall recovery of a RO membrane. Recovery values vary from 35% to 85%, depending on a number of factors including feed composition, feed salinity, and pretreatment. Improved recoveries require increased feed pressure and permeate flux.[144]

**Equation 1.10.**

$$R_W = \frac{Q_P}{Q_F}$$

Baker and colleagues investigated solute flux. Solute flux is an alternative measure of RO performance. Solute transport takes place from a high concentration to low concentration region. Equation 1.11 shows the relationship between solute flux and concentration, where $N_s$ is the solute flux across the membrane, $C_{feed}$ is the ion concentration in the feed solution, and $C_{permeate}$ is the ion concentration in the permeate.[145]

**Equation 1.11.**

$$N_s = B(C_{feed} - C_{permeate})$$

B is a constant based on membrane characteristics. The relationship below shows its dependence on the membrane thickness and solute diffusivity. $D_s$ is the solute diffusivity through the membrane, $K_s$ is the solute partition coefficient between the phases, and l is the membrane thickness.

**Equation 1.12.**

$$B = \frac{D_S - K_S}{l}$$

In summary, RO membranes must meet some criteria for water desalination. First the membrane material must be highly permeable to water, but impermeable to solutes. The membrane must be as thin as possible to maximize water flux, but also it should be thick enough for separation and sufficiently durable to withstand the feed pressure. Lastly, the membrane should be mechanically robust, and chemically inert to resist degradation. In order to meet these requirements researchers studied many polymers for RO membrane applications.

*Cellulosic Membranes*

In the mid-1950s, Reid and colleagues investigated the RO performance of a variety of commercial polymeric films available at the time.[146] They identified cellulose acetate as the most promising membrane material as it exhibited high salt rejection and good chemical stability.[147,148] Reid and coworkers theorized a water transport mechanism in membranes.[147] They claimed that water transported through the membrane via forming hydrogen bonding with carbonyl oxygens in cellulose acetate, and solutes traveled by "hole type diffusion" but that this diffusion process was slow due to small hole size.

In the late 50s, Yuster and others proposed a new approach which involved passing the pressurized solution through a membrane.[133] Later, they discovered that thin asymmetric cellulose acetate membranes had both high water flux and salt rejection. Despite the improved water flux these membranes suffered from limited water flux. Building upon their earlier efforts, Loeb and coworkers developed hand-cast membranes from cellulose acetate solutions in acetone. They immersed the acetone solutions in water which yielded asymmetric membranes.[149]

Manjikian and others made a significant contribution to their predecessors' formulation and casting technique, and they achieved practical membranes with reproducible results.[150] Their research showed that annealing these membranes in hot water improved the properties.[134] The

annealed membranes consisted of a dense skin which served as a barrier and a porous support.[151] An extremely thin surface with a high selectivity towards water have made these membranes commercially viable.[152] However, these membranes had limitations. Annealing improved salt rejection but only to a certain extent. Other disadvantages of these membranes included poor performance for single-pass seawater desalination and loss of water flux with time due to creep under osmotic pressure and membrane fouling.[134] Additionally, cellulose acetate is prone to biodegradation, alkaline degradation, and hydrolytic instability.

*Polyamide Membranes*

In later years, researchers focused on replacing cellulose-based membranes due to their short comings for reverse osmosis application. In the late 1960s, researchers from Dupont developed aromatic polyamides and polyamide-hydrazides that showed potential as RO membranes due to their good mechanical properties.[153] Cadotte and others developed thin film composite membranes in the 1970s.[154,155] Composite membranes were comprised of a polyethylenimine crosslinked with toluene diisocyanate coated on a microporous polysulfone. The first aromatic the polyamide reverse osmosis membranes were prepared via interfacial polymerization that dramatically improved salt rejections and water fluxes.[156] These membranes had good "single-pass" water desalination, excellent resistance to biodegradation, virtually no compaction under high pressure. However, plugging and membrane fouling limited their applications.[157] In the interfacial polymerization method, an aqueous solution of reactive amines is deposited in the pores of a microporous polysulfone support membrane. This amine-loaded support is then immersed in a water-immiscible solvent solution containing aromatic di- and tri-acid chlorides. Upon reaction at the interface an extremely thin, non-porous, dense, highly crosslinked, membrane layer forms. The first interfacial composite membrane was based on polyethylenimine

cross-linked with toluene-2,4-diisocyanate.[156] Highly crosslinked interfacial polymer layer formed on the surface of the support membrane is extremely thin, so it allows high water flux. Due to the crosslinked nature of the film, its selectivity is also high. The first composite asymmetric reverse osmosis membranes were 5–10 times less salt-permeable than the best membranes at the time and composite RO membranes had comparable water fluxes to their predecessors. The state-of-the-art interfacially polymerized polyamide RO membrane was reported in 1980.[158-161] Several monomers are available to produce the aromatic polyamides, but for RO membranes usually phenylene diamines are reacted with various acyl chlorides (Figure 1.13).[162-164] High degree of crosslinking gives state-of-the art material the highest flux and highest rejection. Interfacial polymerization allows that crosslinking occurs simultaneously with polymer film formation at the interface.[164]

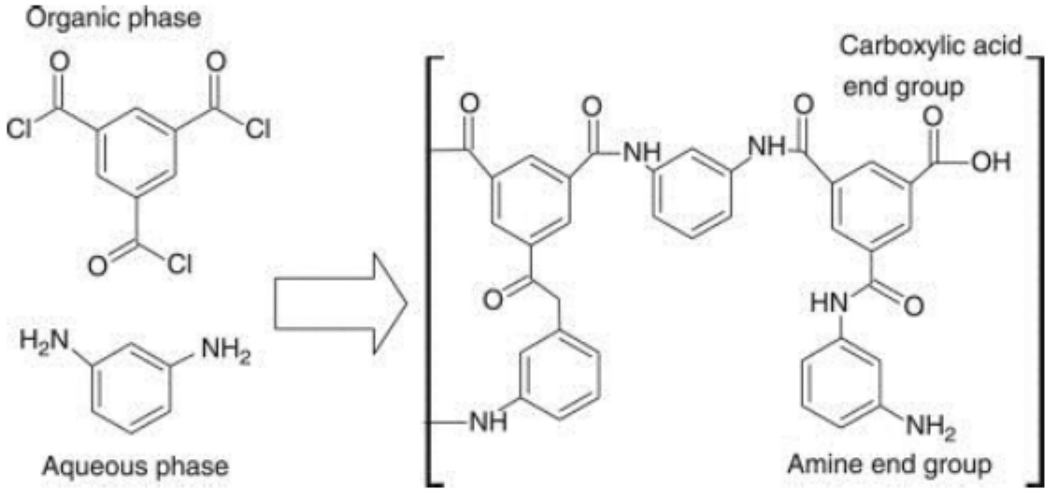


**Figure 1.13.** Polyamide RO membranes[198] Mickols, W. E., 10.41 - Aromatic Poly(amides) for Reverse Osmosis. In *Polymer Science: A Comprehensive Reference*, Matyjaszewski, K.; Möller, M., Eds. Elsevier: Amsterdam, 2012; pp 831-848. Used with permission of Elsevier, 2014.

Over the past three decades, the processing, synthesis and transport properties of these materials have been widely investigated. Further investigation revealed these membranes had

other advantages over their predecessors other than high water permeability, good salt rejection. Aromatic polyamide are more resistant to acid or base induced hydrolysis ,therefore, they can be used at a greater pH range[165]. The high extent of crosslinking reduces swelling and compaction under operating pressures.[166]

Aromatic polyamide films suffer from low chlorine resistance.[157] Kawaguchi and Tamura reported that two chemical processes occur in polyamides including a reversible N-H bond chlorination and irreversible aromatic ring chlorination. They also demonstrated the importance of amide N-H functionality to aromatic ring chlorination. As a result of chlorine substituents on the amide nitrogen or aromatic rings, physical deformation or chemical cleavage at amide linkages in the linear polymer chain can occur.[167]

Several researchers reported performance changes due to chlorine degradation of crosslinked polyamides. Glater *et al.*[168] proposed that flux decline was due to membrane tightening resulting from chlorine substitution, and that the flux increase was due to bond cleavage. A recent report showed that chlorination changed the hydrogen bonding behavior among crosslinked polyamide chains resulting in changes in flexibility of polymer chains followed by deviation from membrane performance. Chlorine concentrations, pH and exposure time affect chlorination of these aromatic polyamides.[169]

The fabrication and performance of polyamide thin film composite membranes greatly improved in the past few decades. Today, nearly all reverse osmosis desalination operations use state of the art polyamide thin film composite membranes. Thin-film composite membranes exhibit high water permeabilities and can reject up to 99.8% of the salts dissolved in the seawater feed. Empirical evidence suggests that it is difficult to further increase the water permeability of these membranes without sacrificing selectivity[136].

Despite such advantages, there are still drawbacks for application. Hollow fiber configurations offer higher packing densities. The polyamide membrane fabrication technique does not extend to hollow fibers. Moreover, the rough surface properties of thin-film composite membranes make them prone to fouling from microorganism/bio growth on the membrane surface and by other impurities in water. This diminishes water flux and overall membrane performance. The susceptibility of the polyamide structure to attack by chlorine requires prevention of the membrane from being exposed to oxidizing agents and increases the operation costs.[136]

*Sulfonated Polysulfone Membranes*

Sulfonated polysulfones are interesting candidates for reverse osmosis membrane materials.[170] Research indicated that sulfonated polysulfone membranes had good acid, alkali and oxidation resistance to oxidizing agents like chlorine.[48] The excellent chlorine resistance of the sulfonated poly(arylene ether sulfone)s compared to current polyamide RO membranes make them attractive candidates compared to aromatic polyamides. Asymmetric semi-permeable membranes were reported from sulfonated poly(arylene ether sulfone)s in 1972.[171] The asymmetric membranes were produced by casting the polymer solutions on glass substrates, then immersing it in a coagulating bath containing a mixture of water, dimethylformamide and NaNO3 and then recovering the membrane. However, precise control of the concentration and location of the sulfonic acid groups were lacking in these polymers due to the post-sulfonation technique utilized for their synthesis, and hence their reproducibility was poor.

McGrath and others developed a "direct copolymerization" synthesis of sulfonated poly(arylene ether sulfone)s using disulfonated activated aromatic dihalide monomers.[59,63-66,172] These aromatic, film-forming copolymers have well-controlled ion concentrations with excellent

oxidative, hydrolytic and mechanical stability. Membranes fabricated from these copolymers have excellent chlorine resistance over a pH range of 4-10. The sulfonated poly(arylene ether sulfone) membrane exposed to chlorine did not show significant change in salt rejection, and this clearly demonstrated its excellent chlorine tolerance relative to conventional desalination membranes. These polymers also exhibit low fouling in oily or protein contaminated water, and high water flux with moderate salt rejection.[173]

### *1.6.2. Gas Separation*

The initial attempts to utilize polymeric membranes for gas separation involved investigation of helium recovery from natural gas.[174] Later research demonstrated the preparation of ultra-thin membranes via coagulation of polymer solutions to yield asymmetric membranes for gas separations.[150] Further efforts revolved around hollow fiber based systems to maximize surface area/volume in membrane modules.[175] Commercial introduction of asymmetric polysulfone hollow fibers for $H_2$ separation from $N_2$ followed which used silicone rubber as a thin permeable film to seal the defects in hollow fibers.[176] The separation of gas mixtures employing polymeric membranes became commercial around the late 1970s.

Gas separation processes utilizing polymer membranes, compared to other techniques such as cryogenic distillation, absorption and pressure-swing adsorption, is a comparatively efficient method. Membrane separation offers the advantage of low energy cost and has a low initial capital expense relative to the more established gas separation processes (e.g. adsorption and cryogenic distillation). With the increased cost of energy, membrane separation is reemerging as an economic option for various gas separations.[177]

Some of the most widely practiced commercial gas separations using membranes include nitrogen from air, recovery of hydrogen from mixtures of nitrogen, methane, and carbon

monoxide, and removal of carbon dioxide from natural gas. Researchers developed membranes with high fluxes and sufficient selectivity to compete with other gas separation technologies. Glassy polymers can provide good materials for gas separation membranes with high selectivities to separate gases based on small differences in size.[178] These polymers are most permeable to the smallest components in a mixture and less permeable to larger components. The Separation of organic vapors from supercritical gases is also an application utilizing membranes.[114] Another application of polymeric gas separation membranes contain the removal of volatile organic compounds (e.g. propylene, ethylene, gasoline from air or nitrogen.[179] The removal of higher hydrocarbons from refinery streams or from natural gas represents promising future applications.[180,181]

In addition to high permeability and selectivity, membranes must also be stable in the industrial process environments, which may be chemically and/or thermally challenging. Due to thermal transition temperatures of polymers used in gas separations, these materials are typically used at or near ambient temperatures.

The following equation describes the relationship between permeability of a polymer film $P_A$ to gas A, where $N_A$ is the gas flux, l is the thickness of the film, $P_{A2}$ and $P_{A1}$ are the upstream and downstream partial pressures of gas A respectively.[114,178,182]

**Equation 1.13.**

$$P_A = \frac{N_A l}{P_{A2} - P_{A1}}$$

Equation 1.14 applies when the downstream pressure is much less than the upstream pressure where $S_A$ is the solubility coefficient and $D_A$ is the diffusion coefficient.[178,182]

**Equation 1.14.**

$$P_A = S_A D_A$$

Equation 1.14 describes the solution-diffusion model of gas transport in polymers.[141] Penetrants first dissolve into the feed side of the film, diffuse through, and desorb at the permeate side of the film. Diffusion is the rate limiting process. As a result, much of the fundamental research related to improvement of membrane gas separation properties focuses on enhancing the diffusion coefficients via systematic modification of polymer chemical structure or processing of polymer membranes.

Polymers separate gas mixtures because of the variations in gas diffusivity and solubility in the membrane. The ability of a polymer to be more permeable to a single component in a mixture relates to a selectivity coefficient which is the ratio of permeabilities of the two components.

**Equation 1.15.**

$$\alpha_{A/B} = \frac{P_A}{P_B} = \frac{D_A S_A}{D_B S_B}$$

Permeation properties vary dramatically from one polymer to another (from glassy to rubbery). Polysulfone membranes are employed for separation of gas mixtures where the more permeable component is the smaller component in the mixture. Examples include air separation, removal of $H_2$ from mixtures with $N_2$, and removal of $CO_2$ from natural gas mixtures.[156,157] This is due to the fact that permeability coefficients generally decrease strongly with increasing penetrant size in the case of polysulfone membranes. Membranes can separate mixture of gases either based on differences in diffusivity or difference in solubility. Research showed that there is a trade-off relationship between permeability and selectivity. Robeson and colleagues recognized an upper bound relationship for the most common gas pairs for different polymeric membranes. They discovered that the log-log plot of permeability coefficient vs. selectivity coefficient (Figure

1.14) showed an upper bound for all polymeric membranes. They published the original paper in 1994[177] and revised it in 2008.[183]

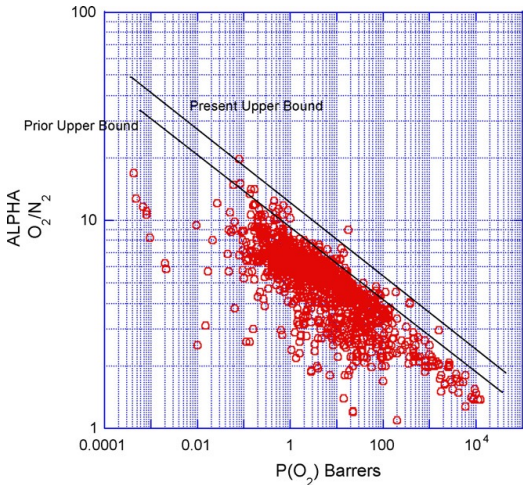


**Figure 1.14.** Updated upper bound relationship for $O_2/N_2$ separation membranes.[183] Robeson, L. M., The upper bound revisited. *J. Membr. Sci.* **2008,** 320, (Copyright (C) 2012 American Chemical Society (ACS). All Rights Reserved.), 390-400. Used with permission of Elsevier, 2014.

### *1.6.3. Separation Membrane Fabrication with Solution Processes*

*Polymer Precipitation by Immersion in a Non-solvent Bath*

This method is the primary way to prepare almost all separation membranes. To prepare a typical membrane film, a ~10-20 wt% casting solution is often used. This solution is cast onto a web, and the cast film is subsequently precipitated by immersion in a water bath. The polymer rapidly precipitates on the surface and forms a dense skin. The skin protects the inner core of the film, letting it precipitate slowly to form a porous substructure. The thickness of the skin of the membranes varies from 0.1 to 1.0 mm depending on the polymer and the casting solution. The original goal to develop this technique was to assemble reverse osmosis membranes,[184] but researchers later adapted such processes to make gas separation membranes.[185,186] The goal is to

make the dense skin as thin as possible, but defect-free. During the process minor defects may occur due to gas bubbles, dust particles, and support fabric imperfections. These defects can diminish the gas separation performance significantly. Research showed that a thin layer of relatively permeable material can seal these defects, and that if the coating is sufficiently thin, it does not change the properties of the underlying permselective layer. It does plug membrane defects, preventing simple convective gas flow through defects.[156,185] This concept has been used to seal defects in polysulfone asymmetric membranes with silicone rubber and it does not significantly restrict permeability, thus improving the overall performance. The polysulfone asymmetric membranes coated with silicone rubber demonstrated this concept. When this coating technique is used, the polysulfone skin layer of the membrane no longer has to be completely free of defects. It also allows the membrane to be produced with a thinner skin. The thinner skin contributes to flux and compensates for the slight reduction due to the presence of the silicone rubber coating.

*Solution-Cast Composite Membranes*

Another important type of composite membrane is formed by solution casting a thin (0.5–2.0 mm) film on a suitable microporous support. Researchers at General Electric and North Star pioneered this research.[187] To prepare membranes using this method, a dilute polymer solution in a volatile, water-immiscible solvent is spread over the surface of a water-filled container. Afterwards, the thin polymer film formed on the water surface is placed on a microporous support. Alternatively, a polymer solution is cast directly onto the microporous support film. The support film must be clean, defect-free, and very finely microporous, to prevent penetration of the coating solution into the pores.

*Interfacially Polymerized Thin Film Composite Membranes*

In the interfacial polymerization method, an aqueous solution of reactive amines is deposited in the pores of a microporous polysulfone support membrane. This amine-loaded support is then immersed in a water-immiscible solvent solution containing aromatic di- and tri-acid chlorides. Upon reaction at the interface an extremely thin, non-porous, densely cross-linked, membrane layer forms. The dense crosslinked polymer layer is extremely thin, so it allows high water flux. Due to the crosslinked nature of the film, its selectivity is also high. In the 1970s the aromatic polyamide reverse osmosis membranes were prepared via interfacial polymerization that dramatically improved salt rejections and water fluxes.[156] The first interfacial composite membrane was based on polyethylenimine cross-linked with toluene-2,4-diisocyanate.[156] Membranes of this kind have a dense, highly crosslinked interfacial polymer layer formed on the surface of the support membrane. The state-of-the-art interfacially polymerized polyamide RO membrane was reported in 1980.[158-161] Several monomers are available to produce the aromatic polyamides, but for RO membranes usually phenylene diamines are reacted with various acyl chlorides.[162-164] High degrees of crosslinking give state-of-the art materials the highest flux and highest rejection. Interfacial polymerization allows for crosslinking to occur simultaneously with polymer film formation at the interface.[164]

### *1.6.4. Photocrosslinked Membrane Designs*

Photopolymerization has found many industrial applications in coatings, adhesives, inks, and printing plates.[188] Industrial UV-curable formulations are mostly radical-initiated unsaturated acrylates and cationically photopolymerized epoxides.[188,189] Photoinitiated curing occurs at room temperature whereas conventional radical (thermal) crosslinking requires elevated temperatures.

Therefore, this advantage makes UV-curing an energy-efficient alternative to thermal curing, and enables applications with large surfaces and temperature sensitive materials.

Photopolymerization refers to a reaction where UV radiation helps to generate the initiating species (Figure 1.15) that are most commonly radicals[189] or cations[190]. Free radical polymerization involves three steps: initiation, propagation, and termination. In the initiation step, a photoinitiator decomposes under UV radiation to generate free radicals. The radical bonds to a monomer and during the propagation steps other monomers are added. The addition of free radicals to the double bond of a monomer generates another radical. Propagation (crosslinking) continues until the active radical is terminated. The most common UV-curable systems are based on multifunctional acrylate oligomers or monomers.

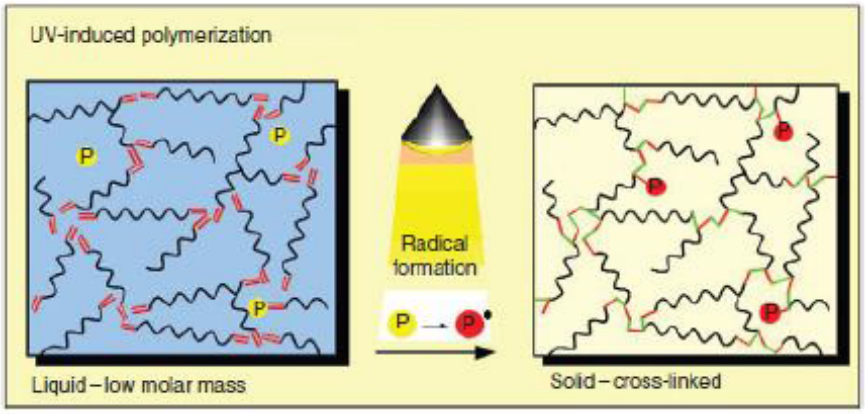


**Figure 1.15.** General Photoinitiated polymerization.[189] Schwalm, R., 10.30 - Radiation-Curing Polymer Systems. In *Polymer Science: A Comprehensive Reference*, Möller, K. M., Ed. Elsevier: Amsterdam, 2012; pp 567-579. Used with permission of Elsevier, 2014

The radiation induces the formation of free radicals, either directly through bond cleavage or indirectly through formation of secondary radicals upon exposure to ultraviolet (UV) irradiation (Figure 1.16).[191] Several different classes of chemicals such as peroxides, disulfides, azo compounds, ketones and aldehydes can form radical species under UV radiation. Aromatic

ketone compounds are among the most common free radical photoinitiators.[191] The initiator efficiency of such ketones was extensively investigated and mechanisms have been elucidated.[192,193] Under exposure to UV radiation, ketone compounds such as 2,2-dimethoxy-2-phenylacetophenone and 1-hydroxycyclohexyl phenyl ketone readily react with acrylates, methacrylates and acrylamides.[194,195] The main UV sources are mercury lamps. The choice of wavelength of UV radiation (UV-A 400-315 nm, UV-B 315-280 nm, UV-C 280-100 nm) depends on the absorption spectrum of the photoinitiator and the oligomer/monomers.[196] For example 2,2-dimethoxy-2phenylacetophenone has the highest UV absorption at 335 nm where it undergoes decomposition to form initiating species.

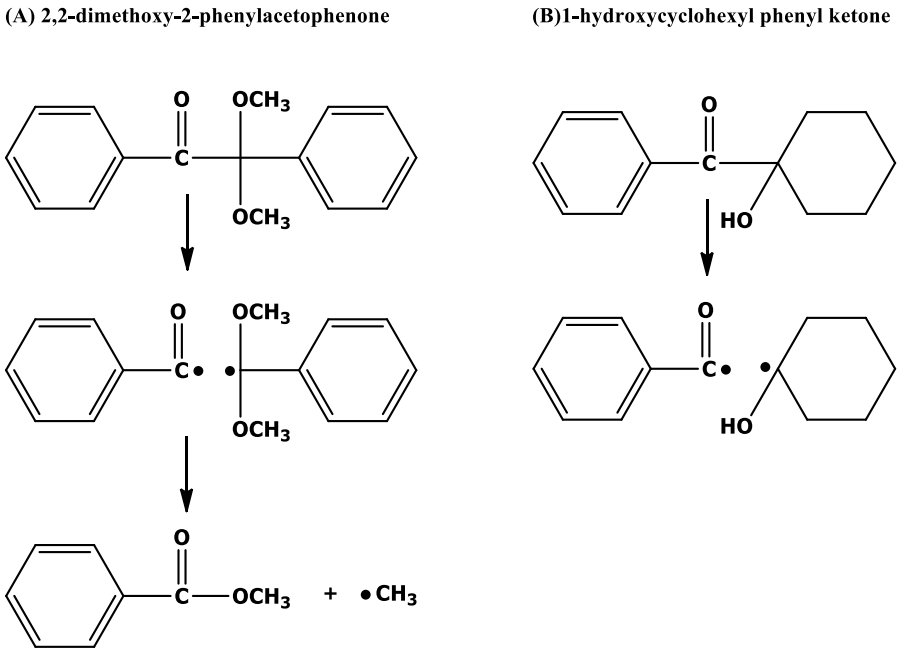


**Figure 1.16.** Formation of initiating species upon bond cleavage (A) 2,2-dimethoxy-2phenylacetophenone (B) 1-hydroxycyclohexyl phenyl ketone

UV crosslinked acrylate-terminated poly(ethylene oxide) (PEO) containing polymers have been identified and extensively investigated as promising membrane material candidates to

selectively permeate $CO_2$.[118-120] Crosslinked membrane designs consisting of UV-crosslinked low molecular weight PEO diacrylates and PEO dimethacrylates are particularly of interest.[113,116,118,121,122] The presence of polar ether oxygens leads to interactions between PEO repeat units and $CO_2$ molecules. Flexible PEO repeat units lack the size sieving separation and this leads to high gas diffusion coefficients. Polar oxygen atoms in the PEO backbone interact favorably with $CO_2$ molecules and thus it enhances solubility in the membranes. These two factors contribute to high diffusion coefficients and high solubility selectivity of $CO_2$ in gas streams.[115,121,123] Crosslinked PEO designs received attention because linear high molecular weight PEO exhibits approximately 12 Barrers of $CO_2$ permeability at 35 ºC[118] whereas $CO_2$ permeability can be as high as 570 Barrers at 35 ºC[123] in crosslinked PEO membranes. This vast difference is due to high crystallinity. Dense crystalline domains in PEO reduce $CO_2$ permeability. Moreover crystalline domains reduce mobility of amorphous regions that reduces $CO_2$ permeability.[118] The influence of crosslink density of PEO-containing networks has been studied.[197] A systematic series of PEO diacrylate and PEO methyl ether acrylates were crosslinked under UV radiation for 90s at 3 $mW/cm^2$. The 1-hydroxycyclohexyl phenyl ketone (Figure 1.16 B) photoinitiator content was kept at 0.1 wt% of the monomer to avoid any significant modifications in the network chemical structure. Wide-angle X-ray diffraction analysis showed a very broad 2θ peak instead of sharp multiple 2θ peaks characteristic of semi-crystalline PEO that suggested crosslinking successfully prevented crystallization. DSC thermograms revealed that the $T_g$'s of these amorphous networks were not dependent on the crosslink density as all samples displayed $T_g$'s of -41 to -42 ºC. The gas transport properties were measured. Interestingly permeability, selectivity, and network $T_g$'s of these membranes was independent of the network crosslink density. It was concluded that the gas diffusion and

permeation depended more on the network $T_g$ than the network crosslink density. In a similar attempt, PEO dimethacrylate were UV crosslinked with a comonomer that contains a methacrylate group on one end and bulky trimethylsiloxane units on the other.[118] Two crosslinking monomers were miscible and formed homogeneous crosslinked films as characterized by single $T_g$'s observed in DSC thermograms. The network density and fractional free volume increased with increasing siloxane monomer as a result of introduction of the flexible comonomer and a decrease in the crosslink density of the network.[118] As predicted, the gas permeability of such membranes increased with increase in the fractional free volume. $CO_2$ permeability improved with the comonomer content but due to the tradeoff relationship, membrane selectivity suffered with increased permeability. Due to unique molecular interactions between PEO repeat units and $CO_2$ molecules, $CO_2$ permeability was the highest (order of permeability $CO_2 > H_2 > CH_4 \approx O_2 > N_2$ ) among the gases tested.[118] To summarize, PEO allows for membranes that selectively permeate $CO_2$ while retaining the light gases such as $H_2$, $O_2$ and $N_2$. Carefully engineered membranes prepared by UV crosslinking of PEO acrylates and methacrylates may find applications in $CO_2$ removal from natural gas, and $H_2$ purification in the industry.

## 1.7. References:


1. Johnson, R. N.; Farnham, A. G.; Clendinning, R. A.; Hale, W. F.; Merriam, C. N., Poly(aryl ethers) by nucleophilic aromatic substitution. I. Synthesis and properties. *Journal of Polymer Science Part A-1: Polymer Chemistry* **1967,** 5, (9), 2375-2398.
2. Rose, J. B., Preparation and properties of poly(arylene ether sulphones). *Polymer* 1974, 15, (7), 456-465.
3. Hale, W. F.; Farnham, A. G.; Johnson, R. N.; Clendinning, R. A., Poly(Aryl ethers) by nucleophilic aromatic substitution. II. Thermal stability. *Journal of Polymer Science Part A-1: Polymer Chemistry* 1967, 5, (9), 2399-2414.
4. Wu, Z.; Zheng, Y.; Yan, H.; Nakamura, T.; Nozawa, T.; Yosomiya, R., Molecular aggregation of PEEK with PES [polyethersulfone] blends and the block copolymers composed of PEEK and PES components. *Angew. Makromol. Chem.* 1989, 173, (Copyright (C) 2012 American Chemical Society (ACS). All Rights Reserved.), 163-81.
5. Dumais, J. J.; Cholli, A. L.; Jelinski, L. W.; Hedrick, J. L.; McGrath, J. E., Molecular basis of the β-transition in poly(arylene ether sulfones). *Macromolecules* 1986, 19, (Copyright (C) 2012 American Chemical Society (ACS). All Rights Reserved.), 1884-9.
6. Robeson, L. M.; Farnham, A. G.; McGrath, J. E., Synthesis and dynamic mechanical characteristics of poly(aryl ethers). *Appl. Polym. Symp.* 1975, 26, (Copyright (C) 2012 American Chemical Society (ACS). All Rights Reserved.), 373-85.
7. Robeson, L. M.; Farnham, A. G.; McGrath, J. E., Dynamic mechanical characteristics of polysulfone and other poly(arylethers). *Midl. Macromol. Monogr.* 1978, 4, (Copyright (C) 2012 American Chemical Society (ACS). All Rights Reserved.), 405-25.
8. Robeson, L. M.; Crisafulli, S. T., Microcavity formation in engineering polymers exposed to hot water. *J. Appl. Polym. Sci.* 1983, 28, (Copyright (C) 2012 American Chemical Society (ACS). All Rights Reserved.), 2925-36.
9. Kambour, R. P.; Romagosa, E. E.; Gruner, C. L., Swelling, crazing, and cracking of an aromatic copolyether-sulfone in organic media. *Macromolecules* 1972, 5, (Copyright (C) 2012 American Chemical Society (ACS). All Rights Reserved.), 335-40.
10. Leslie, V. J. Polysulfone solutions. GB1405052A, 1975.
11. Attwood, T. E.; King, T.; Leslie, V. J.; Rose, J. B., Poly(arylene ether sulfones) by polyetherification. 4. Physical properties in relation to molecular structure. *Polymer* 1977, 18, (Copyright (C) 2012 American Chemical Society (ACS). All Rights Reserved.), 369-74.
12. El-Hibri, M. J., Polymers Containing Sulfur, Polysulfones. In Kirk-Othmer Encyclopedia of Chemical Technology, John Wiley & Sons, Inc.: 2000.
13. Ghosal, K.; Chern, R. T.; Freeman, B. D., Gas permeability of Radel A polysulfone. *J. Polym. Sci., Part B: Polym. Phys*. 1993, 31, (Copyright (C) 2012 American Chemical Society (ACS). All Rights Reserved.), 891-3.
14. McHattie, J. S.; Koros, W. J.; Paul, D. R., Gas transport properties of polysulphones: 2. Effect of bisphenol connector groups. Polymer 1991, 32, (Copyright (C) 2012 American Chemical Society (ACS). All Rights Reserved.), 2618-25.
15. Mohr, J. M.; Paul, D. R.; Tullos, G. L.; Cassidy, P. E., Gas transport properties of a series of poly(ether ketone) polymers. Polymer 1991, 32, (Copyright (C) 2012 American Chemical Society (ACS). All Rights Reserved.), 2387-94.

16. McHattie, J. S.; Koros, W. J.; Paul, D. R., Gas transport properties of polysulfones. 1. Role of symmetry of methyl group placement on bisphenol. Polymer 1991, 32, (Copyright (C) 2012 American Chemical Society (ACS). All Rights Reserved.), 840-50.
17. McGrath, J. E., Wang, S., Polyarylene Ethers": A Review. In Step Polymerization, Long, T. E., Rogers M., Ed. Wiley: 2002.
18. Farnham, A. G.; Johnson, R. N. Polyarylene polyethers. US3332909, 1967.
19. Jurek, M. J.; McGrath, J. E., The synthesis of poly(arylene ethers) via the Ullmann condensation reaction. Polym. Prepr. (Am. Chem. Soc., Div. Polym. Chem.) 1987, 28, (Copyright (C) 2012 American Chemical Society (ACS). All Rights Reserved.), 180-2.
20. Jennings, B. E.; Jones, M. E. B.; Rose, J. B., Synthesis of poly(arylene sulfones) and poly(arylene ketones) by reactions involving substitution at aromatic nuclei. J. Polym. Sci., Polym. Symp. 1967, 16, (Copyright (C) 2012 American Chemical Society (ACS). All Rights Reserved.), 715-24.
21. Stamatoff, G. S. Halogenated polyphenylene ethers. GB1053638, 1967.
22. Burgoyne, W. F., Jr.; Vrtis, R. N.; Robeson, L. M. Nonhalogenated poly(arylene ethers) for dielectric insulating layers. EP755957A1, 1997.
23. Phillips, R. W.; Sheares, V. V.; Samulski, E. T.; DeSimone, J. M. *Isomeric poly(benzophenone)s: synthesis of highly crystalline poly(4,4'-benzophenone) and amorphous poly(2,5-benzophenone), a soluble poly(p-phenylene) derivative*; North Carolina Univ.: 1994; p 14 pp.
24. Pei, J.; Yu, W.-L.; Ni, J.; Lai, Y.-H.; Huang, W.; Heeger, A. J., Thiophene-Based Conjugated Polymers for Light-Emitting Diodes: Effect of Aryl Groups on Photoluminescence Efficiency and Redox Behavior. *Macromolecules* **2001,** 34, (Copyright (C) 2012 American Chemical Society (ACS). All Rights Reserved.), 7241-7248.
25. Ghassemi, H.; McGrath, J. E. In *Proton-conducting polymers derived from poly(p-phenylene)s*, 2002; American Chemical Society: 2002; pp POLY-274.
26. Colon, I.; Kwiatkowski, G. T., High-molecular-weight aromatic polymers by nickel coupling of aryl polychlorides. *J. Polym. Sci., Part A: Polym. Chem.* **1990,** 28, (Copyright (C) 2012 American Chemical Society (ACS). All Rights Reserved.), 367-83.
27. Colon, I.; Maresca, L. M.; Kwiatkowski, G. T. Coupling of aryl and heteroaryl polyhalides. EP25460A1, 1981.
28. Havelka-Rivard, P. A.; Nagai, K.; Freeman, B. D.; Sheares, V. V., Synthesis and Characterization of Poly[[1,1'-biphenyl]-4,4'-diyl[2,2,2-trifluoro-1-(trifluoromethyl)ethylidene]]. *Macromolecules* **1999,** 32, (20), 6418-6424.
29. Olah, G. A.; Kobayashi, S.; Nishimura, J., Aromatic substitution. XXXI. Friedel-Crafts sulfonylation of benzene and toluene with alkyl- and arylsulfonyl halides and anhydrides. *J. Amer. Chem. Soc.* **1973,** 95, (Copyright (C) 2012 American Chemical Society (ACS). All Rights Reserved.), 564-9.
30. Bassin, J. P., Cremlyn, R.J., Swinbourne, F.J, Chlorosulfonation of Aromatic and Heteroaromatic Systems. *Phosphorus Sulfur and Silicon and the Related Elements* **1991,** 56, (1-4), 245.
31. Johnson, R. N.; Farnham, A. G., Poly(aryl ethers) by nucleophilic aromatic substitution. III. Hydrolytic side reactions. *J. Polym. Sci., Part A-1: Polym. Chem.* **1967,** 5, (Copyright (C) 2012 American Chemical Society (ACS). All Rights Reserved.), 2515-27.

32. Bunnett, J. F.; Zahler, R. E., Aromatic nucleophilic substitution reactions. *Chem. Rev. (Washington, DC, U. S.)* **1951,** 49, (Copyright (C) 2012 American Chemical Society (ACS). All Rights Reserved.), 273-412.
33. Meisenheimer, J., Ueber Reactionen aromatischer Nitrokörper. *Justus Liebigs Annalen der Chemie* **1902,** 323, (2), 205-246.
34. March, J., *Advanced Organic Chemistry: Reactions, Mechanisms, and Structure. 2nd Ed*. McGraw-Hill: 1977; p 1328 pp.
35. Freire, H. R.; Miller, J., The SN mechanism in aromatic compounds. Part 42. Para-substituent effects of some groups with C:N function joined to the ring. A possible inverse α-effect. *J. Chem. Soc., Perkin Trans. 2* **1978**, (Copyright (C) 2012 American Chemical Society (ACS). All Rights Reserved.), 108-11.
36. Schulze, S. R.; Baron, A. L., Kinetics of solution polycondensation of aromatic polyethers. *Advan. Chem. Ser.* **1969,** No. 91, (Copyright (C) 2012 American Chemical Society (ACS). All Rights Reserved.), 692-702.
37. Alexander, R.; Ko, E. C. F.; Parker, A. J.; Broxton, T. J., Solvation of ions. XIV. Protic-dipolar aprotic solvent effects on rates of bimolecular reactions. Solvent activity coefficients of reactants and transition states at 25.deg. *J. Amer. Chem. Soc.* **1968,** 90, (Copyright (C) 2012 American Chemical Society (ACS). All Rights Reserved.), 5049-69.
38. Fuchs, R.; Cole, L. L., Transition state enthalpies of transfer in the reaction of nucleophiles with n-hexyl tosylate. *J. Amer. Chem. Soc.* **1973,** 95, (Copyright (C) 2012 American Chemical Society (ACS). All Rights Reserved.), 3194-7.
39. Johnson, R. N.; Farnham, A. G.; Clendinning, R. A.; Hale, W. F.; Merriam, C. N., Poly(aryl ethers) by nucleophilic aromatic substitution. I. Synthesis and properties. *Journal of Polymer Science: Part A Polymer Chemistry* **1967,** 5, 2375-2398.
40. Cotter, R. J., Engineering Plastics, A Handbook of Polyarylethers. Overseas Publishers Association: 1995.
41. Newton, A. B.; Rose, J. B., Relative reactivities of the functional groups involved in synthesis of poly(phenylene ether sulfones) from halogenated derivatives of diphenyl sulfone. *Polymer* 1972, 13, (Copyright (C) 2012 American Chemical Society (ACS). All Rights Reserved.), 465-74.
42. Viswanathan, R.; Johnson, B. C.; McGrath*, J. E., Synthesis, kinetic observations and characteristics of polyarylene ether sulphones prepared via a potassium carbonate DMAC process. In *Polymer*, 1984; Vol. 25, pp 1827-1836.
43. Hedrick, J. L.; Mohanty, D. K.; Johnson, B. C.; Viswanathan, R.; Hinkley, J. A.; McGrath, J. E., Radiation resistant amorphous–all aromatic polyarylene ether sulfones: Synthesis, characterization, and mechanical properties. Journal of Polymer Science Part A: Polymer Chemistry 1986, 24, (2), 287-300.
44. Priddy, D. Ph.D. Thesis. Ph.D. Thesis, VPI&SU, 1994.
45. Harrison, W. L. Synthesis and characterization of sulfonated poly(arylene ether sulfone) copolymers via direct copolymerization: candidates for proton exchange membrane fuel cells. VPI&SU, Virginia, 2002.
46. Smitha, B.; Sridhar, S.; Khan, A. A., Solid polymer electrolyte membranes for fuel cell applications - a review. J. Membr. Sci. 2005, 259, (Copyright (C) 2012 American Chemical Society (ACS). All Rights Reserved.), 10-26.

47. Kucera, F.; Jancar, J., Homogeneous and heterogeneous sulfonation of polymers: a review. Polym. Eng. Sci. 1998, 38, (Copyright (C) 2012 American Chemical Society (ACS). All Rights Reserved.), 783-792.
48. Quentin, J. P.; Ruaud, M. Anion exchange membranes from copolymers of vinyl alcohol and nitrated vinyl monomers. FR1588980, 1970.
49. Genova-Dimitrova, P.; Baradie, B.; Foscallo, D.; Poinsignon, C.; Sanchez, J. Y., Ionomeric membranes for proton exchange membrane fuel cell (PEMFC): sulfonated polysulfone associated with phosphatoantimonic acid. J. Membr. Sci. 2001, 185, (Copyright (C) 2012 American Chemical Society (ACS). All Rights Reserved.), 59-71.
50. Bailly, C.; Williams, D. J.; Karasz, F. E.; MacKnight, W. J., The sodium salts of sulfonated poly(aryl-ether-ether-ketone) (PEEK): preparation and characterization. Polymer 1987, 28, (Copyright (C) 2012 American Chemical Society (ACS). All Rights Reserved.), 1009-16.
51. Johnson, B. C.; Yilgor, I.; Tran, C.; Iqbal, M.; Wightman, J. P.; Lloyd, D. R.; McGrath, J. E., Synthesis and characterization of sulfonated poly(arylene ether sulfones). J. Polym. Sci., Polym. Chem. Ed. 1984, 22, (Copyright (C) 2012 American Chemical Society (ACS). All Rights Reserved.), 721-37.
52. Noshay, A.; Robeson, L. M., Sulfonated polysulfone. J. Appl. Polym. Sci. 1976, 20, (Copyright (C) 2012 American Chemical Society (ACS). All Rights Reserved.), 1885-903.
53. Litter, M. I.; Marvel, C. S., Polyaromatic ether-ketones and polyaromatic ether-ketone sulfonamides from 4-phenoxybenzoyl chloride and from 4,4'-dichloroformyldiphenyl ether. J. Polym. Sci., Polym. Chem. Ed. 1985, 23, (Copyright (C) 2012 American Chemical Society (ACS). All Rights Reserved.), 2205-23.
54. Liu, B.; Robertson, G. P.; Kim, D.-S.; Guiver, M. D.; Hu, W.; Jiang, Z., Aromatic Poly(ether ketone)s with Pendant Sulfonic Acid Phenyl Groups Prepared by a Mild Sulfonation Method for Proton Exchange Membranes. Macromolecules (Washington, DC, U. S.) 2007, 40, (Copyright (C) 2012 American Chemical Society (ACS). All Rights Reserved.), 1934-1944.
55. Le, N. C.; Balland-Longeau, A.; Demattei, D.; Palmas, P.; Saillard, J.; Coutanceau, C.; Lamy, C.; Leger, J. M., Determination of the physicochemical characteristics and electrical performance of post-sulfonated and grafted sulfonated derivatives of poly(para-phenylene) as new proton-conducting membranes for direct methanol fuel cell. J. Appl. Polym. Sci. 2006, 101, (Copyright (C) 2012 American Chemical Society (ACS). All Rights Reserved.), 944-952.
56. Bishop, M. T.; Karasz, F. E.; Russo, P. S.; Langley, K. H., Solubility and properties of a poly(aryl ether ketone) in strong acids. Macromolecules 1985, 18, (Copyright (C) 2012 American Chemical Society (ACS). All Rights Reserved.), 86-93.
57. Nolte, R.; Ledjeff, K.; Bauer, M.; Muelhaupt, R., Partially sulfonated poly(arylene ether sulfone) - a versatile proton conducting membrane material for modern energy conversion technologies. J. Membr. Sci. 1993, 83, (Copyright (C) 2012 American Chemical Society (ACS). All Rights Reserved.), 211-20.
58. Kerres, J.; Cui, W.; Reichle, S., New sulfonated engineering polymers via the metalation route. I. Sulfonated poly(ether sulfone) PSU Udel via metalation-sulfination-oxidation. J. Polym. Sci., Part A: Polym. Chem. 1996, 34, (Copyright (C) 2012 American Chemical Society (ACS). All Rights Reserved.), 2421-2438.

59. Hickner, M. A.; Ghassemi, H.; Kim, Y. S.; Einsla, B. R.; McGrath, J. E., Alternative Polymer Systems for Proton Exchange Membranes (PEMs). Chem. Rev. (Washington, DC, U. S.) 2004, 104, (Copyright (C) 2012 American Chemical Society (ACS). All Rights Reserved.), 4587-4611.
60. Robeson, L. M.; Matzner, M. Flame retardant polyarylate compositions. EP58403A2, 1982.
61. Ueda, M.; Toyota, H.; Ouchi, T.; Sugiyama, J.; Yonetake, K.; Masuko, T.; Teramoto, T., Synthesis and characterization of aromatic poly(ether sulfone)s containing pendent sodium sulfonate groups. J. Polym. Sci., Part A: Polym. Chem. 1993, 31, (Copyright (C) 2012 American Chemical Society (ACS). All Rights Reserved.), 853-8.
62. Genies, C.; Mercier, R.; Sillion, B.; Petiaud, R.; Cornet, N.; Gebel, G.; Pineri, M., Stability study of sulfonated phthalic and naphthalenic polyimide structures in aqueous medium. Polymer 2001, 42, (Copyright (C) 2012 American Chemical Society (ACS). All Rights Reserved.), 5097-5105.
63. Wang, F.; Hickner, M.; Kim, Y. S.; Zawodzinski, T. A.; McGrath, J. E., Direct polymerization of sulfonated poly(arylene ether sulfone) random (statistical) copolymers: candidates for new proton exchange membranes. J. Membr. Sci. 2002, 197, (Copyright (C) 2012 American Chemical Society (ACS). All Rights Reserved.), 231-242.
64. Kim, Y. S.; Hickner, M. A.; Dong, L.; Pivovar, B. S.; McGrath, J. E., Sulfonated poly(arylene ether sulfone) copolymer proton exchange membranes: composition and morphology effects on the methanol permeability. J. Membr. Sci. 2004, 243, (Copyright (C) 2012 American Chemical Society (ACS). All Rights Reserved.), 317-326.
65. Harrison, W. L.; Hickner, M. A.; Kim, Y. S.; McGrath, J. E., Poly(arylene ether sulfone) copolymers and related systems from disulfonated monomer building blocks: synthesis, characterization, and performance - a topical review. Fuel Cells (Weinheim, Ger.) 2005, 5, (Copyright (C) 2012 American Chemical Society (ACS). All Rights Reserved.), 201-212.
66. Sankir, M.; Bhanu, V. A.; Harrison, W. L.; Ghassemi, H.; Wiles, K. B.; Glass, T. E.; Brink, A. E.; Brink, M. H.; McGrath, J. E., Synthesis and characterization of 3,3'-disulfonated-4,4'-dichlorodiphenyl sulfone (SDCDPS) monomer for proton exchange membranes (PEM) in fuel cell applications. J. Appl. Polym. Sci. 2006, 100, (Copyright (C) 2012 American Chemical Society (ACS). All Rights Reserved.), 4595-4602.
67. Wang, F.; Kim, Y.; Hickner, M.; Zawodzinski, T. A.; McGrath, J. E., Synthesis of polyarylene ether block copolymers containing sulfonate groups. *Polym. Mater. Sci. Eng.* **2001,** 85, (Copyright (C) 2012 American Chemical Society (ACS). All Rights Reserved.), 517-518.
68. Wang, F.; Kim, Y.; Hickner, M. A.; Zawodzinski, T. A.; McGrath, J. E. In *Synthesis of polyarylene ether block copolymers containing sulfonate groups*, 2001; American Chemical Society: 2001; pp PMSE-309.
69. Li, Y.; VanHouten, R. A.; Brink, A. E.; McGrath, J. E., Purity characterization of 3,3′-disulfonated-4,4′-dichlorodiphenyl sulfone (SDCDPS) monomer by UV–vis spectroscopy. *Polymer* **2008,** 49, (13–14), 3014-3019.
70. Wurtz, Chemistry. *Cambridge review* **1879,** 1, 159.
71. Dimitrov, I.; Tsvetanov, C. B., 4.21 - High-Molecular-Weight Poly(ethylene oxide). In *Polymer Science: A Comprehensive Reference*, Editors-in-Chief: Krzysztof, M.; Martin, M., Eds. Elsevier: Amsterdam, 2012; pp 551-569.

72. Staudinger, H.; Schweitzer, O., Highly polymerized compounds. H. Staudinger XX. Polyethylene oxides. *Ber. Dtsch. Chem. Ges. B* **1929,** 62B, (Copyright (C) 2012 American Chemical Society (ACS). All Rights Reserved.), 2395-405.
73. Flory, P. J., Molecular size distribution in ethylene oxide polymers. J. Am. Chem. Soc. 1940, 62, (Copyright (C) 2012 American Chemical Society (ACS). All Rights Reserved.), 1561-5.
74. Hill, F. N.; Fitzpatrick, J. T.; Bailey, F. E., Jr. Bivalent metal amide-alcoholate catalysts f or polymerizing epoxides. GB839171, 1960.
75. Ishii, Y.; Sakai, S. In 1,2 Epoxides, 1969; Marcel Dekker: 1969; pp 13-109.
76. Pruitt, M. E.; Baggett, J. M. Solid polymers of propylene oxide. US2706189, 1955.
77. Dimitrov, I.; Tsvetanov, C. B., 4.27 - Oligomeric Poly(ethylene oxide)s. Functionalized Poly(ethylene glycol)s. PEGylation. In *Polymer Science: A Comprehensive Reference*, Editors-in-Chief: Krzysztof, M.; Martin, M., Eds. Elsevier: Amsterdam, 2012; pp 679-693.
78. Pell, A. S.; Pilcher, G., Measurements of heats of combustion by flame calorimetry. III. Ethylene oxide, trimethyl oxide, tetrahydrofuran, and tetrahydropyran. *Trans. Faraday Soc.* **1965,** 61, (Copyright (C) 2012 American Chemical Society (ACS). All Rights Reserved.), 71-77.
79. Kubisa, P., 4.08 - Cationic Ring-Opening Polymerization of Cyclic Ethers. In *Polymer Science: A Comprehensive Reference*, Editors-in-Chief: Krzysztof, M.; Martin, M., Eds. Elsevier: Amsterdam, 2012; pp 141-164.
80. Sawada, H., Thermochemistry of polymerization. III. Thermochemical aspects of propagation of polymerization. *J. Polym. Sci., Part A: Gen. Pap.* **1965,** 3, (Copyright (C) 2012 American Chemical Society (ACS). All Rights Reserved.), 3929-34.
81. Sawada, H., Thermodynamics of polymerization. IV. Free energy changes of binary copolymerization systems. *J. Polym. Sci., Part A-1: Polym. Chem.* **1967,** 5, (Copyright (C) 2012 American Chemical Society (ACS). All Rights Reserved.), 1383-90.
82. Deffieux, A.; Carlotti, S.; Barrère, A., 4.07 - Anionic Ring-Opening Polymerization of Epoxides and Related Nucleophilic Polymerization Processes. In *Polymer Science: A Comprehensive Reference*, Editors-in-Chief: Krzysztof, M.; Martin, M., Eds. Elsevier: Amsterdam, 2012; pp 117-140.
83. Nenna, S.; Figueruelo, J. E., Caesium as counter-ion in the anionic polymerization of ethylene oxide—II: Kinetics in hmpt. *European Polymer Journal* **1975,** 11, (7), 511-513.
84. Price, C. C.; Carmelite, D. D., Reactions of epoxides in dimethyl sulfoxide catalyzed by potassium tert-butoxide. *J. Am. Chem. Soc.* **1966,** 88, (Copyright (C) 2012 American Chemical Society (ACS). All Rights Reserved.), 4039-44.
85. Solov'yanov, A. A.; Kazanskii, K. S., Reactivity of ions and ion pairs during the initiation of ethylene oxide polymerization. *Vysokomol. Soedin., Ser. A* **1974,** 16, (Copyright (C) 2012 American Chemical Society (ACS). All Rights Reserved.), 595-9.
86. Boileau, S.; Deffieux, A.; Lassalle, D.; Menezes, F.; Vidal, B., Reactivities of anionic species for the ring opening of ethylene oxide. *Tetrahedron Letters* **1978,** 19, (20), 1767-1770.
87. Deffieux, A.; Boileau, S., Anionic polymerization of ethylene oxide with cryptates as counterions: 1. *Polymer* **1977,** 18, (10), 1047-1050.
88. Deffieux, A.; Graf, E.; Boileau, S., Anionic polymerization of ethylene oxide with cryptates as counterions: 2. *Polymer* **1981,** 22, (4), 549-552.

89. Kuran, W., Coordination polymerization of heterocyclic and heterounsaturated monomers. *Progress in Polymer Science* **1998,** 23, (6), 919-992.
90. Ebert, P. E.; Price, C. C., Polyethers. VI. Aluminum alkyls as catalysts for polymerization of propylene oxide. *Journal of Polymer Science* **1959,** 34, (127), 157-160.
91. Garty, K. T.; Gibb, T. B., Jr.; Clendenning, R. A., Cocatalysts for the linear polymerization of epoxides by di-butylzinc. *J. Polym. Sci.* **1963,** Pt. A 1, (Copyright (C) 2012 American Chemical Society (ACS). All Rights Reserved.), 85-102.
92. Booth, C.; Higginson, W. C. E.; Powell, E., Polymerization of propylene oxide catalyzed by diethylzinc and water. *Polymer* **1964,** 5, (Copyright (C) 2012 American Chemical Society (ACS). All Rights Reserved.), 479-97.
93. Ueyama, N.; Araki, T.; Tani, H., Behavior of the bis(dialkylaluminum) oxide (R2AlOAlR2) catalyst in the polymerization of propylene oxide. *Macromolecules* **1974,** 7, (Copyright (C) 2012 American Chemical Society (ACS). All Rights Reserved.), 153-60.
94. Vandenberg, E. J., Organometallic catalysts for polymerizing monosubstituted epoxides. *J. Polym. Sci.* **1960,** 47, (Copyright (C) 2012 American Chemical Society (ACS). All Rights Reserved.), 486-9.
95. Imai, H.; Saegusa, T.; Furukawa, J., Polymerization of alkylene oxide by triethylaluminum-water-amine systems. *Makromol. Chem.* **1965,** 82, (Copyright (C) 2012 American Chemical Society (ACS). All Rights Reserved.), 25-31.
96. Vandenberg, E. J., Epoxide polymers: synthesis, stereochemistry, structure, and mechanism. *J. Polym. Sci., Part A-1: Polym. Chem.* **1969,** 7, (Copyright (C) 2012 American Chemical Society (ACS). All Rights Reserved.), 525-67.
97. Tsuruta, T., Stereoselective and asymmetric-selective (or stereoelective) polymerizations. *Journal of Polymer Science: Macromolecular Reviews* **1972,** 6, (1), 179-250.
98. Ishimori, M.; Hsiue, G.; Tsuruta, T., Organometallic compounds as polymerization catalysts. IV. Polymerization of propylene oxide catalyzed by zinc chloride-alkali metal alkoxide systems. *Makromol. Chem.* **1969,** 124, (Copyright (C) 2012 American Chemical Society (ACS). All Rights Reserved.), 143-51.
99. Aida, T.; Inoue, S., Living polymerization of epoxide catalyzed by the porphyrin-chlorodiethylaluminum system. Structure of the living end. *Macromolecules* **1981,** 14, (Copyright (C) 2012 American Chemical Society (ACS). All Rights Reserved.), 1166-9.
100. Aida, T.; Inoue, S., Metalloporphyrins as Initiators for Living and Immortal Polymerizations. *Acc. Chem. Res.* **1996,** 29, (Copyright (C) 2012 American Chemical Society (ACS). All Rights Reserved.), 39-48.
101. Aida, T.; Maekawa, Y.; Asano, S.; Inoue, S., Immortal polymerization: polymerization of epoxide and β-lactone with aluminum porphyrin in the presence of protic compound. *Macromolecules* **1988,** 21, (Copyright (C) 2012 American Chemical Society (ACS). All Rights Reserved.), 1195-202.
102. Aida, T.; Mizuta, R.; Yoshida, Y.; Inoue, S., Polymerization of epoxides catalyzed by metalloporphine. *Makromol. Chem.* **1981,** 182, (Copyright (C) 2012 American Chemical Society (ACS). All Rights Reserved.), 1073-9.
103. Asano, S.; Aida, T.; Inoue, S., 'Immortal' polymerization. Polymerization of epoxide catalyzed by an aluminum porphyrin-alcohol system. *J. Chem. Soc., Chem. Commun.* **1985**, (Copyright (C) 2012 American Chemical Society (ACS). All Rights Reserved.), 1148-9.

104. Sugimoto, H.; Kawamura, C.; Kuroki, M.; Aida, T.; Inoue, S., Lewis Acid-Assisted Anionic Ring-Opening Polymerization of Epoxide by the Aluminum Complexes of Porphyrin, Phthalocyanine, Tetraazaannulene, and Schiff Base as Initiators. *Macromolecules* **1994,** 27, (Copyright (C) 2012 American Chemical Society (ACS). All Rights Reserved.), 2013-18.
105. Sugimoto, H.; Aida, T.; Inoue, S., Ring-opening polymerizations of lactone and epoxide initiated with aluminum complexes of substituted tetraphenylporphyrins. Molecular design of highly active initiators. *Macromolecules* **1990,** 23, (Copyright (C) 2012 American Chemical Society (ACS). All Rights Reserved.), 2869-75.
106. Abetz, V.; Brinkmann, T.; Dijkstra, M.; Ebert, K.; Fritsch, D.; Ohlrogge, K.; Paul, D.; Peinemann, K. V.; Pereira-Nunes, S.; Scharnagl, N.; Schossig, M., Developments in Membrane Research: from Material via Process Design to Industrial Application. *Advanced Engineering Materials* **2006,** 8, (5), 328-358.
107. Ostuni, E.; Chapman, R. G.; Holmlin, R. E.; Takayama, S.; Whitesides, G. M., A Survey of Structure−Property Relationships of Surfaces that Resist the Adsorption of Protein. *Langmuir* **2001,** 17, (18), 5605-5620.
108. Shannon, M. A.; Bohn, P. W.; Elimelech, M.; Georgiadis, J. G.; Marinas, B. J.; Mayes, A. M., Science and technology for water purification in the coming decades. *Nature* **2008,** 452, (Copyright (C) 2012 U.S. National Library of Medicine.), 301-10.
109. Kang, S.; Asatekin, A.; Mayes, A. M.; Elimelech, M., Protein antifouling mechanisms of PAN UF membranes incorporating PAN-g-PEO additive. *J. Membr. Sci.* **2007,** 296, (Copyright (C) 2012 American Chemical Society (ACS). All Rights Reserved.), 42-50.
110. Elimelech, M.; Zhu, X.; Childress, A. E.; Hong, S., Role of membrane surface morphology in colloidal fouling of cellulose acetate and composite aromatic polyamide reverse osmosis membranes. *J. Membr. Sci.* **1997,** 127, (Copyright (C) 2012 American Chemical Society (ACS). All Rights Reserved.), 101-109.
111. Lee, C. H.; Van, H. D.; Lane, O.; McGrath, J. E.; Hou, J.; Madsen, L. A.; Spano, J.; Wi, S.; Cook, J.; Xie, W.; Oh, H. J.; Geise, G. M.; Freeman, B. D., Disulfonated Poly(arylene ether sulfone) Random Copolymer Blends Tuned for Rapid Water Permeation via Cation Complexation with Poly(ethylene glycol) Oligomers. *Chem. Mater.* **2011,** 23, (Copyright (C) 2012 American Chemical Society (ACS). All Rights Reserved.), 1039-1049.
112. Kelman, S.; Lin, H.; Sanders, E. S.; Freeman, B. D., CO2/C2H6 separation using solubility selective membranes. *J. Membr. Sci.* **2007,** 305, (Copyright (C) 2014 American Chemical Society (ACS). All Rights Reserved.), 57-68.
113. Ribeiro, C. P., Jr.; Freeman, B. D.; Paul, D. R., Pure- and mixed-gas carbon dioxide/ethane permeability and diffusivity in a cross-linked poly(ethylene oxide) copolymer. *J. Membr. Sci.* **2011,** 377, (Copyright (C) 2014 American Chemical Society (ACS). All Rights Reserved.), 110-123.
114. Freeman, B. D.; Pinnau, I., Polymeric Materials for Gas Separations. In *Polymer Membranes for Gas and Vapor Separation*, American Chemical Society: 1999; Vol. 733, pp 1-27.
115. Liu, S. L.; Shao, L.; Chua, M. L.; Lau, C. H.; Wang, H.; Quan, S., Recent progress in the design of advanced PEO-containing membranes for CO2 removal. *Prog. Polym. Sci.* **2013,** 38, (Copyright (C) 2014 American Chemical Society (ACS). All Rights Reserved.), 1089-1120.

116. Reijerkerk, S. R.; Nijmeijer, K.; Ribeiro, C. P., Jr.; Freeman, B. D.; Wessling, M., On the effects of plasticization in CO2/light gas separation using polymeric solubility selective membranes. *J. Membr. Sci.* **2011,** 367, (Copyright (C) 2014 American Chemical Society (ACS). All Rights Reserved.), 33-44.
117. Kusuma, V. A.; Gunawan, G.; Smith, Z. P.; Freeman, B. D., Gas permeability of cross-linked poly(ethylene-oxide) based on poly(ethylene glycol) dimethacrylate and a miscible siloxane co-monomer. *Polymer* **2010,** 51, (Copyright (C) 2014 American Chemical Society (ACS). All Rights Reserved.), 5734-5743.
118. Lin, H.; Van Wagner, E.; Freeman, B. D.; Toy, L. G.; Gupta, R. P., Plasticization-enhanced hydrogen purification using polymeric membranes. *Science (Washington, DC, U. S.)* **2006,** 311, (Copyright (C) 2014 American Chemical Society (ACS). All Rights Reserved.), 639-642.
119. Lin, H.; Van Wagner, E.; Swinnea, J. S.; Freeman, B. D.; Pas, S. J.; Hill, A. J.; Kalakkunnath, S.; Kalika, D. S., Transport and structural characteristics of crosslinked poly(ethylene oxide) rubbers. *J. Membr. Sci.* **2006,** 276, (Copyright (C) 2014 American Chemical Society (ACS). All Rights Reserved.), 145-161.
120. Bondar, V. I.; Freeman, B. D.; Pinnau, I., Gas sorption and characterization of poly(ether-b-amide) segmented block copolymers. *J. Polym. Sci., Part B: Polym. Phys.* **1999,** 37, (Copyright (C) 2014 American Chemical Society (ACS). All Rights Reserved.), 2463-2475.
121. Richards, J. J.; Danquah, M. K.; Kalakkunnath, S.; Kalika, D. S.; Kusuma, V. A.; Matteucci, S. T.; Freeman, B. D., Relation between structure and gas transport properties of polyethylene oxide networks based on crosslinked bisphenol A ethoxylate diacrylate. *Chem. Eng. Sci.* **2009,** 64, (Copyright (C) 2012 American Chemical Society (ACS). All Rights Reserved.), 4707-4718.
122. Comer, A. C.; Kalika, D. S.; Kusuma, V. A.; Freeman, B. D., Glass-transition and gas-transport characteristics of polymer nanocomposites based on crosslinked poly(ethylene oxide). *J. Appl. Polym. Sci.* **2010,** 117, (Copyright (C) 2014 American Chemical Society (ACS). All Rights Reserved.), 2395-2405.
123. Lin, H.; Freeman, B. D., Materials selection guidelines for membranes that remove CO2 from gas mixtures. *J. Mol. Struct.* **2005,** 739, (Copyright (C) 2014 American Chemical Society (ACS). All Rights Reserved.), 57-74.
124. Introduction. In *Castable Polyurethane Elastomers*, CRC Press: 2008; pp 1-6.
125. Szycher, M., *Szycher's handbook of polyurethanes*. CRC Press: Boca Raton, 1999.
126. Dodge, J., Polyurethanes and Polyureas. In *Synthetic Methods in Step-Growth Polymers*, John Wiley & Sons, Inc.: 2003; pp 197-263.
127. Das, S.; Cox, D. F.; Wilkes, G. L.; Klinedinst, D. B.; Yilgor, I.; Yilgor, E.; Beyer, F. L., Effect of Symmetry and H-bond Strength of Hard Segments on the Structure-Property Relationships of Segmented, Nonchain Extended Polyurethanes and Polyureas. *J. Macromol. Sci., Part B: Phys.* 2007, 46, (Copyright (C) 2012 American Chemical Society (ACS). All Rights Reserved.), 853-875.
128. Thompson, T., *Desing and Applications of Hydrophilic Polyurethanes*. Technomic: 2000.
129. *The United Nations World Water Development Report*; UN: 2003.
130. Greenlee, L. F.; Lawler, D. F.; Freeman, B. D.; Marrot, B.; Moulin, P., Reverse osmosis desalination: Water sources, technology, and today's challenges. *Water Res.* **2009,** 43,

(Copyright (C) 2012 American Chemical Society (ACS). All Rights Reserved.), 2317-2348.
131. Service, R. F., Desalination Freshens Up. *Science (Washington, DC, U. S.)* **2006,** 313, (Copyright (C) 2012 American Chemical Society (ACS). All Rights Reserved.), 1088-1090.
132. Nollet, J. A., Lecons de physique experimentale,Hippolyte-Louis Guerin and Louis-Francios Delatour. **1748**, 348.
133. Glater, J., The early history of reverse osmosis membrane development. *Desalination* **1998,** 117, (1–3), 297-309.
134. Lonsdale, H. K.; Podall, H. E.; American Chemical, S. In *Reverse osmosis membrane research*, New York, 1972, Plenum Press: New York.
135. Merten, U., *Desalination by reverse osmosis*. M.I.T. Press: Cambridge, 1966; p x, 289 p.
136. Elimelech, M.; Phillip, W. A., The Future of Seawater Desalination: Energy, Technology, and the Environment. *Science (Washington, DC, U. S.)* **2011,** 333, (Copyright (C) 2012 American Chemical Society (ACS). All Rights Reserved.), 712-717.
137. Lonsdale, H. K., Transport properties of cellulose acetate osmotic membranes. *U. Merten and R. L. Riley. J. Appl. Polymer Sci.* **1965,** 9, (Copyright (C) 2012 American Chemical Society (ACS). All Rights Reserved.), 1341-62.
138. Merten, U., Flow Relationships in Reverse Osmosis. *Industrial & Engineering Chemistry Fundamentals* **1963,** 2, (3), 229-232.
139. Paul, D. R., The role of membrane pressure in reverse osmosis. *Journal of Applied Polymer Science* **1972,** 16, (3), 771-782.
140. Paul, D. R., Reformulation of the solution-diffusion theory of reverse osmosis. *Journal of Membrane Science* **2004,** 241, (2), 371-386.
141. Wijmans, J. G.; Baker, R. W., The solution-diffusion model: a review. *Journal of Membrane Science* **1995,** 107, (1–2), 1-21.
142. Bird, R. B., Transport phenomena. *Applied Mechanics Reviews* **2002,** 55, (1), R1-R4.
143. Perry, R. H.; Green, D. W.; Maloney, J. O., *Perry's chemical engineers' handbook*. McGraw-Hill: New York, 1997.
144. Rahardianto, A.; Gao, J.; Gabelich, C. J.; Williams, M. D.; Cohen, Y., High recovery membrane desalting of low-salinity brackish water: Integration of accelerated precipitation softening with membrane RO. *Journal of Membrane Science* **2007,** 289, (1–2), 123-137.
145. Baker, R. W., *Membrane technology and applications*. J. Wiley: Chichester; New York, 2004.
146. United, S., Saline water conversion report. **1955**.
147. Reid, C. E.; Breton, E. J., Water and ion flow across cellulosic membranes. *Journal of Applied Polymer Science* **1959,** 1, (2), 133-143.
148. Reid, C. E.; Kuppers, J. R., Physical characteristics of osmotic membranes of organic polymers. *Journal of Applied Polymer Science* **1959,** 2, (6), 264-272.
149. Sourirajan, S.; Govindan, T. S. In *Membrane separation of some onorganic salts in aqueous solution*, 1967; 1967; pp 251-69, discussion 269-74.
150. Manjikian, S.; Loeb, S.; McCutchan, J. W., Improvement in fabrication techniques for reverse osmosis desalination membranes. *Proc. Int. Symp. Water Desalination, 1st, Washington, D. C., 1965 (Pub. 1967)* **1967,** 2, (Copyright (C) 2012 American Chemical Society (ACS). All Rights Reserved.), 159-79.

151. Riley, R. L.; Merten, U.; Gardner, J. O., Replication electron microscopy of cellulose acetate osmotic membranes. *Desalination* **1966,** 1, (Copyright (C) 2012 American Chemical Society (ACS). All Rights Reserved.), 30-4.
152. Lonsdale, H. K.; Cross, B. P.; Graber, F. M.; Milstead, C. E., Permeability of cellulose acetate membranes to selected solutes. *J. Macromol. Sci., Phys.* **1971,** 5, (Copyright (C) 2012 American Chemical Society (ACS). All Rights Reserved.), 167-87.
153. Richter, J. W.; Hoehn, H. H. Permselective polymer membranes. DE1941022A, 1970.
154. Cadotte, J. E.; Cobian, K. E.; Forester, R. H.; Petersen, R. J. *Continued evaluation of in situ-formed condensation polymers for reverse osmosis membranes*; Midwest Res. Inst.: 1976; p 89 pp.
155. Rozelle, L. T.; Kopp, C. V., Jr.; Cadotte, J. E.; Cobian, K. E., NS-100 membranes for reverse osmosis applications. *J. Eng. Ind.* **1975,** 97, (Copyright (C) 2012 American Chemical Society (ACS). All Rights Reserved.), 220-3.
156. Rozelle, L. T.; Cadotte, J. E.; Cobian, K. E.; Kopp, C. V., Jr. In *Nonpolysaccharide membranes for reverse osmosis: NS-100 membranes*, 1977; NRCC: 1977; pp 249-61.
157. Belfort, G., *Synthetic membrane processes: fundamentals and water applications*. Academic Press: Orlando, Fla., 1984; p xiii, 552 p.
158. Cadotte, J. E.; King, R. S.; Majerle, R. J.; Petersen, R. J., Interfacial synthesis in the preparation of reverse osmosis membranes. *J. Macromol. Sci., Chem.* **1981,** A15, (Copyright (C) 2014 American Chemical Society (ACS). All Rights Reserved.), 727-55.
159. Cadotte, J. E.; Petersen, R. J.; Larson, R. E.; Erickson, E. E., A new thin-film composite seawater reverse osmosis membrane. *Desalination* **1980,** 32, (Copyright (C) 2014 American Chemical Society (ACS). All Rights Reserved.), 25-31.
160. Larson, R. E.; Cadotte, J. E.; Petersen, R. J., The FT-30 sea water reverse osmosis membrane - element test results. *Desalination* **1981,** 38, (Copyright (C) 2014 American Chemical Society (ACS). All Rights Reserved.), 473-83.
161. Cadotte, J. E. Reverse osmosis membrane. US4259183A, 1981.
162. Koros, W. J.; Fleming, G. K.; Jordan, S. M.; Kim, T. H.; Hoehn, H. H., Polymeric membrane materials for solution-diffusion based permeation separations. *Prog. Polym. Sci.* **1988,** 13, 339-401.
163. Glater, J.; Hong, S.-k.; Elimelech, M., The search for a chlorine resistant reverse osmosis membrane. *Desalination* **1994,** 95, 325-345.
164. Xie, W.; Geise, G. M.; Freeman, B. D.; Lee, H.-S.; Byun, G.; McGrath, J. E., Polyamide interfacial composite membranes prepared from m-phenylene diamine, trimesoyl chloride and a new disulfonated diamine. *J. Membr. Sci.* **2012,** 403-404, (Copyright (C) 2014 American Chemical Society (ACS). All Rights Reserved.), 152-161.
165. Cadotte, J. E.; Petersen, R. J.; Larson, R. E.; Erickson, E. E., A new thin-film composite seawater reverse osmosis membrane. *Desalination* **1980,** 32, (Copyright (C) 2012 American Chemical Society (ACS). All Rights Reserved.), 25-31.
166. Credali, L.; Chiolle, A.; Parrini, P., New polymer materials for reverse osmosis membranes. *Desalination* **1974,** 14, (Copyright (C) 2012 American Chemical Society (ACS). All Rights Reserved.), 137-50.
167. Kawaguchi, T.; Tamura, H., Chlorine-resistant membrane for reverse osmosis. I. Correlation between chemical structures and chlorine resistance of polyamides. *Journal of Applied Polymer Science* **1984,** 29, (11), 3359-3367.

168. Glater, J.; Hong, S.-k.; Elimelech, M., The search for a chlorine-resistant reverse osmosis membrane. *Desalination* **1994,** 95, (3), 325-345.
169. Kwon, Y.-N.; Leckie, J. O., Hypochlorite degradation of crosslinked polyamide membranes: I. Changes in chemical/morphological properties. *Journal of Membrane Science* **2006,** 283, (1–2), 21-26.
170. Petersen, R. J., Composite reverse osmosis and nanofiltration membranes. *J. Membr. Sci.* **1993,** 83, (Copyright (C) 2012 American Chemical Society (ACS). All Rights Reserved.), 81-150.
171. Bourganel, J. Anisotropic, semipermeable membranes comprising poly(arylene ether sulfones). DE2225284A1, 1972.
172. Roy, A.; Hickner, M. A.; Yu, X.; Li, Y.; Glass, T. E.; McGrath, J. E., Influence of chemical composition and sequence length on the transport properties of proton exchange membranes. *J. Polym. Sci., Part B: Polym. Phys.* **2006,** 44, (Copyright (C) 2012 American Chemical Society (ACS). All Rights Reserved.), 2226-2239.
173. Park, H. B.; Freeman, B. D.; Zhang, Z.-B.; Sankir, M.; McGrath, J. E., Highly chlorine-tolerant polymers for desalination. *Angew. Chem., Int. Ed.* **2008,** 47, (Copyright (C) 2012 American Chemical Society (ACS). All Rights Reserved.), 6019-6024.
174. Stern, S. A.; Sinclair, T. F.; Gareis, P. J.; Vahldieck, N. P.; Mohr, P. H., Helium recovery by permeation. *J. Ind. Eng. Chem. (Washington, D. C.)* **1965,** 57, (Copyright (C) 2012 American Chemical Society (ACS). All Rights Reserved.), 49-60.
175. Puri, P. S., Fabrication of hollow fiber gas separation membranes. *Gas Sep. Purif.* **1990,** 4, (Copyright (C) 2012 American Chemical Society (ACS). All Rights Reserved.), 29-36.
176. Henis, J. M. S.; Tripodi, M. K., Composite hollow fiber membranes for gas separation: the resistance model approach. *J. Membr. Sci.* **1981,** 8, (Copyright (C) 2012 American Chemical Society (ACS). All Rights Reserved.), 233-46.
177. Robeson, L. M.; Burgoyne, W. F.; Langsam, M.; Savoca, A. C.; Tien, C. F., High performance polymers for membrane separation. *Polymer* **1994,** 35, (Copyright (C) 2012 American Chemical Society (ACS). All Rights Reserved.), 4970-8.
178. Stern, S. A., Polymers for gas separations: the next decade. *J. Membr. Sci.* **1994,** 94, (Copyright (C) 2012 American Chemical Society (ACS). All Rights Reserved.), 1-65.
179. Baker, R. W.; Wijmans, J. G. In *Membrane separation of organic vapors from gas streams*, 1994; CRC: 1994; pp 353-97.
180. Freeman, B.; Pinnau, I., Separation of gases using solubility-selective polymers. *Trends in Polymer Science* **1997,** 5, (5), 167-173.
181. Baker, R. W.; Yoshioka, N.; Mohr, J. M.; Khan, A. J., Separation of organic vapors from air. *J. Membr. Sci.* **1987,** 31, (Copyright (C) 2012 American Chemical Society (ACS). All Rights Reserved.), 259-71.
182. Ghosal, K.; Freeman, B. D., Gas separation using polymer membranes: an overview. *Polym. Adv. Technol.* **1994,** 5, (Copyright (C) 2012 American Chemical Society (ACS). All Rights Reserved.), 673-97.
183. Robeson, L. M., The upper bound revisited. *J. Membr. Sci.* **2008,** 320, (Copyright (C) 2012 American Chemical Society (ACS). All Rights Reserved.), 390-400.
184. Sourirajan, S.; Editor, *Reverse Osmosis and Synthetic Membranes. Theory-Technology-Engineering*. NRCC: 1977; p 598 pp.

185. Henis, J. M. S.; Tripodi, M. K., A novel approach to gas separations using composite hollow fiber membranes. *Sep. Sci. Technol.* **1980,** 15, (Copyright (C) 2012 American Chemical Society (ACS). All Rights Reserved.), 1059-68.
186. Pinnau, I.; Koros, W. J., A qualitative skin layer formation mechanism for membranes made by dry/wet phase inversion. *Journal of Polymer Science Part B: Polymer Physics* **1993,** 31, (4), 419-427.
187. Ward, W. J., III; Browall, W. R.; Salemme, R. M., Ultrathin silicone/polycarbonate membranes for gas separation processes. *J. Membr. Sci.* **1976,** 1, (Copyright (C) 2012 American Chemical Society (ACS). All Rights Reserved.), 99-108.
188. Yagci, Y.; Jockusch, S.; Turro, N. J., Photoinitiated Polymerization: Advances, Challenges, and Opportunities. *Macromolecules* **2010,** 43, (15), 6245-6260.
189. Schwalm, R., 10.30 - Radiation-Curing Polymer Systems. In *Polymer Science: A Comprehensive Reference*, Möller, K. M., Ed. Elsevier: Amsterdam, 2012; pp 567-579.
190. Sangermano, M.; Razza, N.; Crivello, J. V., Cationic UV-Curing: Technology and Applications. *Macromol. Mater. Eng.* **2014,** 299, (Copyright (C) 2014 American Chemical Society (ACS). All Rights Reserved.), 775-793.
191. Bhowmik, P. K., Light-Associated Reactions of Synthetic Polymers By A. Ravve (Consultant, Niles, IL). Springer Science + Business Media, LLC: New York. 2006. ISBN 0-387-31803-8. *Journal of the American Chemical Society* **2006,** 128, (50), 16412-16412.
192. Kurdikar, D. L.; Peppas, N. A., Method of determination of initiator efficiency: application to UV polymerizations using 2,2-dimethoxy-2-phenylacetophenone. *Macromolecules* **1994,** 27, (3), 733-738.
193. Groenenbook, C. J.; Hageman, H. J.; Overeem, T.; Weber, A. J. M., Photoinitiators and photoinitiation, 3. Comparison of the photodecompositions of α-methoxy- and α,α-dimethoxydeoxybenzoin in 1,1-diphenylethylene as model substrate. *Die Makromolekulare Chemie* **1982,** 183, (2), 281-292.
194. Bradley, G.; Davidson, R. S.; Howgate, G. J.; Mouillat, C. G. J.; Turner, P. J., Photoinitiated polymerization reactions: Application of a new real-time FTIR system for following the rate of polymerization. *Journal of Photochemistry and Photobiology A: Chemistry* **1996,** 100, (1–3), 109-118.
195. Phan, X. T.; Grubb, M. B., Effects of Additives on the Laser-Initiated Polymerization of 1,6-Hexanediol Diacrylate. *Journal of Macromolecular Science: Part A - Chemistry* **1988,** 25, (2), 143-158.
196. Endruweit, A.; Johnson, M. S.; Long, A. C., Curing of Composite Components by Ultraviolet Radiation: A Review. *Polymer Composites* **2006,** 27, (2), 119-128.
197. Lin, H.; Kai, T.; Freeman, B. D.; Kalakkunnath, S.; Kalika, D. S., The Effect of Cross-Linking on Gas Permeability in Cross-Linked Poly(Ethylene Glycol Diacrylate). *Macromolecules* **2005,** 38, (20), 8381-8393.
198. Mickols, W. E., 10.41 - Aromatic Poly(amides) for Reverse Osmosis. In *Polymer Science: A Comprehensive Reference*, Matyjaszewski, K.; Möller, M., Eds. Elsevier: Amsterdam, 2012; pp 831-848.
199. Robeson, L. M., 8.13 - Polymer Membranes. In *Polymer Science: A Comprehensive Reference*, Matyjaszewski, K.; Möller, M., Eds. Elsevier: Amsterdam, 2012; pp 325-347.

## 2. UV Crosslinked Telechelic Disulfonated Poly(arylene ether sulfone) Copolymers for Reverse Osmosis Membranes

*Ali Nebipasagil,[1] Benjamin J. Sundell,[1] Ozma R. Lane,[1] Euisong Jang[2] Sue J. Mecham,[1] Benny D. Freeman,[2] and James E. McGrath[1]*

[1]Macromolecules and Interfaces Institute, Virginia Tech, Blacksburg, VA 24061, USA

[2]Department of Chemical Engineering, Center for Energy and Environmental Resources, The University of Texas at Austin, Austin, TX, 78758, USA

**Keywords**: disulfonated poly(arylene ether sulfone); oligomer synthesis; UV crosslinking; reverse osmosis; thin film composite; chlorine resistant polymer membrane

### 2.1. Abstract:

Disulfonated poly(arylene ether sulfone) random copolymers with controlled oligomeric molecular weights were synthesized via nucleophilic aromatic substitution step polymerization. A monofunctional endcapping reagent, *meta*-aminophenol, was utilized to control the molecular weight of the oligomers and to achieve telechelic amine endgroups. The *meta*-aminophenol end-capped oligomers were reacted with 2-propenoyl chloride (acryloyl chloride) to obtain novel crosslinkable poly(arylene ether sulfone) oligomers with acrylamide groups on both ends. The chemical compositions of the functional oligomers were characterized by $^{1}$H NMR spectroscopy to determine the degree of disulfonation and concentrations of acrylamide endgroups. The acrylamide-terminated oligomers were crosslinked with UV radiation in the presence of a multifunctional acrylate and a UV initiator. Transparent, free-standing, dense films were obtained with high gel fractions. FTIR spectroscopy was utilized to observe the progress of the photo-crosslinking reaction. Mechanically robust thin film composite (TFC) membranes were

prepared from either aqueous or water-methanol solutions cast onto a commercial UDEL® foam support. Crosslinked disulfonated poly(arylene ether sulfone) copolymers exhibit reduced water uptake and swelling relative to their linear counterparts, which is expected to enhance membrane properties. SEM and AFM showed that the photo-crosslinked thin film composites had smooth surfaces. The combination of smooth and hydrophilic surface properties is expected to enhance resistance of these membranes against fouling.

## 2.2. Introduction

The Earth's seas and oceans cover more than two thirds of the planet's surface and contain about 97% of all available water.[1] The scarcity of fresh water is an increasing global concern. Forty percent of the world's population live in water-stressed areas, and half of those people do not have access to potable water.[2] Seawater desalination which long has been a means for providing a source of clean water. Over the past several decades, thermal- and membrane-based separation technologies have been used to augment desalination as a viable source of fresh water.[2]

Reverse osmosis is a membrane-based separation method where saline water is pressurized against a semipermeable membrane. The process selectively rejects the salt and drives water to diffuse through the membrane. Substantial reductions in energy costs relative to thermal separation methods, coupled with increased membrane efficiency, make RO a critical technology for seawater desalination.[3,4] State-of-the-art RO membranes are thin film composites with a highly crosslinked aromatic polyamide as the selective membrane. Commercial TFC's are produced by synthesizing a polyamide interfacially directly onto the surface of a poly(arylene ether sulfone) microporous support structure, and this results in a thin selective layer of

crosslinked polyamide. The resulting thin film composites have high salt rejection, high water flux, low compaction under the pressures involved, and reasonable chemical stability.[5-8]

Fouling remains a major problem for efficient operation of RO membranes. Fouling diminishes both water flux and salt rejection of membrane modules.[9,10] Chlorine-based disinfectants are commonly used to sterilize municipal water supplies. The instability of the polyamide selective layer of TFC membranes to chlorinated disinfectants requires removal of the disinfectants prior to the RO process. Chlorine exposure causes chain scission and oxidative degradation in crosslinked polyamide membranes. These irreversible reactions lead to permanent performance loss over time.[11-15] Disulfonated poly(arylene ether sulfone)s are significantly more chlorine resistant than current commercial membranes.[11,16-18]

Poly(arylene ether sulfone) microporous asymmetric films are the primary support material used in state-of-the-art RO thin film composites.[7] Poly(arylene ether sulfone)s are well-known hydrophobic, amorphous polymers that display excellent thermal and mechanical properties, as well as high chemical resistance against oxidation and hydrolysis.[19-22] Given their excellent attributes, these materials are ideal for the porous support layer. They are not suitable for the selective layer in membrane separations which requires hydrophilicity to produce reasonable levels of water permeability. Incorporation of sulfonate moieties into poly(arylene ether sulfone)s introduces hydrophilicity into these hydrophobic polymers, and also modifies other physical properties such as $T_g$.[23,24] Therefore sulfonated poly(arylene ether sulfone)s have been considered as potential candidates for the selective layers on reverse osmosis thin film composites.

The direct copolymerization of sulfonated and non-sulfonated comonomers to synthesize sulfonated poly(arylene ether sulfone)s avoids the unwanted side reactions and degradation of

polymers that often occur using post-sulfonation. Additionally, direct copolymerization provides the advantages of precise control over the distribution of sulfonate units homogeneously throughout the polymer, as well as the control over the degree of sulfonation. The method leads to high molecular weight copolymers and good reproducibility.[25-27] McGrath et al. have demonstrated that disulfonated random copolymers can have high water flux and modest levels of salt rejection.[11,16] Additional research investigated the fundamental water and salt transport properties,[28,29] the tradeoff relationship between salt rejection and water permeability,[30] and the effect of free volume on transport properties of these sulfonated poly(arylene ether sulfone)s.[31] A limitation of these copolymers is that polymer membranes with high ion densities swell strongly in water. The swelling of the polymer matrix leads to a loss in mechanical stability and an increase in salt diffusion.[28,30] Crosslinking can reduce the swelling of these highly hydrophilic membranes and improve their mechanical stability and salt rejection without significantly reducing water flux.[17] We have previously investigated crosslinking of phenoxide-terminated polysulfones with 50% of the repeat units disulfonated with a tetrafunctional epoxide, and shown that networks with gel fractions up to 85% could be produced. The crosslinks reduced membrane swelling by 70% and increased salt rejection up to 97% with only a slight decrease in water permeability.[17]

It has been demonstrated that the processing methods applied to these membranes after they have been solvent cast can affect their transport properties. For example, a random copolymer prepared from biphenol, dichlorodiphenyl sulfone and 3,3'-disulfonated dichlorodiphenyl sulfone with 32% of the units disulfonated was investigated.[32] Acidified membranes had higher water uptake and permeability along with lower salt rejections than their salt form (Na, K, and Ca) counterparts. Additionally, thermal treatment of dense films in water resulted in different

transport properties as a function of the thermal treatment history. Thermal treatment of dense films increased water uptake, water permeability as well as salt permeability of these membranes resulting in a decrease in water/salt selectivity. These results suggest that post production treatment can be used to tune the final properties of these partially-disulfonated poly(arylene ether sulfone) membranes.

The fabrication of thin film composite (TFC) membranes is another approach to preparing RO membranes utilizing disulfonated poly(arylene ether sulfone)s.[33] Multiple layers of high molecular weight random copolymer prepared from biphenol, dichlorodiphenyl sulfone and 3,3'-disulfonated dichlorodiphenyl sulfone with either 20 or 32 mol % of the units disulfonated were cast into thin films from dilute solutions onto the microporous support. This yielded a disulfonated polysulfone selective layer, similar to the state-of-the-art TFCs used commercially. Di(ethylene glycol) (DEG) was identified as a benign solvent which selectively dissolved the disulfonated poly(arylene ether sulfone) copolymers and in which the UDEL® support foam was insoluble. It was shown that thermal treatment at elevated temperatures to remove the casting solvent caused the pores of the microporous UDEL® support to shrink which led to substantial decrease in water permeability. Therefore, this casting method required pretreatment to protect the support and remove the high boiling casting solvent without altering the microporous structure of the UDEL® support. Multilayer casting of dilute solutions produced films with a thickness ($L_{actual}$) of about 500 nm; however the average effective thickness ($L_{effective}$) which was calculated based on the water and salt transport data was around 750 nm. The discrepancy ($L_{actual} < L_{effective}$) between the thickness measurements indicates defects in the composite membrane structure such as pore penetration within the supporting foam layer. To avoid pore penetration, support membranes were initially immersed in an IPA/glycerin mixture, which left glycerin

within the pores of the membranes after the IPA was allowed to evaporate. This pretreatment procedure allowed the TFC membranes to be dried under vacuum at elevated temperatures while preventing pore collapse during the drying procedures. Upon preparation of membranes, glycerin was extracted via water treatment. Defect free films had salt rejection around 97% with a significant improvement in water flux relative to their dense membrane counterparts.[33]

Our group has reported the synthesis of telechelic disulfonated oligomers with phenol and aromatic amine functionalities crosslinked with epoxy reagents previously.[17,35] We now report the synthesis of acrylamide-terminated disulfonated poly(arylene ether sulfone) oligomers and crosslinking of the new materials with UV light. This study focuses on the synthesis, characterization and fabrication of these crosslinkable materials into TFCs, as well as an analysis of the factors that influence the composite assembly.

## 2.3. Experimental

### *2.3.1. Materials*

4,4'-(Propane-2,2-diyl)diphenol (bisphenol A) and 4,4'-dichlorodiphenylsulfone (DCDPS, 99%) were kindly provided by Solvay and recrystallized from toluene before use. 3,3'-Disulfonated-4,4'-dichlorodiphenylsulfone (SDCDPS, 98%) was purchased from Akron Polymer Systems (Akron, OH).[34] Potassium carbonate ($K_2CO_3$, 99%), 2-propenoyl chloride (acryloyl chloride, 96%), triethylamine (TEA, 99.5%), pentaerythritol tetraacrylate (PETA), di(ethylene glycol) diacrylate (DEGDA), glycerol propoxylate triacrylate (GPTA), trimethylolpropane ethoxylate triacrylate (TMPTA), 2,2-dimethoxy-2-phenylacetophenone (DMPA, 99%) 1-hydroxycyclohexyl phenyl ketone (HCPK) and 4Å molecular sieves were purchased from Sigma Aldrich. Calcium hydride ($CaH_2$, 90-95%) was purchased from Alfa Aesar. 3-Aminophenol (*m*-AP, 99%) and *N,N*-dimethylacetamide (DMAc, 99%) were purchased from Acros Organics.

DMAc was distilled from calcium hydride and stored over activated molecular sieves before use. HPLC-grade water was purchased from Spectrum Chemicals. Toluene and 2-propanol (IPA) were purchased from Fisher Scientific. The solvents were used as received unless noted otherwise.

### *2.3.2. Synthesis of an ~5,000 g/mol ($M_n$) amine-endcapped disulfonated polysulfone copolymer (am-BisASXX, Figure 2.1)*

Poly(arylene ether sulfone) oligomers with controlled degrees of disulfonation and controlled molecular weights were synthesized via nucleophilic aromatic substitution (Figure 2.1). SDCDPS was incorporated into the oligomer via a direct copolymerization route as previously reported.[26,27]

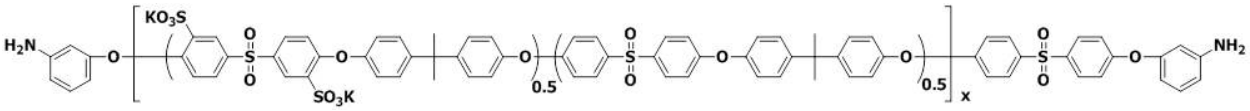


**Figure 2.1.** Amine-endcapped disulfonated poly(arylene ether sulfone) with 50 % of the repeat units disulfonated

High monomer purity and a strict monomer ratio are imperative to obtain high conversion with precisely controlled molecular weights and composition. Bisphenol A and DCDPS were recrystallized from toluene to eliminate impurities. Hygroscopic reagents can absorb moisture under ambient conditions. Thus $K_2CO_3$ was dried for 24 h and SDCDPS for 72 h at 160$^oC$ under vacuum to remove moisture. NaCl is a by-product of SDCDPS synthesis and remains as an inert impurity in SDCDPS. The NaCl content in the SDCDPS was quantified as 3 mol% by UV-VIS spectroscopy before it was used in the oligomer synthesis.[35] A representative synthetic procedure is provided below. Bisphenol A (43.6 mmol, 9.9534 g), DCDPS (25 mmol, 7.1790 g), SDCDPS (25 mmol, 12.6611 g), *m*-aminophenol (12.7 mmol, 1.3999 g), were weighed into a 250-mL

three-necked flask and dissolved in DMAc (130 mL). The reaction flask was equipped with a mechanical stirrer, nitrogen inlet, and Dean-Stark trap filled with toluene. A stirred oil bath equipped with a thermocouple was used to regulate the reaction temperature. The oil bath temperature was raised to 155$^{o}$C to bring the reaction to reflux and subsequently $K_2CO_3$ (78.48 mmol, 10.8467 g) and toluene (65 mL) were added into the flask. The reaction was azeotropically dehydrated at 155 $^{o}$C until water condensation ceased (6h). The temperature was gradually increased to 175 $^{o}$C and the water-toluene mixture was drained from the Dean-Stark trap and the toluene in the reaction was collected. After 48 h, the reaction was cooled to room temperature. The polymer solution was filtered to remove salt and then was precipitated in isopropyl alcohol as a white solid. The oligomer was filtered, washed with IPA, and dried under vacuum at 120 $^{o}$C for 24 h (yield>90 %).

### *2.3.3. Conversion of amine-endcapped oligomers to acrylamide-endcapped oligomers (AA-BisASXX, Figure 2.2)*

A representative acrylamide functionalization reaction was conducted as follows. Am-BisAS50 (0.517 mmol, 3.000 g) was dissolved in DMAc (45 mL) in a 100-mL round bottom flask equipped with a magnetic stir bar. The flask was sealed with a septum, purged with nitrogen, and placed in an ice bath. An acid scavenger, triethylamine (TEA, 10 mmol, 0.5856 g), was injected into the flask. An excess of acryloyl chloride (3.47 mmol, 0.3143 g) dissolved in DMAc (5 mL) was slowly injected into the reaction flask to avoid a rapid exothermic reaction, yielding an opaque solution due to formation of insoluble triethylamine hydrochloride salt. A large excess of acryloyl chloride was used to ensure 100% endgroup conversion. The reaction was allowed to proceed for 4 h. Triethylamine hydrochloride salt is soluble in alcohols; the acrylamide-terminated product was precipitated in isopropyl alcohol as a white solid. The

product was filtered, washed with isopropyl alcohol to eliminate any residual salt or reaction solvent, and dried in a vacuum oven at 120 °C for 24 h.

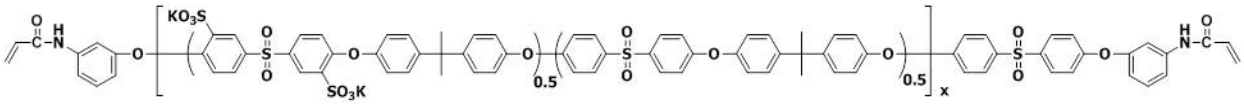

**Figure 2.2.** Acrylamide-functional poly(arylene ether sulfone) oligomer with 50 % of the repeat units disulfonated

### *2.3.4. Synthesis of an acrylamide-functional crosslinking agent: bis-acrylamide disulfonated diphenyl sulfone*

SDCDPS (25 mmol, 12.6611 g) and *m*-aminophenol (50.0 mmol, 5.5114 g) were weighed into a 250-mL three-necked flask and dissolved in DMAc (50 mL). The reaction flask was equipped with a mechanical stirrer, nitrogen inlet, and Dean-Stark trap filled with toluene. A stirred oil bath regulated with a thermocouple was used to control the reaction temperature. The oil bath temperature was raised to 155°C to bring the reaction to reflux and then $K_2CO_3$ (78.48 mmol, 10.8467 g) and toluene (65 mL) were added to the flask. The reaction was azeotropically dehydrated at 155 °C until water condensation ceased. The temperature was gradually increased to 175 °C and the water-toluene mixture was drained. After 48 h, the reaction was allowed to cool to room temperature. The solution was filtered and precipitated in isopropyl alcohol as amber solid. The product was filtered, washed with isopropyl alcohol, and dried in a vacuum oven at 120 °C for 24 h. Next, this amino-functional reagent (20 mmol, 15.538 g) was dissolved in DMAc (45 mL) in a 100-mL round bottom flask. The flask was sealed with a septum, purged with nitrogen and placed in an ice bath. Triethylamine (TEA, 30 mmol, 1.7568 g) was injected into the flask to function as an acid scavenger. An excess of acryloyl chloride (140 mmol, 12.68 g) dissolved in DMAc (25 mL) was injected into the reaction flask, yielding an opaque solution

due to triethylamine hydrochloride salt. The reaction was allowed to proceed for 4 h. The acrylamide-functional crosslinking agent was isolated by precipitating it in isopropyl alcohol as a white solid. The product was filtered, washed with isopropyl alcohol, and dried under vacuum at 120 $^{o}$C for 24 h (Yield >90 %). The structure was confirmed by $^{1}$H NMR spectroscopy.

### *2.3.5. Crosslinking and dense film fabrication of acrylamide-functional disulfonated poly(arylene ether sulfone) oligomers (AA-BisASXX)*

AA-BisASXXs were photocrosslinked in combination with multifunctional acrylates or acrylamides. The crosslinking experimental conditions were optimized via crosslinking experiments of AA-BisAS50 with pentaerythritol tetraacrylate (PETA) and 2,2-dimethoxy-2-phenylacetophenone (DMPA) in DMAc solutions. A series of oligomer to PETA molar ratios (1:1, 1:1.5, 1:2 and 1:2.5) were investigated, as well as the effect of DMPA concentration on the degree of crosslinking. Experiments with two, five and ten % (wt/wt) initiator relative to total monomer mass were conducted. A representative photo-crosslinking reaction of AA-BisAS50 is described. AA-BisAS50 (0.1 mmol, 0.500 g) and PETA (0.25 mmol, 0.088 g) were dissolved in DMAc (2.0 mL) in a glass vial. DMPA (2 wt %, 0.05 mmol, 0.012 g) was added. The solution was cast on a glass substrate on a level surface and crosslinked using a Heraeus LC6B benchtop conveyor instrument (315-400 nm broad range irradiation, 1.988 W/cm$^2$, 1200 J/cm$^2$, 15 s/pass on the conveyor belt) for a total of 150 s. UV curing yielded transparent ,free standing yet fragile polymer films. The films were dried under vacuum at 120 $^{o}$C for one day to remove residual solvent. Crosslinking reactions of water soluble AA-BisASXX with 60, 80 and 100% of the repeat units disulfonated were conducted in aqueous solutions using 1-hydroxycyclohexyl phenyl ketone (HCPK) as the photoinitiator and diethylene glycol diacrylate (DEGDA) or bis-acrylamide disulfonated diphenylsulfone (SDPSDA) instead of PETA as the crosslinking agent.

Similarly, AA-BisASXX (60, 80 and 100) films were crosslinked from methanol-water (50:50, v:v) solutions in the presence of one of the multifunctional acrylates: di(ethylene glycol) diacrylate (DEGDA), glycerol propoxylate triacrylate (GPTA), or trimethylolpropane ethoxylate triacrylate (TMPTA).

### *2.3.6. Polymer Characterization*

*Nuclear Magnetic Resonance Spectroscopy (NMR)*

$^{1}H$ and $^{19}F$ NMR analysis of the oligomers was performed on a Varian Unity Plus spectrometer and a Varian Inova spectrometer, both operating at 400 MHz. The spectra of the oligomers were obtained from a 15% (w/v) 1-mL solution in DMSO-$d_6$.

*Fourier Transform Infrared Spectroscopy (FT-IR)*

FT-IR experiments were conducted on a Varian 670-IR spectrometer. A background spectrum of polished KBr disc was collected before taking sample spectra. Thin films of polymer solutions were coated on the discs and FT-IR spectra were collected in quick succession after UV exposure.

*Atomic Force Microscopy (AFM)*

Samples were imaged using a Veeco Multimode AFM. The samples were equilibrated for 12 h at 30 ºC and 40% relative humidity and then sealed prior to imaging. Humidity was measured to be between 25 and 40% during AFM microscopy sessions. A low force constant Nanosensors Point probe-Plus Si tip was used, with a force constant between 1.2-29 N/m.

*Scanning Electron Microscopy (SEM)*

A LEO (Zeiss) 1550 field-emission SEM was used to conduct FE-SEM microscopy. Prior to FE-SEM experiments, the nonwoven backing of the thin film composites was manually

removed. The remaining layers which included a dense UV-crosslinked top layer and a UDEL® foam support were freeze-fractured using liquid nitrogen. Freeze-fractured samples were sputter coated with 10-12 nm of a gold-palladium alloy immediately before SEM imaging.

*Water Uptake*

Water uptake of crosslinked films was measured gravimetrically. Films were dried at 120 °C under vacuum overnight to obtain the dry weight ($W_{dry}$). The films were then immersed in DI water at ambient temperature for at least 48 h. The films were removed, quickly blotted to remove water droplets on the surface and weighed to obtain the wet weight ($W_{wet}$). Equation 2.1 shows the calculation used to determine the gravimetric percent water uptake.

$$\text{Water Uptake}(\%) = \frac{W_{wet} - W_{dry}}{W_{dry}} \times 100$$

**Equation 2.1.**

*Gel fractions*

Gel fraction measurements were performed to determine the extent of crosslinking. Crosslinked films were dried at 120 °C under vacuum overnight. Then ~0.2 g of initial sample was placed in a 20-mL scintillation vial filled with DMAc and stirred at 100 °C overnight. The remaining solid was filtered, transferred to a pre-weighed vial, and dried at 120 °C under vacuum overnight. The final weight was taken the next day. At least three extractions were conducted per sample. Gel fraction values were calculated using equation 2.2.

$$\text{Gel Fraction}(\%) = \frac{W_{final}}{W_{initial}} \times 100$$

**Equation 2.2.**

*Water Transport and Salt Rejection*

The water flux, and salt rejection (%) were determined at 25 °C in a cross-flow filtration system using stainless steel crossflow cells machined at the University of Texas at Austin. The pressure difference across the membrane (38 $cm^2$) is listed in Table 2.4. The aqueous feed contained ~2000 ppm NaCl, and the feed solution was circulated past the samples at a continuous flow rate of 4 (L/min). The feed pH was adjusted to a range between 6.5 and 7.5 using a 10 g/L sodium bicarbonate solution. NaCl concentrations in the feed water and permeate were measured with an Oakton 100 digital conductivity meter.

## 2.4. Results and Discussion

### *2.4.1. Oligomer Synthesis*

Direct copolymerization of partially disulfonated poly(arylene ether sulfones) synthesized via nucleophilic aromatic substitution step polymerizations have been previously described by McGrath et al.[17,26,29,36-39] The 3,3'-disulfonated-4,4'-dichlorodiphenylsulfone (SDCDPS) monomer was used to control of the degree of disulfonation and therefore the hydrophilicity of the copolymers.[26,27] Oligomers with targeted molecular weights of ~5,000 g/mol were investigated in this research utilizing a monofunctional endcapping reagent to limit the molecular weights. A modified Carothers equation was used to calculate the required amount of *m*-aminophenol endcapping agent which also provided aromatic amine endgroup functionality.[40] *m*-Aminophenol was preferred over *p*-aminophenol because *m*-aminophenol produces more oxidatively stable oligomers.[40,41] Thus, the *m*-aminophenol endgroup greatly extends the shelf life of these oligomers.[41] Toluene was used as the azeotropic solvent to remove the byproduct water that the $K_2CO_3$ reaction produces. Toluene reflux was continued until no more water was

observed in the distillate. The temperature was raised slowly to 175$^{o}$C, and toluene was slowly collected until the initial charged volume was obtained. The viscosity of the reaction solution increased slightly after 48 hours. Since the targeted molecular weight was 5,000 g/mol, no drastic change in viscosity was anticipated. The nucleophilic substitution reaction between amine-terminated oligomers and acryloyl chloride occurs rapidly. Therefore the reaction was cooled to 0 $^{o}$C before adding triethylamine and acryloyl chloride. The am-BisAS50 was dried prior to reaction with the acid chloride to avoid reactions of water with the acryloyl chloride.

### *2.4.2. Oligomer Characterization*

The composition of the amino-functional oligomer was characterized by $^{1}$H NMR to determine the degree of disulfonation (D.S.) and to estimate the $M_n$,. A $^{1}$H NMR spectrum of the am-BisAS50 oligomer is shown in Figure 2.3. The spectrum showed no side products, residual monomer or reaction solvent. The D.S. was calculated using equation 2.3. The measured D.S. was 49% compared to the targeted D.S. of 50%.

$$\text{D.S.}\,(\%) = \frac{[(\text{H}_a + \text{H}_b + \text{H}_c)/3]/2}{[(\text{H}_a + \text{H}_b + \text{H}_c)/3]/2 \; + [(\text{H}_f + \text{H}_g)/2]/4} \times 100$$

**Equation 2.3.**

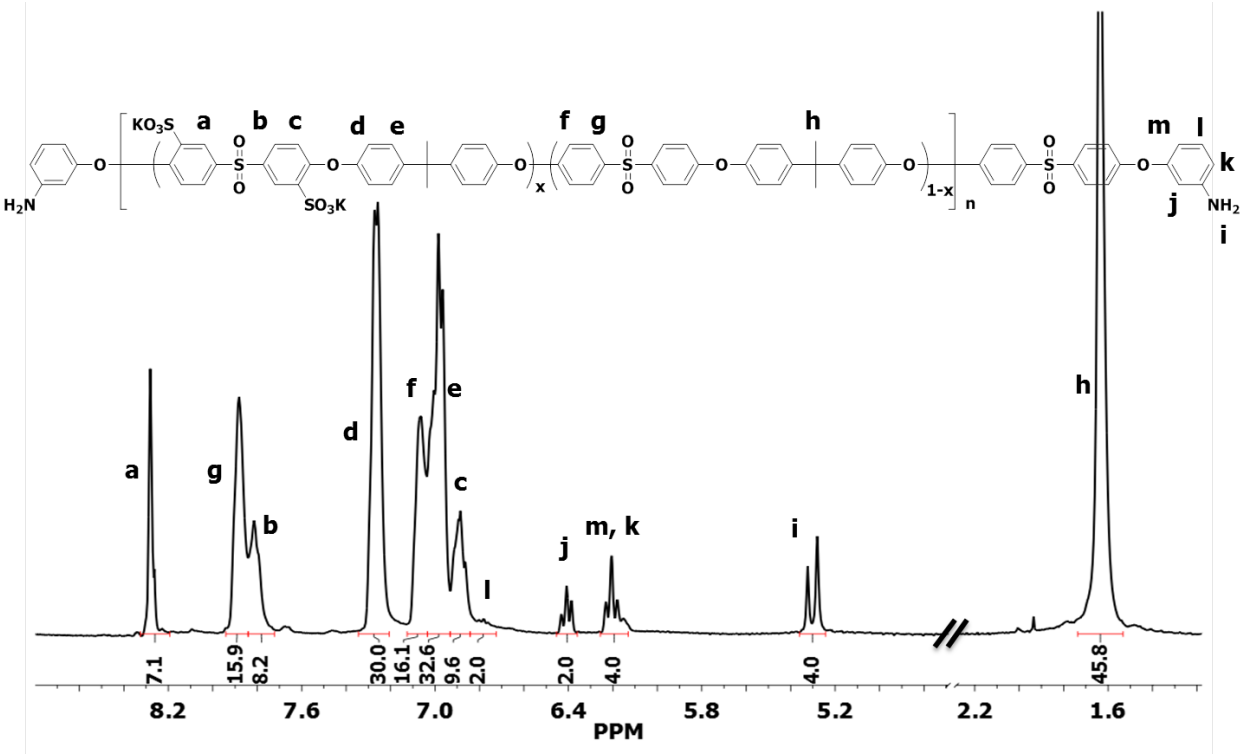


**Figure 2.3.** $^{1}$H NMR of am-BisAS50

The *m*-aminophenol endgroups can be attached to a non-sulfonated or a disulfonated unit so the positions of the *m*-aminophenol protons shift slightly depending on which monomer is the adjacent group. For example, the singlets (**i**) are due to amine protons bonded to DCDPS (further downfield) and SDCDPS. Similarly, endgroup peaks (**j**), (**m**), and (**k**) have overlapping, slightly shifted signals depending on the adjacent group.

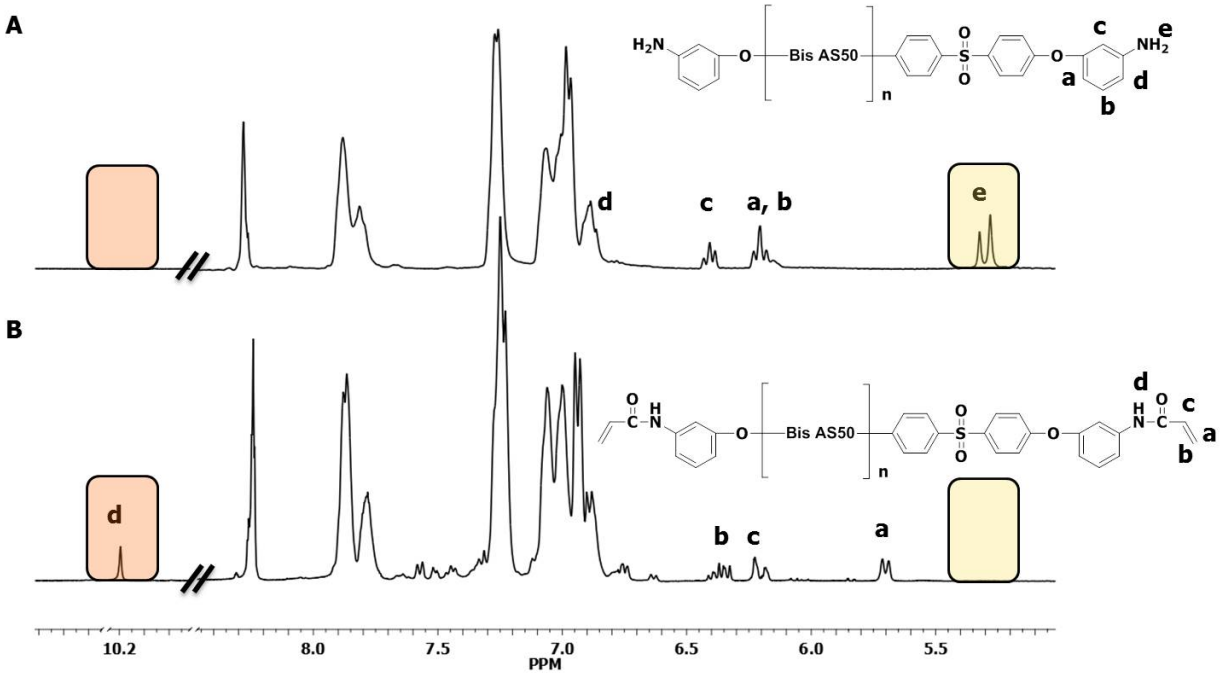


**Figure 2.4.** The endgroup of oligomers were modified as evidenced by $^{1}$H NMR Spectra

Spectrum A: $^{1}$H NMR of am-BisAS50, Spectrum B: $^{1}$H NMR of AA-BisAS50

$^{1}$H NMR was also utilized to confirm the endgroup structures of the acrylamide-functional oligomers (Figure 2.4). As expected, the amine peak disappeared upon conversion to the acrylamide while the amide proton at approximately 10.2 ppm. The $M_n$ calculated by $^{1}$H NMR endgroup analysis was 4,900 g/mol, determined by ratio of the integration values of the DCDPS and SDCDPS aromatic protons that are adjacent to sulfonyl groups and the acrylamide endgroup peak (a).

### *2.4.3. Crosslinking and Film Fabrication of AA-BisASXX Oligomers*

The acrylamide-functional oligomers were photochemically crosslinked using 2,2-dimethoxy-2-phenylacetophenone (DMPA) or 1-hydroxycyclohexyl phenyl ketone (HCPK) as the photoinitiator in the presence of multifunctional acrylates. The efficiencies of these

photoinitiators and the mechanisms involved in their crosslinking reactions with acrylates and acrylamides have been extensively studied.[42] The crosslinking yielded transparent and fragile polymer films. Reactions of the acrylamide-functional polysulfone copolymer in the absence of a multifunctional acrylate comonomer, however, only produced networks with gel fractions ranging from 13 to 45%. Addition of a highly functional crosslinking agent increases the concentration of reacting groups and drives the crosslinking reaction to high gel fraction.

FT-IR is a powerful tool for characterizing crosslinked networks. FT-IR experiments were conducted to observe the photo-crosslinking of these acrylamide-terminated oligomers with the multifunctional acrylates. The bending =C-H vibrational mode of the unsaturated endgroups shows a characteristic peak at 812 $cm^{-1}$. The FT-IR spectrum (1) of mixture of BISAS50, PETA and DMPA shows the peak at 812 $cm^{-1}$ in Figure 2.5, indicating the presence of acrylate groups prior to photo-crosslinking the acrylate group. Upon exposure to UV light the peak at 812 $cm^{-1}$ disappears, confirming a photo-crosslinking reaction takes place between acrylamide functional Bis-ASXX and multifunctional acrylate crosslinking agent. Ultrathin films were coated on polished KBr discs for FT-IR experiments. FT-IR Spectra showed these ultrathin films were completely crosslinked after 30 seconds of UV irradiation. Table 2.1 summarizes the gel fraction analysis of the dense membranes with the same composition. Gel fraction analysis indicated that dense membranes required up to 150 s of UV irradiation to form a densely crosslinked network structure.

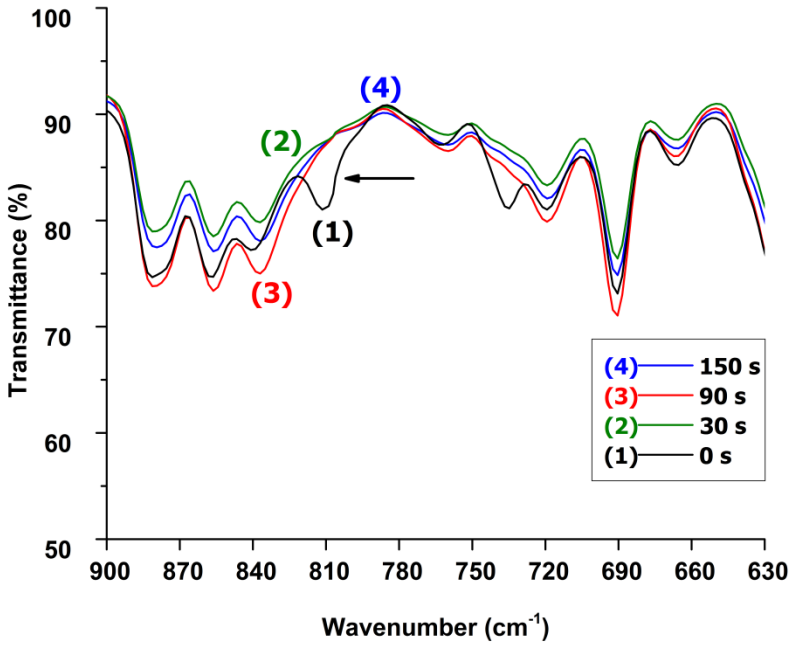


**Figure 2.5.** FT-IR spectra of mixture of BisAS50, PETA and DMPA before (1) and after (2, 3, 4) photo-crosslinking

### *2.4.4. Crosslinking Agent and Photoinitiator Concentration*

The role of the ratio of PETA to AA-BisAS50 was studied to investigate the influence of the crosslinking agent concentration on the degree of crosslinking of dense films with a thickness of ~150 μm. The AA-BisAS50 to PETA molar concentration ratio ranged from 1.0:1.0 to 1.0:2.5. Gel fractions of up to 87% were obtained. The gel fraction increased linearly and plateaued around 87% with increasing PETA concentration. This systematic study indicated that at least a 1.0 to 2.0 molar ratio of AA-BisAS50 to PETA is required to achieve a high degree of crosslinking with these oligomers. Experiments to investigate the effect of photoinitiator concentration on the degree of crosslinking were also conducted. Initiator concentration was varied from 2, 5 and 10 % relative to the total amount of AA-BisAS50 and PETA. Increasing the initiator concentration did not yield a significant increase in the crosslink density. In fact, gel

fractions decreased at higher initiator concentrations which we ascribed to radical recombination as a result of increasing radical concentration as previously addressed in the literature.[42]

### *2.4.5. The Effect of Film Thickness on Dense Film Degree of Crosslinking*

The Beer-Lambert law[43,44] states that absorbance correlates with molar absorptivity, concentration and thickness of the light absorbing medium. Therefore, high thickness of a dense film may have an adverse effect on the total degree of crosslinking. To investigate this theory, dense films with two distinct thicknesses were prepared. 150 μm films were cast directly from solution onto a glass substrate and 50 μm films were cast with the aid of a doctor blade. Gel fraction analysis of crosslinked films of both thicknesses showed no significant difference in the gel fractions. This behavior indicates that the UV absorption and photo-initiation was similar over the thickness range of dense films tested, likely due to the high energy output of the crosslinking instrument that was used.

### *2.4.6. The Influence of UV Exposure on Crosslinking of AA-BisAS50-PETA Films*

Bisphenol A-based poly(arylene ether sulfone) absorbs UV radiation between wavelengths 230 and 310 nm with a maxima around 270 nm.[45] Photo degradation, chain scission and crosslinking can occur in a broad temperature window ranging from ambient temperature to 250 ºC. The extent of these photochemical reactions depends on temperature and exposure time.[45,46] Elevated temperature extended exposure of high energy UV radiation is required to photochemically degrade Bisphenol A-based poly(arylene ether sulfone)s. Photocrosslinking of AA-BisASXX copolymers was conducted utilizing a broad range UV radiation (315-400 nm) wavelength outside the absorbance window of such copolymers. Additionally, materials were exposed to UV radiation for a limited time (not more than 150 s) and at 75 ºC; therefore any significant photo degradation was avoided through the choice of crosslinking conditions. In the

course of optimization of the crosslinking conditions, the effect of the length of UV exposure was studied. Duration of exposure to UV irradiation influenced the gel fractions of these crosslinked films. Increasing the UV exposure from 90 to 150 seconds resulted in up to a 20 % increase in gel fraction of the resultant crosslinked films. We ascribe increase this to the amount of energy absorbed during photocrosslinking reaction. Rate of photopolymerization ($R_p$) depends on the polymerization quantum yield ($\Phi_m$) which defines the number of monomer polymerized per photon absorbed and the amount of the energy absorbed at a specific wavelength ($I_{abs}$). The equation 2.4 shows the relationship between these variables. Similarly equation 2.5 where $R_i$ rate of initiation depends on the initiation quantum yield $\Phi_i$ which describes number of starting chains per photon absorbed and $I_{abs}$.[42] Therefore prolonging the UV exposure increases amount of energy absorbed $I_{abs}$ which both increases $R_p$ and $R_i$ of photopolymerization reaction.

$$R_p = \phi_m I_{abs}$$

**Equation 2.4.**

$$R_i = \phi_i I_{abs}$$

**Equation 2.5.**

**Table 2.1.** Gel fractions of crosslinked films with varied molar ratio as well as the duration of UV exposure in presence of DMPA 2% photoinitiator.

| AA-BISAS50: PETA Molar Ratio | % Gel Fraction after Photocrosslinking | | |
|---|---|---|---|
| | 30 seconds | 90 seconds | 150 seconds |
| 1.0 : 1.0 | 29.2 ± 1.8 | 62.7 ± 2.2 | 81.5 ± 0.1 |
| 1.0 : 1.5 | 29.8 ± 0.6 | 70.1 ± 1.2 | 85.1 ± 0.1 |
| 1.0 : 2.0 | 36.8 ±0.9 | 73.7 ± 2.4 | 87.0 ± 0.3 |
| 1.0 : 2.5 | 42.8 ± 1.0 | 74.8 ± 1.9 | 86.6 ± 0.4 |

The presence of the photoinitiator is crucial in achieving a high degree of crosslinking. Photocrosslinking experiments without a photoinitiator failed to produce crosslinked films, thus

this method requires a photoinitiator which is soluble in the casting solvent. DMPA is a water-insoluble photoinitiator; thus, HCPK was the choice of photoinitiator for crosslinking in aqueous solutions. To compare the performance of HCPK to DMPA, dense films were crosslinked utilizing HCPK instead of DMPA in DMAc solutions. Results indicated that crosslinked films in the presence of HCPK had slightly lower gel fractions than their DMPA crosslinked counterparts, plateauing around 80%. This may be attributed to the different quantum efficiency of each photoinitiator under these experimental conditions.

### *2.4.7. Preparation of UV Crosslinked AA-BisASXX from Benign Solutions*

In order to obtain very thin films with high water permeability, TFC membranes were prepared. Solutions containing AA-BisASXX, acrylate crosslinker and 2% photoinitiator were cast and UV crosslinked as the selective layer of the thin film composite on a commercial UDEL® foam support. DMAc, as well as other organic solvents such as DMF, DMSO, and NMP are good solvents for disulfonated oligomers, acrylate crosslinkers and photoinitiators. For example dense membrane casting solutions of BisAS50, PETA and DMPA were prepared in DMAc, however, these solvents also dissolve the UDEL®foam support which excludes them as potential casting solvents for TFC applications.[33] Table 2.2 shows the structures, and acronyms of crosslinkers and photoinitiators.

**Table 2.2.** Names and structures of crosslinking agents and photoinitiators

| | |
|---|---|
| 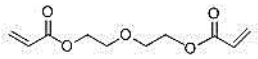 | di(ethylene glycol) diacrylate (DEGDA) |
| 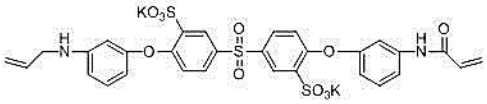 | sulfonated diphenyl acrylamide sulfone (SDPSDA) |
| 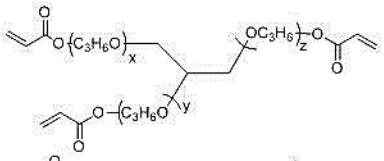 | glycerol propoxylate triacrylate (GPTA) |
| 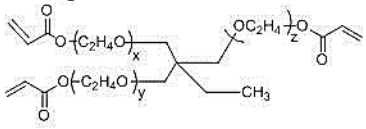 | trimethylolpropane ethoxylate triacrylate (TMPTA) |
| 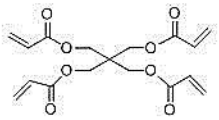 | pentaerythritol tetraacrylate (PETA) |
| 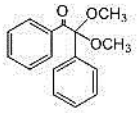 | 2,2-dimethoxy-2-phenylacetophenone (DMPA) |
| 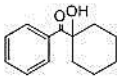 | 1-hydroxycyclohexyl phenyl ketone (HCPK) |

### *2.4.8. Aqueous Casting Solution*

Water is a non-solvent for UDEL® polysulfone. Dissolving reagents in a benign solvent for polysulfone foam preserves the foam structure which is crucial to prevent pore plugging, foam densification or collapse of the foam due to solvent swelling. Avoiding these undesirable outcomes is critical to preparing a thin film composite (TFC) with good transport properties. Developing a thin selective layer on the TFC membrane influences water flux as it is a function of membrane thickness.[29] Di(ethylene glycol) diacrylate (DEGDA) is a water soluble reagent which can be utilized as a crosslinker. In order to evaluate its effect on the degree of crosslinking of dense films, AA-BisAS50 and DEGDA were cast and photocrosslinked from DMAc solutions

in the presence of 2% HCPK photoinitiator. Films produced with this formulation showed slightly lower (~70%) gel fractions relative to films with PETA as the crosslinking agent. This result may be attributed to the lower functionality of DEGDA (f=4) compared to PETA (f=8). Replacing PETA with DEGDA yielded similar gel fractions (~75%) upon photo-crosslinking of the water-soluble oligomers AA-BisAS60, AA-BisAS80, and AA-BisAS100 from aqueous solutions. These results confirmed that sulfonated poly(arylene ether sulfone)s form photo-crosslinked networks from aqueous solutions. An acrylamide-endcapped derivative of SDCDPS (SDPSDA) was also employed as a crosslinker as an alternative to DEGDA. SDPSA crosslinked films had low gel fractions (varied between 9 and 21%) and lacked the mechanical properties that are required for TFCs.

#### *2.4.9. Water:Methanol (50:50, v:v) Casting Solution*

In addition to water, other polar solvents such as alcohols are also non-solvents for the UDEL® polysulfone support. The high degree of sulfonation of AA-BisASXX oligomers imparts high polarities of these materials. Di(ethylene glycol) diacrylate, glycerol propoxylate triacrylate, trimethylolpropane ethoxylate triacrylate are multifunctional acrylates and soluble in polar solvents such as alcohols including methanol and methanol-water mixtures. Trimethylolpropane ethoxylate triacrylate and glycerol propoxylate triacrylate have higher functionality than di(ethylene glycol) diacrylate (f=6 vs f=4) which is expected to provide a higher degree of crosslinking. AA-BisAS60 samples were crosslinked from water:methanol (50:50, v:v) solutions in the presence of HCPK. Trimethylolpropane ethoxylate triacrylate and glycerol propoxylate triacrylate containing solutions yielded films with gel fractions above 90%.

**Table 2.3.** Gel fractions of films crosslinked with di(ethylene glycol) diacrylate, trimethylolpropane ethoxylate triacrylate and glycerol propoxylate triacrylate in the presence of HCPK as the photoinitiator.

| Crosslinking Agent | Functionality | AA-BISAS60 % Gel Fraction |
|---|---|---|
| di(ethylene glycol) diacrylate | 4 | 82.5 ± 4.8 |
| trimethylolpropane ethoxylate triacrylate | 6 | 93.8 ± 5.3 |
| glycerol propoxylate triacrylate | 6 | 98.3 ± 0.7 |

Table 2.3 summarizes the results of gel fraction analysis of AA-BisAS60 films crosslinked with a 2.5 molar excess crosslinking agent. Both aqueous and water-methanol solutions produced high gel fractions that enabled successful fabrication of TFC membranes from benign solvents.

### *2.4.10. Water Uptake*

Crosslinking produced insoluble membranes from otherwise water-soluble non-film forming oligomers. Incorporating a hydrophilic comonomer imparts hydrophilicity into the hydrophobic polysulfones, and thus the degree of disulfonation correlates with water solubility of linear polymers and water uptake in crosslinked films. Water uptake of the BisAS60, BisAS80 and BisAS100 crosslinked films were measured to be 49, 90 and 143 % respectively. It is hypothesized that a selective layer with high water uptake cast on a UDEL® foam would result in a TFC membrane with significantly higher flux compared to a conventional TFC prepared with a crosslinked polyamide selective layer.

### *2.4.11. Surface Morphology of Photo-Crosslinked Membranes by Atomic Force Microscopy (AFM) and Scanning Electron Microscopy (SEM)*

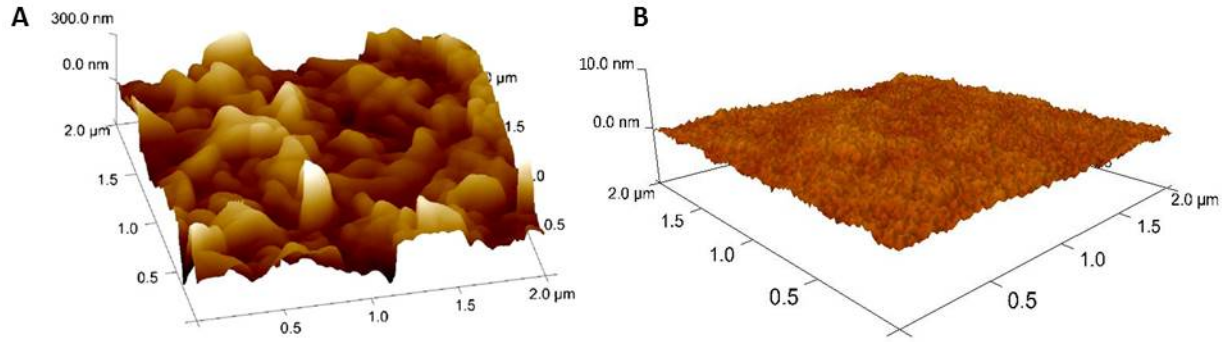


**Figure 2.6.** AFM Micrograph of (A) polyamide TFC membrane[33] and (B) AA-BisAS60 TFC membrane

State-of-the-art polyamide TFC membranes display a very different surface topography when compared to those of BisASXX TFC membranes due to differing methods of manufacture. The polyamide TFC membrane surface retains a rough surface texture as a result of the interfacial polymerization and simultaneous crosslinking reactions of aromatic tri-functional acid chlorides and aromatic diamines.[13,47] Root-mean-square (RMS) roughness can be used to quantify the surface roughness. RMS roughness is defined as the square-root of mean values of deviation of the indicated surfaces in AFM micrographs relative to a reference surface. This provides information about surface topography; therefore, smooth surfaces have small RMS values. Figure 2.6 (A) presents an AFM micrograph of a polyamide TFC membrane.[33] Fouling has been attributed to the rough surface structure of these polyamide membranes. The rough surface leads to membrane fouling which significantly diminishes water flux through the membranes over time. The fouling behavior has been explained by interaction energies between depositing particles and the rough surface. Interaction energies favor enhancement of membrane fouling,

thus, rougher surfaces suffer more from fouling compared to smoother surfaces.[9,10,48] Moreover, the AFM micrograph of a BisAS60 membrane shown in Figure 2.6 (B) shows a smooth surface which is confirmed by the RMS values of both surfaces. BisASXX TFC membranes have RMS surface roughness values between 0.4–0.7 nm whereas polyamide TFCs have been measured as 56.2 nm previously by our group.[33] The smooth surface of the photo-crosslinked membrane coupled with the hydrophilic surface will contribute to reducing fouling resistance and therefore maintaining water flux over the membrane service life. In addition to the surface smoothness and chemistry advantages, the poly(arylene ether sulfone)s have been shown to exhibit significant resistance to chlorine[16] meaning that incorporation of this class of polymer as a replacement for polyamides could lead to the use of chlorinated water treatment, eliminating a major issue of membrane biofouling in the future.

SEM micrographs confirm the smoothness of the photo-crosslinked membrane surface. Figure 2.7 displays cross-sectional SEM micrographs of a TFC with a photo-crosslinked BisAS60 skin. The skin surface illustrates the absence of the "ridges and valleys" type surface roughness that is inherent to interfacially polymerized crosslinked polyamide membranes. Cross-sectional images show a selective dense top layer with a relatively uniform thickness of approximately 600 nm and a smooth surface.

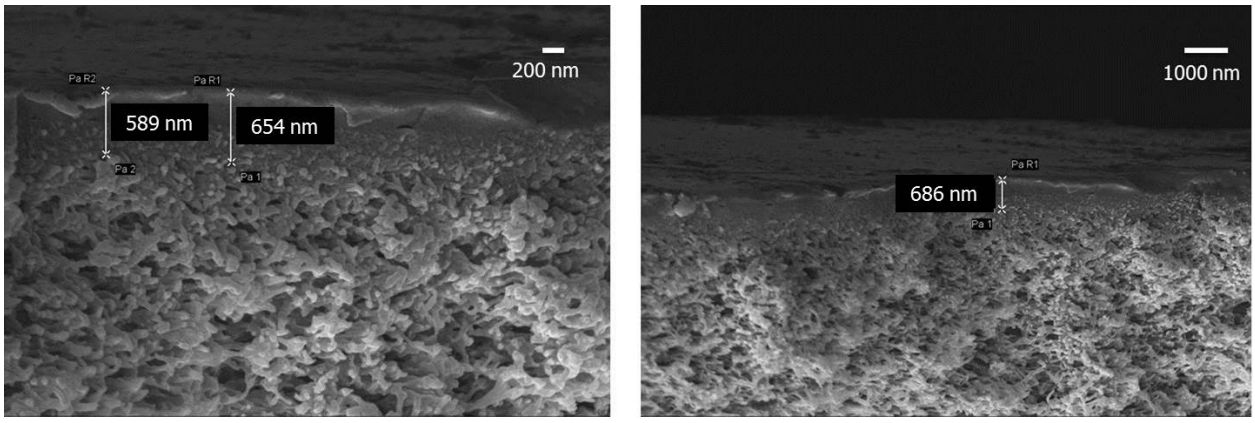


**Figure 2.7.** SEM Micrograph of AA-BisAS60 TFC membrane cross-sectional micrographs

### *2.4.12. Initial Investigations of Water Transport Properties*

The water flux and salt rejection were determined at 25 °C. The aqueous feed contained 2000 ppm NaCl, and the feed solution was circulated past the samples at a continuous flow rate of 4 (L/min) at 225 psi. The water flux and salt rejection results in table 2.4 indicate that these membranes have good water flux but insufficient salt rejection compared to the state of the art DOW membrane. This result was attributed to the possible presence of pinhole defects on the membrane surfaces. Further research will be required to prepare defect-free thin film composite membranes, which would lead to a several fold improvement in salt rejection values.

**Table 2.4**. Water Flux and salt rejection of thin film composite films

| Thin Film Composite | Pressure (psi) | Feed NaCl Concentration (ppm) | Permeate Flux (LMH) | NaCl Rejection (%) |
|---|---|---|---|---|
| DOW FilmTec FT35 | 225 | 2032 | 5.4±1.1 | 98.2±0.4 |
| AA-BisAS60 | 225 | 1990 | 9.0 ±2.0 | 72.1 ±2.7 |
| AA-BisAS80 | 225 | 2009 | 144.4 ± 7.6 | 46.6± 2.0 |
| AA-BisAS100 | 225 | 2006 | 169.5± 44.4 | 12.4 ± 1.1 |

## 2.5. Conclusions

Our research has focused on the synthesis of novel UV crosslinkable oligomers and preparation of TFC's utilizing a potentially aqueous based UV curing procedure. Novel UV crosslinkable oligomers were synthesized for use as water purification membranes and their structures were confirmed by $^{1}$H NMR. The UV crosslinking reaction conditions such as molar ratio of reactants, type and concentration of crosslinking agent and photoinitiator were evaluated. For the first time, UV crosslinking of partially or fully sulfonated, endgroup functionalized poly(arylene ether sulfone)s was demonstrated from methanol-water and aqueous solutions,

thereby enabling application onto a commercially utilized polysulfone support structure. UV crosslinking produced films with up to 98% gel fraction. Preparation of well-defined initial thin film composite membranes was demonstrated utilizing a rapid aqueous based casting/crosslinking procedure under UV radiation. AFM was used to demonstrate that the composite membranes exhibited two orders of magnitude lower RMS values compared to conventional polyamide composite membranes. Low RMS values indicate a smooth surface feature which has been shown to contribute to lower surface fouling. SEM micrographs corroborate the AFM measurements. Moreover, SEM cross-sectional micrographs showed the presence of a top selective layer with a thickness of ~600 nm. Further studies involving the preparation of defect-free membranes, water transport, salt rejection and fouling studies are underway.

### 2.6. Acknowledgements

The authors are grateful for the support of Dow Water & Process Solutions, Inc. This research was also supported by the U.S. National Science Foundation Partnerships for Innovation-Accelerating Innovative Research (PFI-AIR, Grant #1237858), Partnerships for Innovation (PFI) -Partnerships for Water Purification (Grant #0650277), and DMR 1263248 (MRI).

## 2.7. References:


1. Schneider, S. H., *Encyclopedia of climate and weather*. Oxford University Press: New York, 1996.
2. Service, R. F., Desalination Freshens Up. *Science* **2006,** 313, (5790), 1088-1090.
3. *Desalination: A National Perspective*. The National Academies Press: 2008.
4. Elimelech, M.; Phillip, W. A., The Future of Seawater Desalination: Energy, Technology, and the Environment. *Science (Washington, DC, U. S.)* **2011,** 333, (Copyright (C) 2012 American Chemical Society (ACS). All Rights Reserved.), 712-717.
5. Cadotte, J. E. Reverse osmosis membrane. US4259183A, 1981.
6. Cadotte, J. E.; King, R. S.; Majerle, R. J.; Petersen, R. J., Interfacial synthesis in the preparation of reverse osmosis membranes. *J. Macromol. Sci., Chem.* **1981,** A15, (Copyright (C) 2014 American Chemical Society (ACS). All Rights Reserved.), 727-55.
7. Cadotte, J. E.; Petersen, R. J.; Larson, R. E.; Erickson, E. E., A new thin-film composite seawater reverse osmosis membrane. *Desalination* **1980,** 32, (Copyright (C) 2014 American Chemical Society (ACS). All Rights Reserved.), 25-31.
8. Larson, R. E.; Cadotte, J. E.; Petersen, R. J., The FT-30 sea water reverse osmosis membrane - element test results. *Desalination* **1981,** 38, (Copyright (C) 2014 American Chemical Society (ACS). All Rights Reserved.), 473-83.
9. Lee, S.; Cho, J.; Elimelech, M., Influence of colloidal fouling and feed water recovery on salt rejection of RO and NF membranes. *Desalination* **2004,** 160, (1), 1-12.
10. Vrijenhoek, E. M.; Hong, S.; Elimelech, M., Influence of membrane surface properties on initial rate of colloidal fouling of reverse osmosis and nanofiltration membranes. *Journal of Membrane Science* **2001,** 188, (1), 115-128.
11. Park, H. B.; Freeman, B. D.; Zhang, Z.-B.; Sankir, M.; McGrath, J. E., Highly chlorine-tolerant polymers for desalination. *Angew. Chem., Int. Ed.* **2008,** 47, (Copyright (C) 2012 American Chemical Society (ACS). All Rights Reserved.), 6019-6024.
12. Orton, K. J. P.; Soper, F. G.; Williams, G., CXXXII.-The chlorination of anilides. Part III. N-chlorination and C-chlorination as simultaneous side reactions. *Journal of the Chemical Society (Resumed)* **1928**, (0), 998-1005.
13. Xie, W.; Geise, G. M.; Freeman, B. D.; Lee, H.-S.; Byun, G.; McGrath, J. E., Polyamide interfacial composite membranes prepared from m-phenylene diamine, trimesoyl chloride and a new disulfonated diamine. *J. Membr. Sci.* **2012,** 403-404, (Copyright (C) 2014 American Chemical Society (ACS). All Rights Reserved.), 152-161.
14. Do, V. T.; Tang, C. Y.; Reinhard, M.; Leckie, J. O., Degradation of Polyamide Nanofiltration and Reverse Osmosis Membranes by Hypochlorite. *Environ. Sci. Technol.* **2012,** 46, (Copyright (C) 2014 American Chemical Society (ACS). All Rights Reserved.), 852-859.
15. Kang, G.-D.; Gao, C.-J.; Chen, W.-D.; Jie, X.-M.; Cao, Y.-M.; Yuan, Q., Study on hypochlorite degradation of aromatic polyamide reverse osmosis membrane. *Journal of Membrane Science* **2007,** 300, (1–2), 165-171.
16. Park, H. B.; Xie, W.; Freeman, B. D.; Paul, M.; Roy, A.; Sankir, M.; Lee, H.-S.; Riffle, J. S.; McGrath, J. E. In *Chlorine-tolerant desalination membranes*, 2008; American Chemical Society: 2008; pp POLY-312.
17. Paul, M.; Park, H. B.; Freeman, B. D.; Roy, A.; McGrath, J. E.; Riffle, J. S., Synthesis and crosslinking of partially disulfonated poly(arylene ether sulfone) random copolymers

as candidates for chlorine resistant reverse osmosis membranes. *Polymer* **2008,** 49, (9), 2243-2252.
18. Zhang, Y.; Zhao, C.; Yan, H.; Pan, G.; Guo, M.; Na, H.; Liu, Y., Highly chlorine-resistant multilayer reverse osmosis membranes based on sulfonated poly(arylene ether sulfone) and poly(vinyl alcohol) for water desalination. *Desalination* **2014,** 336, (Copyright (C) 2014 American Chemical Society (ACS). All Rights Reserved.), 58-63.
19. Rose, J. B., Preparation and properties of poly(arylene ether sulphones). *Polymer* **1974,** 15, (7), 456-465.
20. Jennings, B. E.; Jones, M. E. B.; Rose, J. B., Synthesis of poly(arylene sulfones) and poly(arylene ketones) by reactions involving substitution at aromatic nuclei. *J. Polym. Sci., Polym. Symp.* **1967,** 16, (Copyright (C) 2012 American Chemical Society (ACS). All Rights Reserved.), 715-24.
21. Johnson, R. N.; Farnham, A. G.; Clendinning, R. A.; Hale, W. F.; Merriam, C. N., Poly(aryl ethers) by nucleophilic aromatic substitution. I. Synthesis and properties. *Journal of Polymer Science Part A-1: Polymer Chemistry* **1967,** 5, (9), 2375-2398.
22. Robeson, L. M.; Farnham, A. G.; McGrath, J. E., Dynamic mechanical characteristics of polysulfone and other poly(arylethers). *Midl. Macromol. Monogr.* **1978,** 4, (Copyright (C) 2012 American Chemical Society (ACS). All Rights Reserved.), 405-25.
23. Noshay, A.; Robeson, L. M., Sulfonated polysulfone. *J. Appl. Polym. Sci.* **1976,** 20, (Copyright (C) 2012 American Chemical Society (ACS). All Rights Reserved.), 1885-903.
24. Johnson, B. C.; Yilgor, I.; Tran, C.; Iqbal, M.; Wightman, J. P.; Lloyd, D. R.; McGrath, J. E., Synthesis and characterization of sulfonated poly(arylene ether sulfones). *J. Polym. Sci., Polym. Chem. Ed.* **1984,** 22, (Copyright (C) 2012 American Chemical Society (ACS). All Rights Reserved.), 721-37.
25. Ueda, M.; Toyota, H.; Ouchi, T.; Sugiyama, J.; Yonetake, K.; Masuko, T.; Teramoto, T., Synthesis and characterization of aromatic poly(ether sulfone)s containing pendent sodium sulfonate groups. *J. Polym. Sci., Part A: Polym. Chem.* **1993,** 31, (Copyright (C) 2012 American Chemical Society (ACS). All Rights Reserved.), 853-8.
26. Wang, F.; Hickner, M.; Kim, Y. S.; Zawodzinski, T. A.; McGrath, J. E., Direct polymerization of sulfonated poly(arylene ether sulfone) random (statistical) copolymers: candidates for new proton exchange membranes. *J. Membr. Sci.* **2002,** 197, (Copyright (C) 2012 American Chemical Society (ACS). All Rights Reserved.), 231-242.
27. Wang, F.; Kim, Y.; Hickner, M.; Zawodzinski, T. A.; McGrath, J. E., Synthesis of polyarylene ether block copolymers containing sulfonate groups. *Polym. Mater. Sci. Eng.* **2001,** 85, (Copyright (C) 2012 American Chemical Society (ACS). All Rights Reserved.), 517-518.
28. Wei, X.; Ho-Bum, P.; Cook, J.; Chang Hyun, L.; Gwangsu, B.; Freeman, B. D.; McGrath, J. E., Advances in membrane materials: desalination membranes based on directly copolymerized disulfonated poly(arylene ether sulfone) random copolymers. *Water Science & Technology* **2010,** 61, (3), 619-624.
29. Xie, W.; Cook, J.; Park, H. B.; Freeman, B. D.; Lee, C. H.; McGrath, J. E., Fundamental salt and water transport properties in directly copolymerized disulfonated poly(arylene ether sulfone) random copolymers. *Polymer* **2011,** 52, (9), 2032-2043.

30. Geise, G. M.; Park, H. B.; Sagle, A. C.; Freeman, B. D.; McGrath, J. E., Water permeability and water/salt selectivity tradeoff in polymers for desalination. *Journal of Membrane Science* **2011,** 369, (1–2), 130-138.
31. Xie, W.; Ju, H.; Geise, G. M.; Freeman, B. D.; Mardel, J. I.; Hill, A. J.; McGrath, J. E., Effect of Free Volume on Water and Salt Transport Properties in Directly Copolymerized Disulfonated Poly(arylene ether sulfone) Random Copolymers. *Macromolecules* **2011,** 44, (11), 4428-4438.
32. Xie, W.; Geise, G. M.; Freeman, B. D.; Lee, C. H.; McGrath, J. E., Influence of processing history on water and salt transport properties of disulfonated polysulfone random copolymers. *Polymer* **2012,** 53, (7), 1581-1592.
33. Lee, C. H.; McCloskey, B. D.; Cook, J.; Lane, O.; Xie, W.; Freeman, B. D.; Lee, Y. M.; McGrath, J. E., Disulfonated poly(arylene ether sulfone) random copolymer thin film composite membrane fabricated using a benign solvent for reverse osmosis applications. *Journal of Membrane Science* **2012,** 389, (0), 363-371.
34. Sankir, M.; Bhanu, V. A.; Harrison, W. L.; Ghassemi, H.; Wiles, K. B.; Glass, T. E.; Brink, A. E.; Brink, M. H.; McGrath, J. E., Synthesis and characterization of 3,3'-disulfonated-4,4'-dichlorodiphenyl sulfone (SDCDPS) monomer for proton exchange membranes (PEM) in fuel cell applications. *J. Appl. Polym. Sci.* **2006,** 100, (Copyright (C) 2012 American Chemical Society (ACS). All Rights Reserved.), 4595-4602.
35. Li, Y.; VanHouten, R. A.; Brink, A. E.; McGrath, J. E., Purity characterization of 3,3′-disulfonated-4,4′-dichlorodiphenyl sulfone (SDCDPS) monomer by UV–vis spectroscopy. *Polymer* **2008,** 49, (13–14), 3014-3019.
36. Kim, Y. S.; Hickner, M. A.; Dong, L.; Pivovar, B. S.; McGrath, J. E., Sulfonated poly(arylene ether sulfone) copolymer proton exchange membranes: composition and morphology effects on the methanol permeability. *J. Membr. Sci.* **2004,** 243, (Copyright (C) 2012 American Chemical Society (ACS). All Rights Reserved.), 317-326.
37. Harrison, W. L.; Hickner, M. A.; Kim, Y. S.; McGrath, J. E., Poly(arylene ether sulfone) copolymers and related systems from disulfonated monomer building blocks: synthesis, characterization, and performance - a topical review. *Fuel Cells (Weinheim, Ger.)* **2005,** 5, (Copyright (C) 2012 American Chemical Society (ACS). All Rights Reserved.), 201-212.
38. Park, H. B.; Freeman, B. D.; Zhang, Z.-B.; Fan, G.-Y.; Sankir, M.; McGrath, J. E., Water and salt transport behavior through hydrophilic-hydrophobic copolymer membranes and their relations to reverse osmosis membrane performance. *PMSE Prepr.* **2006,** 95, (Copyright (C) 2014 American Chemical Society (ACS). All Rights Reserved.), 889-891.
39. Sundell, B. J.; Lee, K.-s.; Nebipasagil, A.; Shaver, A.; Cook, J. R.; Jang, E.-S.; Freeman, B. D.; McGrath, J. E., Cross-Linking Disulfonated Poly(arylene ether sulfone) Telechelic Oligomers. 1. Synthesis, Characterization, and Membrane Preparation. *Ind. Eng. Chem. Res.* **2014,** 53, (Copyright (C) 2014 American Chemical Society (ACS). All Rights Reserved.), 2583-2593.
40. Jurek, M. J.; McGrath, J. E., Synthesis and characterization of amine terminated poly(arylene ether sulphone) oligomers. *Polymer* **1989,** 30, (8), 1552-1557.
41. Lyle, G. D.; Senger, J. S.; Chen, D. H.; Kilic, S.; Wu, S. D.; Mohanty, D. K.; McGrath, J. E., Synthesis, curing and physical behaviour of maleimide-terminated poly(ether ketones). *Polymer* **1989,** 30, (6), 978-985.

42. Fouassier, J. P.; Lalevée, J., *Photoinitiators for Polymer Synthesis*. Wiley: Somerset, NJ, USA, 2012.
43. Guvendiren, M.; Purcell, B.; Burdick, J. A., 9.22 - Photopolymerizable Systems. In *Polymer Science: A Comprehensive Reference*, Matyjaszewski, K.; Möller, M., Eds. Elsevier: Amsterdam, 2012; pp 413-438.
44. Krebs, R. E., *Encyclopedia of scientific principles, laws, and theories*. Greenwood Press: Westport, Conn., 2008.
45. Kuroda, S.; Nagura, A.; Horie, K.; Mita, I., Degradation of aromatic polymers. III. Crosslinking and chain scission during photodegradation of polysulfones. *Eur. Polym. J.* **1989,** 25, (Copyright (C) 2014 American Chemical Society (ACS). All Rights Reserved.), 621-7.
46. Yamashita, T.; Tomitaka, H.; Kudo, T.; Horie, K.; Mita, I., Degradation of sulfur-containing aromatic polymers: photodegradation of poly(ether sulfone) and polysulfone. *Polym. Degrad. Stab.* **1993,** 39, (Copyright (C) 2014 American Chemical Society (ACS). All Rights Reserved.), 47-54.
47. Mickols, W. E., 10.41 - Aromatic Poly(amides) for Reverse Osmosis. In *Polymer Science: A Comprehensive Reference*, Matyjaszewski, K.; Möller, M., Eds. Elsevier: Amsterdam, 2012; pp 831-848.
48. Elimelech, M.; Zhu, X.; Childress, A. E.; Hong, S., Role of membrane surface morphology in colloidal fouling of cellulose acetate and composite aromatic polyamide reverse osmosis membranes. *J. Membr. Sci.* **1997,** 127, (Copyright (C) 2012 American Chemical Society (ACS). All Rights Reserved.), 101-109.

## 3. Polyurethanes Containing Poly(arylene ether sulfone) and Poly(ethylene oxide) Segments for Gas Separation Membranes

*Ali Nebipasagil,[1] Jaesung Park,[2] Benjamin J. Sundell,[1] Sue J. Mecham,[1] Benny D. Freeman,[2] Judy S. Riffle[1] and James E. McGrath[1]*

[1]Macromolecules and Interfaces Institute, Virginia Polytechnic Institute and State University, Blacksburg, VA 24061, USA

[2]Department of Chemical Engineering, Center for Energy and Environmental Resources, The University of Texas at Austin, Austin, TX, 78758, USA

**Keywords**: Poly(arylene ether sulfone) copolymers; PEO polyurethane; Membranes

### 3.1. Abstract:

Poly(arylene ether sulfone) and poly(ethylene oxide) (PEO)-based segmented polyurethanes were synthesized for potential application as gas separation membranes. Poly(arylene ether sulfone) oligomers with controlled molecular weights (15,000 and 20,000 g/mol $M_n$) were prepared with phenol endgroups by nucleophilic aromatic substitution step growth polymerization of 4,4`-dichlorodiphenyl sulfone with a calculated excess of 4,4'-(propane-2,2-diyl) diphenol (bisphenol A). The oligomers with phenolic endgroups were subsequently reacted with ethylene carbonate to obtain aliphatic hydroxyethyl terminal functionality. The hydroxyethyl terminated oligomers and α,ω-hydroxy-terminated PEO were reacted with 4,4'-methylene diphenyl diisocyanate (MDI) to obtain segmented polyurethanes. Compositions with high poly(arylene ether sulfone) content relative to the hydrophilic PEO blocks were of particular interest due to their mechanical integrity. Size exclusion chromatograms confirmed

that the polyurethanes had high molecular weights with unimodal molecular weight distributions. DMA thermograms revealed polyurethanes with two distinct $T_g$'s. Incorporation of PEO into polyurethanes improved $CO_2/CH_4$, $CO_2/N_2$ and $CO_2/O_2$ selectivities but slightly decreased the permeability of all of the gases that were tested.

### 3.2. Introduction

Polymeric membrane-based gas separation is a prominent process used for diverse industrial applications. Membrane technology has several advantages over conventional separation methods including low energy consumption and lower capital investment.[1] Excellent reviews document the recent progress in membrane materials[2] and industrial applications[3-6] that include natural gas sweetening ($CO_2/CH_4$), post-combustion carbon capture ($CO_2/N_2$), syngas purification ($H_2/CO_2$), and food packaging, nitrogen blanketing and purge gas recovery applications ($O_2/N_2$).

Membrane gas transport is a pressure-driven permeation process. The solution-diffusion mechanism is the widely accepted model that describes gas transport through dense polymeric membranes.[1,6] According to this model, molecules dissolve in the high-pressure upstream surface of the membrane and then diffuse across the thickness of the membrane and desorb on the low-pressure downstream surface. Permeability is a material property that describes the quantity of gas that diffuses through a membrane at a given temperature. Permeability is the product of two coefficients: (1) solubility and (2) diffusivity of the gas in the membrane. Membrane selectivity is a material property that defines separation efficiency. The solution-diffusion model describes membrane selectivity as the ratio of permeabilities. Therefore, membrane selectivity depends on the ratio of diffusivity coefficients (diffusivity selectivity) and the ratio of solubility coefficients (solubility selectivity). The size of the gas molecule and polymer chain rigidity and free volume

determine the diffusivity selectivity, whereas the interactions between the polymer and the gas dominate the solubility selectivity.[7,8] Ideally a good gas separation membrane has both high selectivity and high permeability, however, a trade-off relationship has been identified between these properties. In 1991 Robeson mapped a large set of experimental data with selectivity versus permeability of gas pairs that showed an "upper bound" trade-off relationship.[7,9,10] Freeman et al. derived the fundamental basis for this phenomenon.[11]

$CO_2$ occurs as either a natural impurity or by-product of industrial chemical processes and must be separated from gas mixtures. Natural gas streams contain impurities such as $CO_2$ along with low molecular weight hydrocarbons and olefins. Hydrocarbons, $C_2H_6$ for example, is a commercially important petrochemical feed stock to be recovered and $CO_2$ has to be removed to meet natural gas pipeline specifications. This separation has been conducted via conventional methods such as chemical absorption with amine solutions, selective solvent (NMP) absorption, and cryogenic distillation. However, these methods are capital and energy intensive and require complex equipment and maintenance.[12-14]

Conventional commercial membranes used for $CO_2$ separations rely on diffusivity selectivity.[6,15] In a heavy/light gas separation such as $CO_2$ separation from $H_2$, $N_2$ or $O_2$, diffusivity selective membranes yield low pressure light gas products due to the higher permeability of light gases compared to $CO_2$.[15,16] At the end of the separation process the product must be re-pressurized and this complicates the process and increases the production cost. Thus, to separate $CO_2$ from a light gas stream a highly $CO_2$ permeable membrane is desired.

$H_2$ production involves steam reforming of hydrocarbons which produces a mixture of $H_2$ with $CO_2$ and other byproduct gases, therefore highly selective and permeable membranes are required for $CO_2/H_2$ separation.[17,18] $CO_2$ recovery from flue gas ($CO_2/N_2$) is increasingly

important due to increasing levels of $CO_2$ in the atmosphere. Coal power plants are responsible for about 40% of $CO_2$ emission in the US alone.[19,20] Carbon capture and sequestration that involves separating $CO_2$ from light gases such as $N_2$ and $O_2$ can significantly reduce $CO_2$ emissions.[20] Amine absorption is an effective method to capture $CO_2$, however, this expensive procedure significantly increases the cost of energy production.

Poly(ethylene oxide) (PEO) containing polymers have been identified and extensively investigated as promising membrane material candidates to selectively permeate $CO_2$.[17,18,21] PEO-containing linear polymer designs include PEO components in polyesters, polyamides, polyimides and segmented polyurethanes.[6] The PEO-containing polyurethanes and polyurethane ureas were studied for gas separation and PEOs with different molecular weights (400 and 600 g/mol) were used as soft segments.[22] In all cases the soft segment contents were less than 50% wt of the polymers. PEO600-containing membranes had higher $CO_2$ permeability and $CO_2/N_2$ and $CO_2/CH_4$ selectivities than the PEO400-containing membranes. This was due to better phase separation and larger PEO-domains in PEO600-containing membranes. The solubility selectivities for PEO600-containing membranes were between 183 and 198 whereas solubility selectivities for the same gas pair for PEO400-containing membranes were around 68 and 69. Moreover, the solubility selectivities of all membranes were significantly higher than their diffusivity selectivities for the $CO_2/N_2$ gas pair. Crosslinked membrane designs consisting of UV-crosslinked low molecular weight PEO diacrylates are particularly of interest.[13,15,18,23,24] The presence of polar ether oxygens leads to interactions between PEO repeat units and $CO_2$ molecules. This interaction enhances solubility and thus the solubility selectivity of $CO_2$ in gas streams.[6,24,25]

This current work reports the synthesis and characterization of segmented polyurethanes containing a major fraction of glassy poly(arylene ether sulfone) and a minor fraction of rubbery poly(ethylene oxide) for $CO_2$/light gas separations. Compositions with high poly(arylene ether sulfone) content relative to the PEO segments were investigated because of their desirable mechanical properties and phase separated morphologies. Viscoelastic properties, morphologies and transport properties are discussed. SEC confirmed that the polyurethanes had high molecular weights with unimodal molecular weight distributions.

## 3.3. Experimental

### *3.3.1. Materials*

4,4'-(Propane-2,2-diyl)diphenol (bisphenol A) and 4,4'-dichlorodiphenylsulfone (DCDPS, 99%) were kindly provided by Solvay and recrystallized from toluene before use. Potassium carbonate ($K_2CO_3$, ACS reagent grade, 99%) was purchased from Sigma Aldrich and dried in a vacuum oven at 150 ºC for at least 24 h. Ethylene carbonate (98%), trifluoroacetic anhydride (reagent plus grade, >99%) and 4Å molecular sieves were purchased from Sigma Aldrich and used as received. α,ω-Hydroxy-terminated poly(ethylene oxide) (PEO labeled $M_n$ 600, 1050, and 2050 g/mol) were purchased from Sigma Aldrich and dried at 80 ºC under vacuum for 24 h. The PEO oligomers were titrated by a method adapted from the literature.[26] Lithium Bromide (LiBr) was purchased from Sigma Aldrich and dried in a vacuum oven before use. Celite 545 was purchased from EMD chemicals. 4,4'-Methylene diphenyl diisocyanate (MDI, >99.5%) was graciously donated by Bayer Material Science. Calcium hydride (90-95%) was purchased from Alfa Aesar. *N,N*-Dimethylacetamide (DMAc, 99%) was purchased from Acros Organics. DMAc was dried over $CaH_2$ and distilled under reduced pressure before use. HPLC grade water was purchased from Spectrum Chemicals. Toluene, chloroform and isopropanol were purchased from Fisher Scientific and used as received. The SEC mobile phase,

*N*-methylpyrrolidone (NMP), was purchased from Fisher Scientific and distilled from phosphorus pentoxide under reduced pressure, and filtered through a 0.2 μm PTFE filter before use.

### *3.3.2. Synthesis of an ~15,000 g/mol ($M_n$) phenol-endcapped poly(arylene ether sulfone) (PAES15K)*

Poly(arylene ether sulfone) copolymers (PAES's) with controlled molecular weights were synthesized via nucleophilic aromatic substitution reactions. High monomer purity, high conversion and strict stoichiometric ratios are imperative to achieve targeted number average molecular weights. Bisphenol A and DCDPS were recrystallized from toluene to eliminate impurities. Bisphenol A was charged in excess to ensure a product with phenol endgroups of controlled molecular weight. The ratio of bisphenol A to DCDPS was calculated according to the Carothers equation to obtain the target molecular weight. A representative procedure adapted from the literature[27] which yielded a 15,100 g/mol phenol terminated PAES was conducted. Bisphenol A (49.072 g, 214.96 mmol), DCDPS (60.000 g, 208.96 mmol), $K_2CO_3$ (35.440 g, 256 mmol) and DMAc (320 mL) were charged into a three neck 500-mL flask equipped with a condenser, Dean-Stark trap filled with toluene, thermometer, nitrogen inlet/outlet, and mechanical stirrer. A thermocouple-regulated oil bath was used to control the reaction temperature. After the monomers dissolved, toluene (80 mL) was added to the reaction flask. The oil bath temperature was raised to 135 ºC to bring the solution to reflux. The reaction was azeotropically dehydrated for 6 h until all water condensation ceased. Subsequently, toluene in the Dean-Stark trap was drained and toluene in the reaction flask was completely removed by slowly increasing the temperature to 155 ºC. After 48 h, the reaction was cooled to room temperature. The polymer solution was diluted with 200 mL of chloroform and filtered to

remove salt and then was precipitated into stirring isopropanol as a white solid. The polymer was filtered, washed with isopropanol and dried under vacuum at 100 ºC for overnight. The next day, the polymer was re-dissolved in chloroform, filtered twice through Celite, and then was precipitated into isopropanol. The product was dried at 100 ºC under vacuum for 24 h. (yield>90 %) Synthesis of a PAES with a molecular weight of 20,500 g/mol was synthesized in a similar way utilizing a different stoichiometry of monomers calculated with the Carothers equation.

### *3.3.3. Conversion of phenol-endcapped copolymers to hydroxyethyl end-capped copolymers (PAES-hydroxyethyl)*

A representative reaction was conducted as previously reported.[27] Phenol terminated PAES (58.0 g, 3.84 mmol), ethylene carbonate (5.11 g, 76.8 mmol), $K_2CO_3$ (0.80 g, 7.68 mmol) were dissolved in DMAc (300 mL) in a 500-mL flask equipped with a magnetic stir bar. The flask was sealed with a rubber septum, flame dried and purged with $N_2$ to eliminate moisture. A large excess of ethylene carbonate was used to ensure 100% endgroup conversion. The flask was placed in an oil bath and the temperature was regulated with a thermocouple. The reaction flask was purged with nitrogen for 15 min, then the temperature was gradually increased to 125 ºC and the reaction was stirred for 24 h. The solution was cooled to room temperature and filtered to remove salt. The polymer was precipitated into isopropanol, filtered and dried at 100 ºC overnight under vacuum. The next day polymer was re-dissolved in chloroform, filtered twice through Celite, and then precipitated into isopropanol. The product was dried at 100 ºC under vacuum for 24 h. (yield>90 %)

### *3.3.4. Poly(arylene ether sulfone) and poly(ethylene oxide)-containing segmented polyurethanes*

A typical reaction to synthesize poly(arylene ether sulfone) (PAES) and poly(ethylene oxide) (PEO)-containing segmented polyurethanes was conducted as follows. PAES-hydroxyethyl (0.199 mmol, 3.009 g) and PEO with a titrated $M_n$ of 920 g/mole (0.445 mmol, 0.409 g) were dissolved in DMAc (16 mL) in a 100-mL three-neck round bottom flask. The flask was equipped with a condenser, Dean-Stark trap filled with toluene, thermometer, nitrogen inlet/outlet, and a mechanical stirrer. A thermocouple-regulated oil bath was used to control the reaction temperature. After PAES-hydroxyethyl and the PEO dissolved, toluene (10 mL) was added into the reaction flask. The solution was refluxed at 135 ºC for 4 h until all moisture was azeotropically removed with toluene. Subsequently toluene in the Dean-Stark trap was drained and the toluene in the reaction was completely removed. The reaction temperature was gradually reduced to 60 ºC. MDI (0.644 mmol, 0.168 g) was dissolved in 4 mL of anhydrous DMAc and added drop-wise into the stirring PAES-hydroxyethyl/PEO mixture. The reaction was purged with dry $N_2$ to protect the reactants from ambient humidity. Reaction vessel temperature was brought down to 60 ºC to start polyurethane synthesis. The reaction was allowed to proceed at 60 ºC for 6 h. The viscous polymer mixture was cooled to room temperature and diluted with 30 mL of DMAc. The solution was precipitated into stirring isopropanol as a white solid. The polymer was filtered, washed with isopropanol and dried under vacuum at 100 ºC for 24 h. (Yield>95 %) The acronym for each polyol (PAES and PEO) followed by number average molecular weight and weight percent in the polyurethane was used to identify each sample. For example PAES15K PEO1000(11) stands for a polyurethane containing a 15,000 g/mol hydroxyethyl end-capped poly(arylene ether sulfone) and 11 % by weight of a ~1000 g/mol poly(ethylene oxide).

### *3.3.5. Polymer Characterization*

*Nuclear magnetic resonance spectroscopy (NMR)*

$^1$H NMR analysis of the copolymers was performed on a Varian Inova spectrometer operating at 400 MHz. 64 scans for each spectrum were collected at ambient temperature. The spectra were obtained from a 0.25 g/mL 1-mL solution in $CDCl_3$.

*Size Exclusion Chromatography (SEC)*

The SEC mobile phase, *N*-methylpyrrolidone (NMP), was dehydrated. After distillation, a 0.05 M solution of lithium bromide (LiBr) was prepared in NMP. Three Agilent PL gel 10-µm mixed bed polystyrene-divinylbenzene columns 300 x 7.5 mm connected in series were used as the stationary phase. A system of multiple detectors connected in series was used for the analysis. A multi-angle laser light scattering (MALS) detector (DAWN-HELEOS II, Wyatt Technology Corporation, USA), operating at a wavelength of 658 nm, a viscometer detector (Viscostar, Wyatt Technology Corporation), and a refractive index detector operating at a wavelength of 658 nm (Optilab T-rEX, Wyatt Technology Corporation) provided online results. The system was corrected for interdetector delay, band broadening, and the MALS signals were normalized using a 21,720 g/mole polystyrene standard obtained from Agilent Technologies with each set of samples. Data acquisition and analysis was completed using Astra 6 software from Wyatt Technology Corporation. The samples were analyzed at a concentration of approximately 3 mg/mL in NMP + 0.05 M LiBr at a flow rate of 0.5 mL/min. The polyurethanes were analyzed via light scattering. The $d_n/d_c$ was also calculated using the Astra 6 software to calculate the $d_n/d_c$ by assuming 100% recovery of the sample.

*Dynamic Mechanical Analysis (DMA)*

DMA was performed on a TA Instruments Q800 Dynamic Mechanical Analyzer in tension mode at a frequency of 1 Hz, an oscillatory amplitude of 15 μm, and a static force of 0.01 N. The temperature ramp was 2 °C/min.

*Differential Scanning Calorimetry (DSC)*

DSC was conducted on a TA Instruments Q2000, under nitrogen at 10 ºC/min heating/cooling rate. A heat/cool/heat protocol was used. First, samples were equilibrated at -85 ºC, then heated up to 200 ºC and cooled back down to -85 ºC. In the last cycle, it was heated up to 250 ºC, second heat is shown.

*Tensile Testing (Instron)*

Micro dogbone tensile specimens were prepared using a cutting die. Tensile samples were prepared and tested according to ASTM standard D1708-13. Stress-strain tests were performed at ambient temperature with a strain rate of 0.25 mm/min.

*Water Uptake*

Water uptakes of polyurethanes were measured gravimetrically. Films were dried at 120°C under vacuum overnight to obtain the dry weight ($W_{dry}$). The films were then immersed in DI water at ambient temperature for at least 48 h. The films were removed, quickly blotted to remove water droplets on the surface and weighed to obtain the wet weight ($W_{wet}$). Equation 3.1 shows the calculation used to determine the gravimetric percent water uptake.

$$\text{Water Uptake}(\%) = \frac{W_{wet} - W_{dry}}{W_{dry}} \times 100$$

**Equation 3.1**

*Gas permeation Measurements*

Gas permeation properties were measured using a constant volume/ variable pressure method. The upstream portion of the system was constructed from commercially available Swagelok parts using Swagelok tube fittings. Welded joints and VCR connections were used in the downstream portion to minimize leaks. The membrane was housed in a stainless steel Millipore filter holder (Millipore, Billerica, MA, USA) with an included support. A Honeywell Super TJE 1500 psi (10.3 MPa) transducer (Honeywell Sensotec, Columbus, Ohio, USA) was used to track upstream pressure, and a MKS Baratron 626 transducer (MKS, Andover, MA, USA) was used to measure downstream pressure. The permeabilities of gases were measured at 35 ºC at 10 atm feed pressure.

## 3.4. Results and Discussion

### *3.4.1. Synthesis of phenol and hydroxyethyl end-capped PAES copolymers (Figure 3.1)*

PAES polymers with phenol endgroups were synthesized via a nucleophilic aromatic substitution reaction (Figure 3.1) between bisphenol A and DCDPS. The targeted number average molecular weights were calculated utilizing the Carothers equation. The amount of excess bisphenol A relative to DCDPS were calculated to achieve either 15,000 or 20,000 g/mole phenol end-capped PAES's.

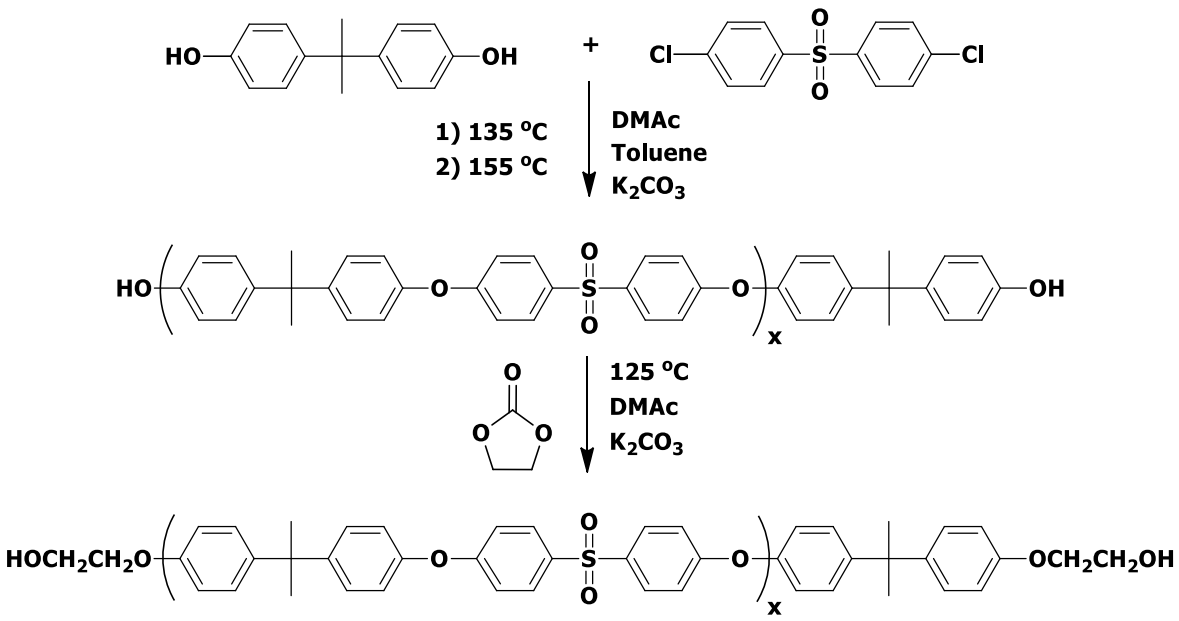


**Figure 3.1.** Synthesis of a hydroxyethyl terminated PAES with controlled molecular weight

The $^{1}$H NMR spectrum in Figure 3.2 illustrates the differences between the chemical compositions of phenol (Figure 3.2 A) and hydroxyethyl terminated (Figure 3.2 B) PAES polymers and validates their endgroup functionality. The bisphenol A endgroup phenol protons resonate at 6.75, 6.78 ppm (f) and at 7.07, 7.09 ppm (g) respectively. Backbone DCDPS protons adjacent to the sulfonyl group (a) resonate at 7.84 and 7.86 ppm and protons next to the ether linkage (b) resonate at 7.23 and 7.25 ppm respectively. The DCDPS backbone peak (b) overlaps partially with the solvent peak (chloroform at 7.26 ppm). Isopropylidene protons (e) of the bisphenol A groups resonate at 1.70 ppm. Doublets at 6.93, 6.95 and 6.99, 7.01 were assigned to backbone aromatic bisphenol A peaks (d) and (c) respectively. The number average molecular weights of PAES's were calculated using the endgroup (f) peak and the backbone peaks (c) and (d). This calculation assumes that the polymer chains were quantitatively terminated with bisphenol A groups. The absence of DCDPS endgroup peaks supports this assumption. The

NMR endgroup analyses yielded 15,100 and 20,500 g/mole number average molecular weights, which was in excellent agreement with the targeted number average molecular weights.

Chemical modification of bisphenol A endgroups with ethylene carbonate is an efficient reaction.[27-29] Bisphenol A terminated PAES polymers were reacted with a large excess of ethylene carbonate in the presence of $K_2CO_3$. This reaction converted the phenolic endgroups of the PAES polymers to aliphatic hydroxyethyl telechelic functionalities (Figure 3.1). Nucleophilic attack of the phenoxide ion on one of the alkyl carbons of the ethylene carbonate opens the ethylene carbonate ring, and loss of $CO_2$ yields the hydroxyethyl functional polymer.[28] $^1$H NMR (Figure 3.2 B) demonstrated the presence of aliphatic ethyl protons resonating at 3.95 and 4.05 ppm, which confirms that this reaction produced hydroxyethyl functionalities under relatively mild conditions. Under these reaction conditions, NMR peak integrations showed approximately one hydroxyethyl unit per phenol endgroup.

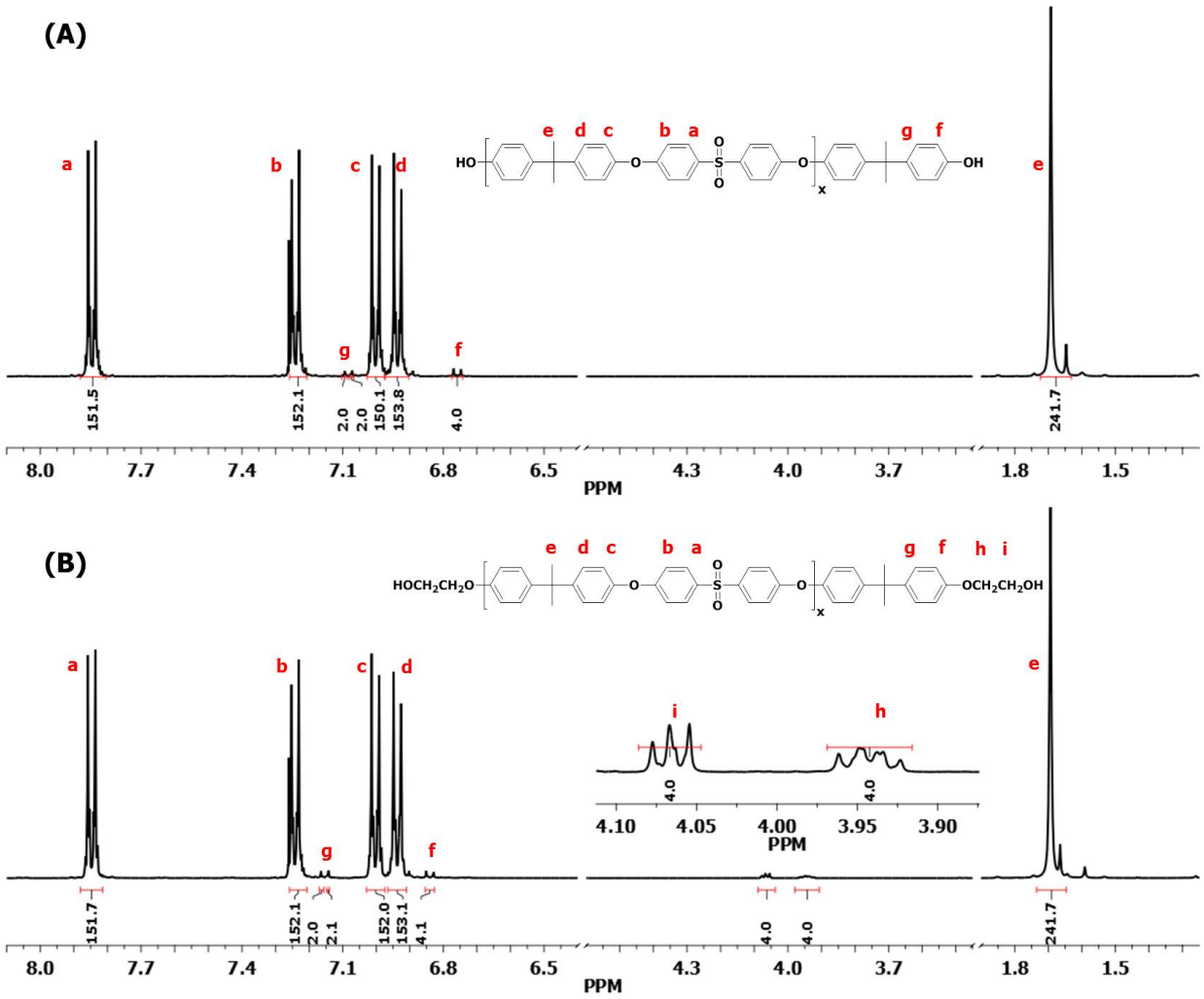


**Figure 3.2.** [1]H NMR spectra of (A) phenol and (B) hydroxyethyl end-capped PAES copolymers

[19]F NMR is a versatile method which can distinguish fluorine modified aliphatic hydroxyl endgroups versus fluorine modified phenol endgroups.[30] Trifluoroacetic anhydride derivatization of phenol and hydroxyethyl terminated polymers produce distinct [19]F signals due to the different shielding effects of their respective trifluoroacetates.[30] Phenol and hydroxyethyl terminated polymers were reacted with trifluoroacetic anhydride to prepare trifluoroacetates. This derivatization quantitatively verified the complete conversion of bisphenol A endgroups to hydroxyethyl functionalities (Figure 3.3).

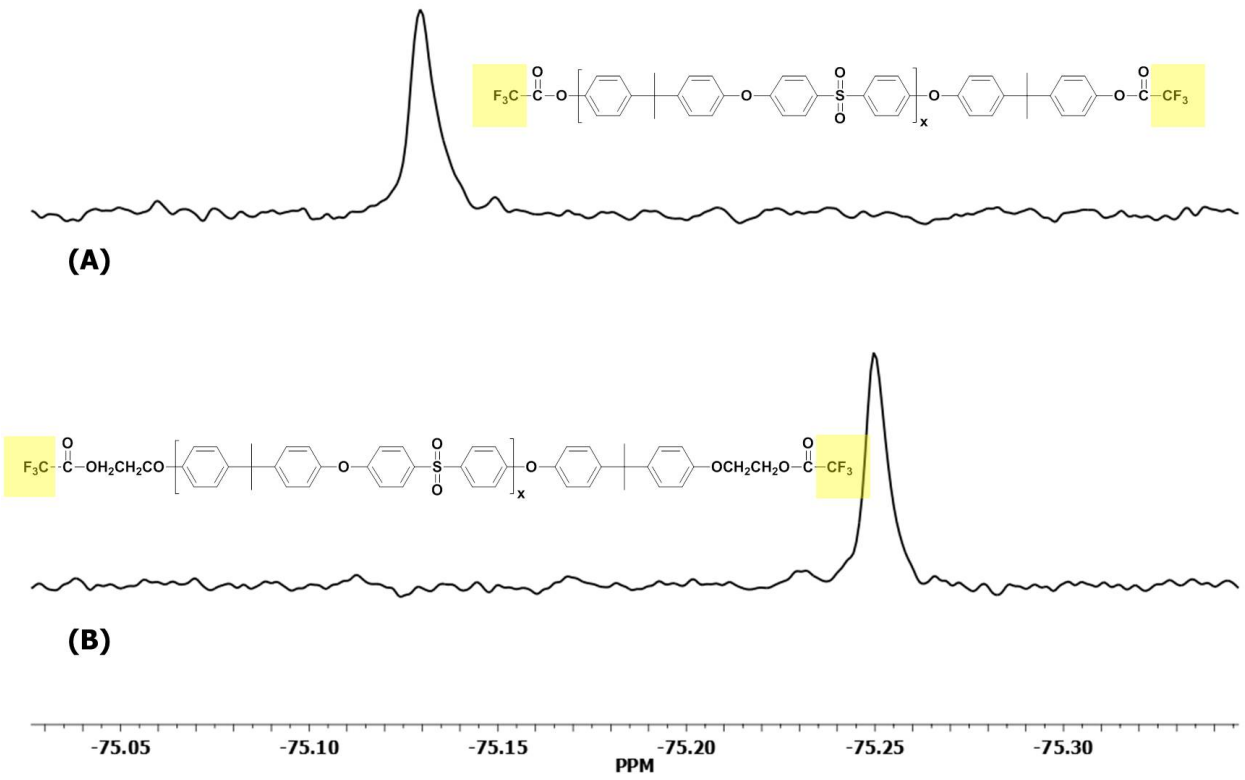


**Figure 3.3.** $^{19}F$ NMR spectra of (A) trifluoroacetic anhydride end-capped phenol- and (B) hydroxyethyl end-capped PAES's

### *3.4.2. Synthesis of poly(arylene ether sulfone) and poly(ethylene oxide) containing segmented polyurethanes (Figure 3.4)*

Primary alcohols are more reactive towards isocyanates in comparison to secondary and tertiary aliphatic alcohols and phenols.[31,32] Isocyanate reacts with proton-bearing nucleophiles via nucleophilic addition across the carbon-nitrogen bond of the NCO group. In this perspective, phenols (pKa~10) react much more slowly than the aliphatic alcohols (pKa~16) due to the large difference between their acidities. The phenol-isocyanate reaction yields unstable polyurethanes compared to polyurethanes derived from aliphatic alcohols. Moreover, the phenol-isocyanate

bond is reversible at temperatures as low as 100 ºC.[31] Bisphenol A terminated PAES's were modified with ethylene carbonate to yield oligomers with primary hydroxyl endgroups.[31] Hydroxyethyl derivatized PAES and a series of PEO oligomers were utilized as polyols for the synthesis of segmented polyurethanes. Accurately determining the hydroxyl content of PEO oligomers ensured the stoichiometric balance between polyol and diisocyanate monomers. The PEO oligomers were acetylated with acetic anhydride, excess anhydride was hydrolyzed, then the acetic acid content was back-titrated with potassium hydroxide.[26] Isocyanates are very susceptible to reactions with water. Therefore, PAES and the PEO were dried overnight at 100 ºC under vacuum to remove moisture. Toluene was used as the azeotropic solvent to ensure that the PAES-PEO mixture was moisture-free prior to addition of isocyanate. The viscosity of the reaction solution visibly increased after 1 hour following the addition of MDI.

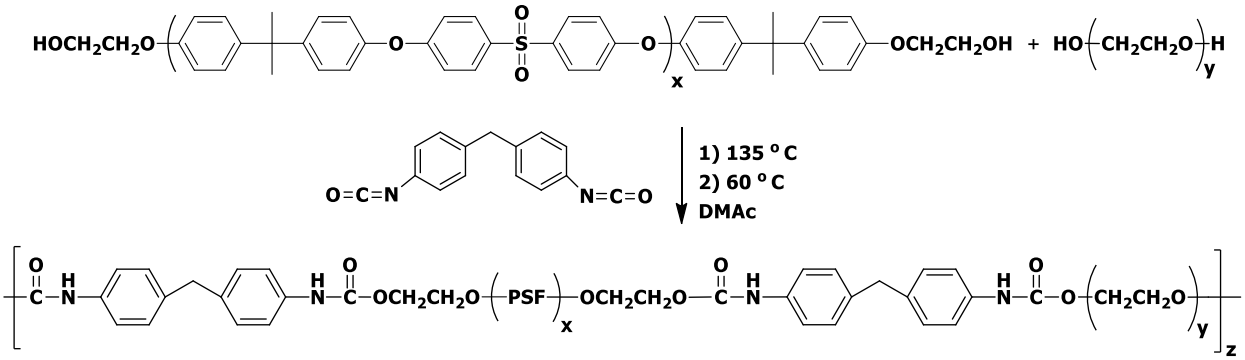


**Figure 3.4.** Synthesis of poly(arylene ether sulfone) and poly(ethylene oxide) containing polyurethanes

Figure 3.5 presents the $^{1}H$ NMR spectra comparison of PAES-PEO segmented polyurethanes. PAES15K PEO(0), was synthesized utilizing only PAES as a control. In addition to PAES-polyol backbone peaks, the incorporation of PEO segments resulted in appearance of broad ethylene peaks at 3.63 ppm. The intensity of the ethylene peaks grew as the weight percent

PEO increased in the polyurethanes. The control polyurethane did not exhibit these resonances as anticipated.

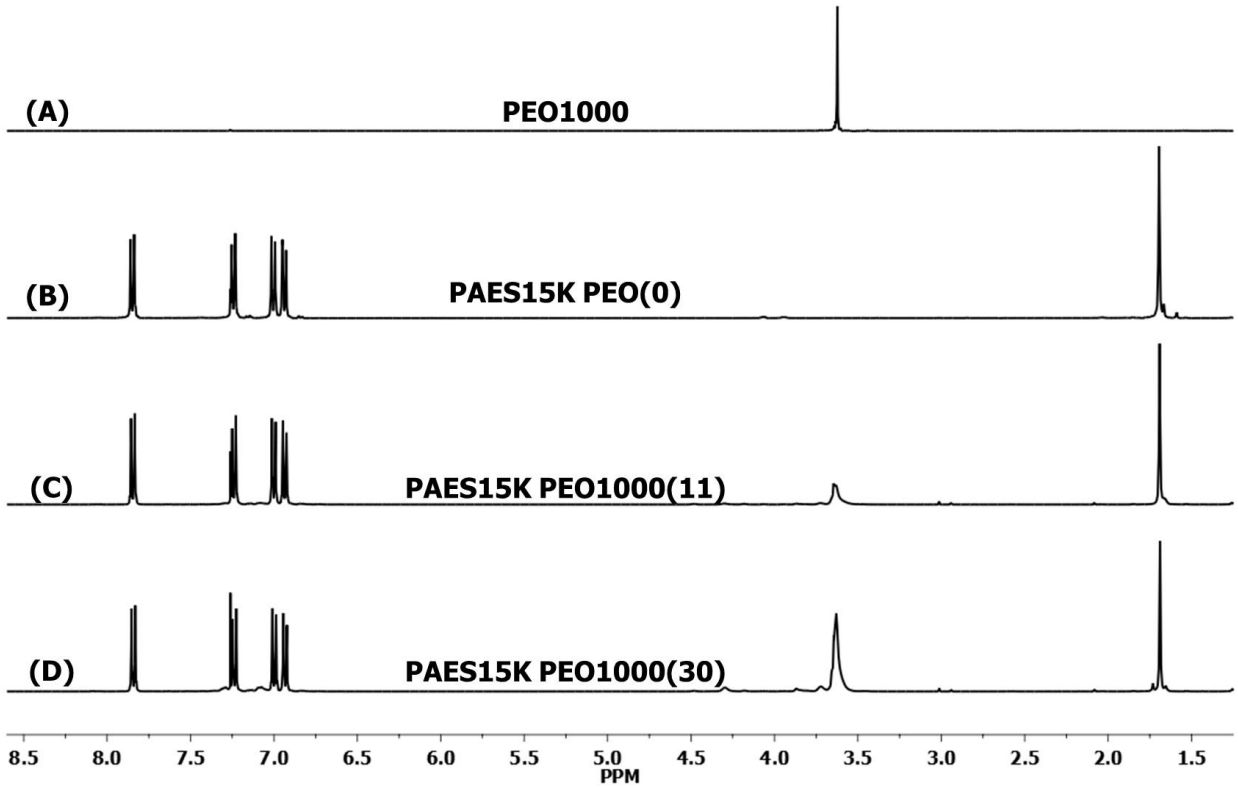


**Figure 3.5** $^{1}$H NMR spectra of (A) PEO1000 polyol, (B)PAES15K-hydroxyethyl that was chain extended with MDI, (C and D) the polymer with PAES15K-hydroxyethyl and 11wt.% and 30 wt.% PEO1000

SEC was utilized to determine the molecular weights and molecular weight distributions of the segmented polyurethanes. The SEC mobile phase was 0.05 M LiBr solution in NMP. LiBr salt was added to reduce intermolecular polymer interactions. Figure 3.6 shows the comparison of SEC chromatograms of the PAES-hydroxyethyl and the 0, 11 and 30 wt % PEO containing polyurethanes. All of the polymers yielded unimodal symmetrical chromatograms. The reaction of hydroxyethyl terminated PAES with MDI resulted in chain extension of PAES-hydroxyethyl

which increased the molecular weight of the product. This increase was reflected as a shift to lower elution volumes in the chromatograms.

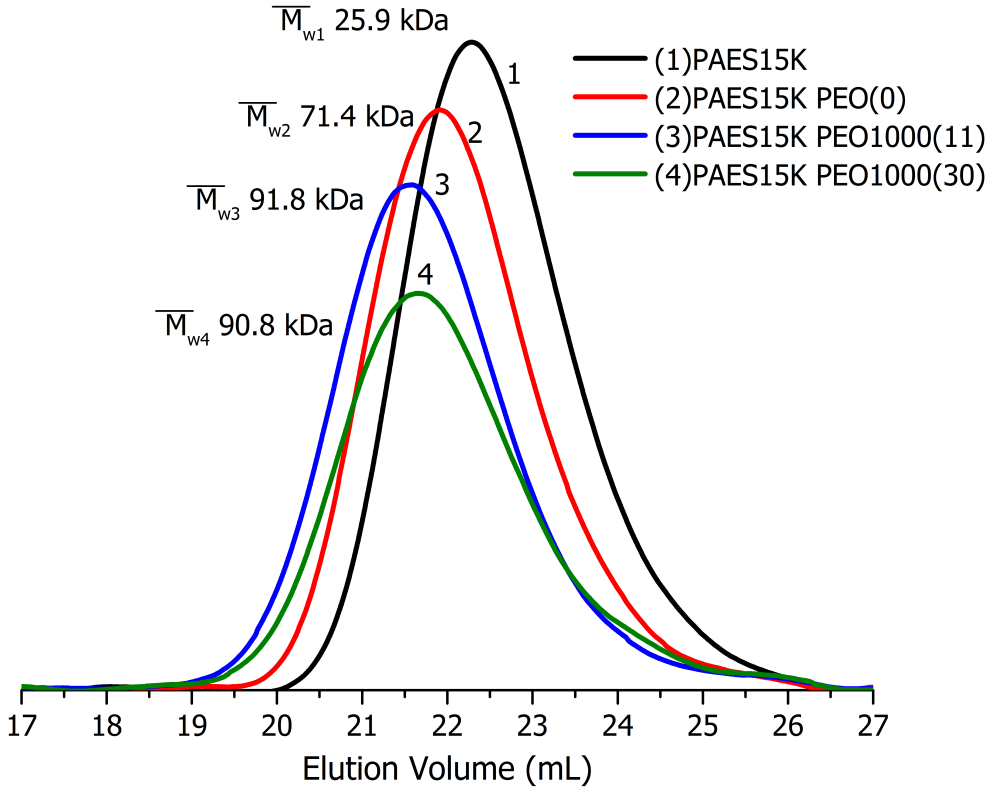


**Figure 3.6**. SEC chromatograms of (1) PAES15K-hydroxyethyl, (2)PAES15K-hydroxyethyl that was chain extended with MDI, (3 and 4) the polyurethane with PAES15K-hydroxyethyl and 11wt.% and 30 wt.% PEO1000

The solid state thermal properties of the PAES-PEO containing polyurethanes were investigated to probe the phase structures of the membranes (Figure 3.7). DSC thermograms of the polyurethanes revealed that the PAES 15K PEO1000(11) have one $T_g$ around 134 ºC, whereas PAES 15K PEO1000(30) showed two distinct $T_g$ transitions at -33 ºC and 110 ºC. The $T_g$ at -33 ºC, corresponding to the PEO segments, was detected as the PEO content was increased

from 11 to 30 weight percent, which indicated phase separation between PAES and PEO segments. This PEO $T_g$ was higher than any value reported in the literature.[33]

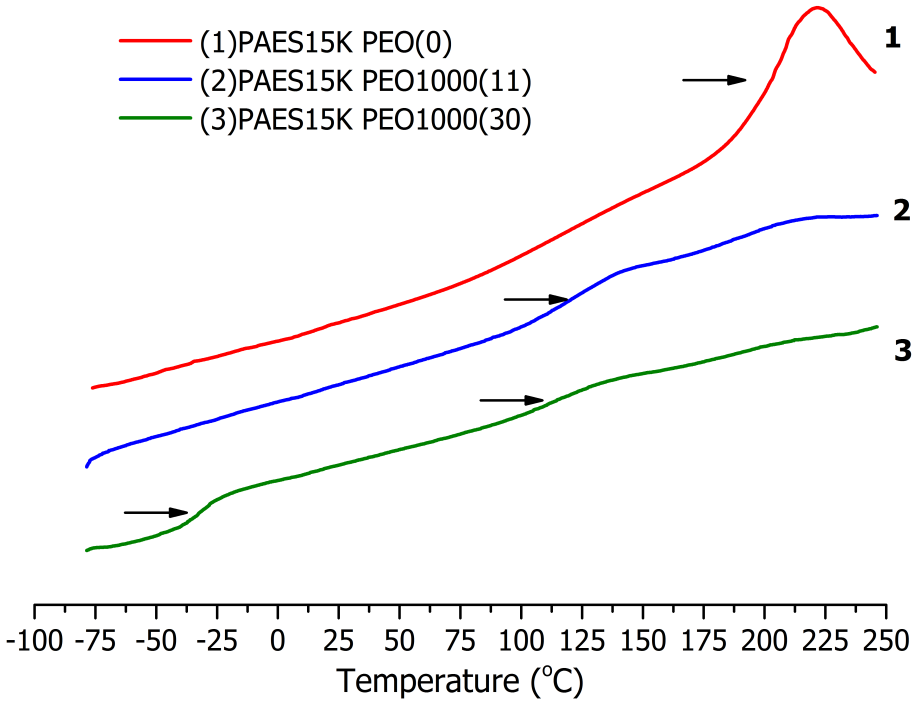


**Figure 3.7.** DSC Thermograms(exo down) of polyurethanes (1)PAES15K-hydroxyethyl that was chain extended with MDI, (2 and 3) containing PAES15K-hydroxyethyl and 11wt.% and 30 wt.% PEO1000

The $T_g$ of the control PAES 15K PEO (0) polyurethane was observed around 200 ºC which was slightly higher than the $T_g$ of bisphenol A polysulfone (UDEL®) at 186 ºC.[33] The difference between the $T_g$'s was attributed to decreasing concentration of the mobile endgroups with increase in the molecular weight due to chain extension of the rigid polysulfone with MDI. The $T_g$'s of both copolymer compositions (examples of thermograms of polyurethanes

containing the 1000 g/mol $M_n$ PEO are shown in Figure 3.7) indicate at least partial phase mixing between the PAES and PEO segments. The transitions in the DSC thermograms of the PEO-containing polyurethanes above 100 ºC are attributed to PAES-rich segments. This phenomenon occurs due to phase mixing of the PEO and PAES phases and plasticization of the PAES by short, flexible PEO segments. Phase behavior of a variety of polysulfone- and disulfonated polysulfone-PEO blends has been investigated and the compatibility of these blends has been previously established.[34-36] Due to their high $T_g$'s disulfonated polysulfones are susceptible to degradation during processing by melt extrusion. In disulfonated polysulfones $T_g$ increases and degradation temperature generally decreases with increasing degree of sulfonation. Low molecular weight PEOs can depress the polysulfone $T_g$ to the 100 to 150 ºC range.[35] Moreover blends of disulfonated polysulfones and PEO show a single $T_g$ [35] which indicates miscibility between these two polymers, and these blends show shear thinning rheological behavior due to relaxation of entanglements.[34]

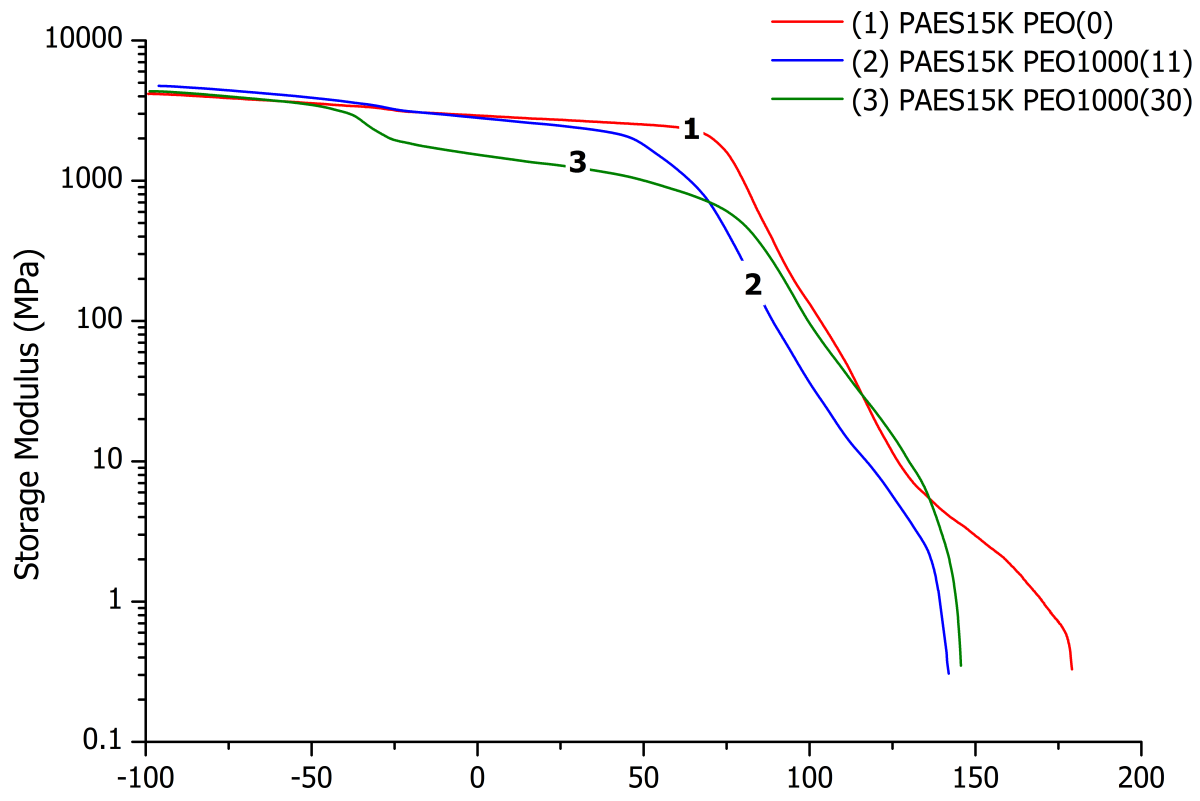


**Figure 3.8.** DMA thermograms(exo down) of polyurethanes (1)PAES15K-hydroxyethyl that was chain extended with MDI, (2 and 3) containing PAES15K-hydroxyethyl and 11wt.% and 30 wt.% PEO1000

DMA thermograms revealed more information about the thermal properties of the polyurethanes than DSC (Figure 3.8). DMA of PAES 15K PEO (0) showed two separate but close thermal transitions: an α transition just above 175 ºC and an additional thermal transition undetected by DSC around 90 ºC. This signal has been attributed to the β relaxation of bisphenol A-containing polysulfone chains.[33] These two transitions cover a broad temperature range and almost appear to be a single transition in the storage modulus plot of PAES 15K PEO (0). DMA thermograms of the polyurethanes containing 10 and 30 weight % of PEO exhibit the $T_g$

depression also observed in DSC. Consequently $T_g$ overlaps with the β relaxation of PAES-hydroxyethyl. Due to this overlap, DMA thermograms of the PEO-containing polyurethanes exhibit only a single thermal transition at temperatures starting around the expected β relaxation. Moreover, the DMA thermogram of the PAES 15K PEO (30) showed he expected $T_g$ around -30 ºC (PEO segment $T_g$), that is consistent with the DSC data.

Mechanical robustness is a critical quality for dense gas separation membranes as they must withstand feed pressures up to 10 atmospheres.[3] Figure 3.9 shows representative stress-strain curves of three polyurethanes comprised of 0, 11 and 30 weight % PEO segments. The incorporation of PEO into these polymers resulted in increasing elongations at break and lower failure stresses. While 11 wt% PEO toughens the segmented polyurethanes without a large decrease in break stress, raising the PEO amount to 30 percent yields a more significant reduction in stress at break. Table 3.1 and Figure 3.9 display the tensile properties of the polymers. The results of different specimens were quite consistent.

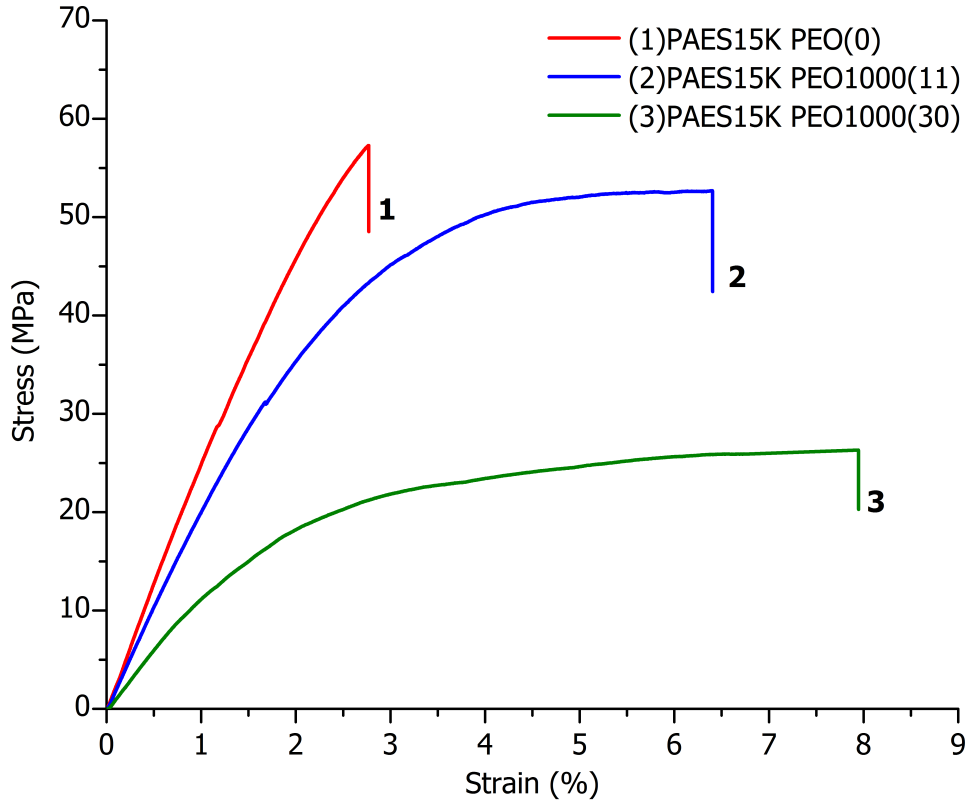


**Figure 3.9.** Representative tensile plots of polyurethanes (1)PAES15K-hydroxyethyl that was chain extended with MDI, (2 and 3) containing PAES15K-hydroxyethyl and 11wt.% and 30 wt.% PEO1000

**Table 3.1.** Tensile properties of polyurethanes in Figure 3.9

| Sample | Strain at Break (%) | Stress at Break (MPa) |
|---|---|---|
| PAES15K PEO1000(0) | 2.76±0.26 | 49.60±6.73 |
| PAES15K PEO1000(11) | 6.93±0.23 | 42.00±8.08 |
| PAES15K PEO1000(30) | 8.71±0.67 | 21.63±3.42 |

The influence of PAES or PEO polyol $M_n$ on tensile properties was much more limited. Comparison of segmented polyurethanes containing 15K and 20K PAES oligomers did not show a substantial difference in strain or stress at break. Table 3.2 compares three segmented

polyurethanes which contain PEO 600, 1000 and 2000 polyols. The molecular weight of these three polyurethanes are within a narrow range, thus, the influence of prepolymer molecular weight was limited. Stress and strain at break of these materials are within the error of the experiments.

**Table 3.2.** Tensile properties of PAES15K-hydroxyethyl and ~30 wt.%, PEO600, 1000 and 2000 containing polyurethanes

| Sample | Strain at Break (%) | Stress at Break (MPa) |
|---|---|---|
| PAES15K PEO 600(29) | 8.31±1.13 | 21.51±0.54 |
| PAES15K PEO1000(30) | 8.71±0.67 | 21.63±3.42 |
| PAES15K PEO2000(33) | 6.92±0.69 | 22.44±2.94 |

Copolymerization of PEO with hydrophobic polysulfones introduced hydrophilic character into these membranes. Water uptake is often used to evaluate the hydrophilicity of a membrane and the weight percent of increasing PEO correlated with increased water uptake. Table 3.3 presents the water uptake data of segmented polyurethanes with a 15K PAES. Increasing the composition of PEO from 0 to 30 wt% in these segmented copolymers lead to a modest increase in the water uptake of between 3.5 and 6.3 % This very small increase in water uptake was attributed to the partial phase mixing between hydrophilic and hydrophobic segments of these polyurethanes. Small differences between the water uptake values of these polyurethanes were observed based on the PEO molecular weight. In general, water uptake increased with increasing PEO molecular weight, which may be due to the increasing concentration of PEO-rich domains in these polyurethanes.

**Table 3.3.** Water uptake of segmented PAES-PEO polyurethanes

| Sample | % Water Uptake |
|---|---|
| PAES 15K | < 1 |
| PAES 15K PEO(0) | < 1 |
| PAES 15K PEO600(11) | < 1 |
| PAES 15K PEO600(29) | 3.4 ± 0.4 |
| PAES 15K PEO1000(11) | < 1 |
| PAES 15K PEO1000(30) | 4.9 ± 0.3 |
| PAES 15K PEO2000(11) | < 1 |
| PAES 15K PEO2000(33) | 6.3 ± 0.5 |

Polymer composition is one of the main contributors that define polymer performance. Initial single gas transport experiments showed a close correlation between gas permeability/selectivity and polyurethane PEO-content. Table 3.4 presents single gas transport properties of PEO1000-containing PAES 15K polyurethane membranes. Membrane permeability decreased for a variety gasses that have different kinetic diameters with increasing PEO-content in the polyurethane composition. This inverse result was attributed to partial phase mixing between PAES and PEO segments of polyurethanes. On the contrary to this decrease in permeability, an increase in $CO_2/CH_4$ and $CO_2/N_2$ selectivity was observed. It was reasoned that due to high solubility coefficient of $CO_2$ in PEO, $CO_2$ permeate relatively faster and $CO_2$ selectivity over $CH_4$ and $CO_2$ became favorable as PEO content increased up to 30 weight percent. For example, $CO_2/CH_4$ selectivity increase from 25 for PAES 15K PEO(0) to 34 for PAES 15K PEO1000(30) membranes. Increase in polyurethane PEO-content made almost no-change for selectivity of other gas pairs such as $O_2/N_2$.

**Table 3.4.** Initial gas transport properties of PAES15K-hydroxyethyl and PEO1000-containing polyurethane membranes

| Permeability (Barrer) | | | | | | |
|---|---|---|---|---|---|---|
| PAES 15K | He | $H_2$ | $CO_2$ | $O_2$ | $N_2$ | $CH_4$ |
| PEO(0) | 9.4 | 9.5 | 3.1 | 0.779 | 0.123 | 0.125 |
| PEO1000(11) | 5.3 | 4.3 | 1.2 | 0.253 | 0.036 | 0.035 |
| PEO1000(30) | 4 | 3.5 | 1.6 | 0.248 | 0.034 | 0.045 |
| Selectivity | | | | | | |
| PAES 15K | $CO_2/CH_4$ | $CO_2/N_2$ | $CO_2/O_2$ | $CO_2/H_2$ | $CO_2$/He | $O_2/N_2$ |
| PEO(0) | 25 | 25 | 4 | 0.3 | 0.3 | 6 |
| PEO1000(11) | 33 | 32 | 5 | 0.3 | 0.2 | 7 |
| PEO1000(30) | 34 | 46 | 6.5 | 0.4 | 0.4 | 7 |

Single gas transport experiments also showed that PEO-polyol molecular weight didn't have a significant impact on gas permeability or selectivity. Table 3.5 presents single gas transport properties of 30 weight percent PEO-containing PAES 15K polyurethane membranes that contain PEO polyols with molecular weights between 600 and 2000 g/mol. These membranes had comparable transport properties for gases with some minor variations that can be due to slight variations during membrane preparation.

**Table 3.5.** Initial gas transport properties of PAES15K-hydroxyethyl and ~30 wt%, PEO600, 1000 and 2000 containing polyurethanes

| Permeability (Barrer) | | | | | | |
|---|---|---|---|---|---|---|
| PAES 15K | He | $H_2$ | $CO_2$ | $O_2$ | $N_2$ | $CH_4$ |
| PEO(0) | 9.4 | 9.5 | 3.1 | 0.779 | 0.123 | 0.125 |
| PEO600 (29) | 3.7 | 3.2 | 1.9 | 0.246 | 0.045 | 0.063 |
| PEO1000 (30) | 4.0 | 3.5 | 1.6 | 0.248 | 0.034 | 0.045 |
| PEO2000 (33) | 3.2 | 2.6 | 1.5 | 0.197 | 0.034 | 0.049 |
| Selectivity | | | | | | |
| PAES 15K | $CO_2/CH_4$ | $CO_2/N_2$ | $CO_2/O_2$ | $CO_2/H_2$ | $CO_2$/He | $O_2/N_2$ |
| PEO(0) | 25 | 25 | 4.0 | 0.3 | 0.3 | 6 |
| PEO600 (29) | 30 | 42 | 7.7 | 0.6 | 0.5 | 5 |
| PEO1000 (30) | 34 | 46 | 6.5 | 0.4 | 0.4 | 7 |
| PEO2000 (33) | 31 | 45 | 7.6 | 0.6 | 0.5 | 6 |

### 3.5. Conclusions

In this current work, the synthesis of novel segmented polyurethanes that contain both a glassy high $T_g$ poly(arylene ether sulfone) and a flexible low $T_g$ poly(ethylene oxide) segment were described. These polyurethanes were prepared for gas separation membrane applications. Solid state thermal characterizations of these membranes revealed that at low PEO-content, PAES and PEO segments were at least partially phase-mixed. Thermo-mechanical analysis of polyurethane membranes displayed a decrease in the $T_g$ which corroborated with solid-state thermal analysis results. Membranes that contain PEO >10% by weight displayed two-distinct glass transition temperatures which indicated a phase separated morphology. Tensile properties showed that incorporation of flexible PEO segments toughened these polyurethanes at 10% and enhanced strain at break, however at 30 weight%, PEO segments started to compromise excellent tensile properties observed at lower PEO contents. These polyurethanes had remarkably low water uptake which was due to at least partial phase mixing between hydrophobic poly(arylene ether sulfone) and hydrophilic PEO segments. Single gas transport experiments showed a 25% improvement in $CO_2/CH_4$ and 80% improvement in $CO_2/N_2$ selectivities of polyurethanes membranes as PEO-content increased from 0 to 30 weight percent.

### 3.6. References:


1. Baker, R. W., *Membrane technology and applications*. J. Wiley: Chichester; New York, 2004.
2. Pandey, P.; Chauhan, R. S., Membranes for gas separation. *Prog. Polym. Sci.* **2001,** 26, (Copyright (C) 2014 American Chemical Society (ACS). All Rights Reserved.), 853-893.
3. Baker, R. W., Future Directions of Membrane Gas Separation Technology. *Ind. Eng. Chem. Res.* **2002,** 41, (Copyright (C) 2014 American Chemical Society (ACS). All Rights Reserved.), 1393-1411.
4. Bernardo, P.; Drioli, E.; Golemme, G., Membrane Gas Separation: A Review/State of the Art. *Ind. Eng. Chem. Res.* **2009,** 48, (Copyright (C) 2014 American Chemical Society (ACS). All Rights Reserved.), 4638-4663.
5. Robeson, L. M.; Burgoyne, W. F.; Langsam, M.; Savoca, A. C.; Tien, C. F., High performance polymers for membrane separation. *Polymer* **1994,** 35, (Copyright (C) 2012 American Chemical Society (ACS). All Rights Reserved.), 4970-8.
6. Liu, S. L.; Shao, L.; Chua, M. L.; Lau, C. H.; Wang, H.; Quan, S., Recent progress in the design of advanced PEO-containing membranes for CO2 removal. *Prog. Polym. Sci.* **2013,** 38, (Copyright (C) 2014 American Chemical Society (ACS). All Rights Reserved.), 1089-1120.
7. Robeson, L. M., 8.13 - Polymer Membranes. In *Polymer Science: A Comprehensive Reference*, Matyjaszewski, K.; Möller, M., Eds. Elsevier: Amsterdam, 2012; pp 325-347.
8. Freeman, B. D., *Polymer membranes for gas and vapor separation : chemistry and materials science*. American Chemical Society: 1999.
9. Robeson, L. M., Correlation of separation factor versus permeability for polymeric membranes. *J. Membr. Sci.* **1991,** 62, (Copyright (C) 2014 American Chemical Society (ACS). All Rights Reserved.), 165-85.
10. Robeson, L. M., The upper bound revisited. *J. Membr. Sci.* **2008,** 320, (Copyright (C) 2012 American Chemical Society (ACS). All Rights Reserved.), 390-400.
11. Freeman, B. D., Basis of Permeability/Selectivity Tradeoff Relations in Polymeric Gas Separation Membranes. *Macromolecules* **1999,** 32, (Copyright (C) 2014 American Chemical Society (ACS). All Rights Reserved.), 375-380.
12. Kelman, S.; Lin, H.; Sanders, E. S.; Freeman, B. D., CO2/C2H6 separation using solubility selective membranes. *J. Membr. Sci.* **2007,** 305, (Copyright (C) 2014 American Chemical Society (ACS). All Rights Reserved.), 57-68.
13. Ribeiro, C. P., Jr.; Freeman, B. D.; Paul, D. R., Pure- and mixed-gas carbon dioxide/ethane permeability and diffusivity in a cross-linked poly(ethylene oxide) copolymer. *J. Membr. Sci.* **2011,** 377, (Copyright (C) 2014 American Chemical Society (ACS). All Rights Reserved.), 110-123.
14. Freeman, B. D.; Pinnau, I., Polymeric Materials for Gas Separations. In *Polymer Membranes for Gas and Vapor Separation*, American Chemical Society: 1999; Vol. 733, pp 1-27.
15. Reijerkerk, S. R.; Nijmeijer, K.; Ribeiro, C. P., Jr.; Freeman, B. D.; Wessling, M., On the effects of plasticization in CO2/light gas separation using polymeric solubility selective membranes. *J. Membr. Sci.* **2011,** 367, (Copyright (C) 2014 American Chemical Society (ACS). All Rights Reserved.), 33-44.

16. Kusuma, V. A.; Gunawan, G.; Smith, Z. P.; Freeman, B. D., Gas permeability of cross-linked poly(ethylene-oxide) based on poly(ethylene glycol) dimethacrylate and a miscible siloxane co-monomer. *Polymer* **2010,** 51, (Copyright (C) 2014 American Chemical Society (ACS). All Rights Reserved.), 5734-5743.
17. Lin, H.; Van Wagner, E.; Swinnea, J. S.; Freeman, B. D.; Pas, S. J.; Hill, A. J.; Kalakkunnath, S.; Kalika, D. S., Transport and structural characteristics of crosslinked poly(ethylene oxide) rubbers. *J. Membr. Sci.* **2006,** 276, (Copyright (C) 2014 American Chemical Society (ACS). All Rights Reserved.), 145-161.
18. Lin, H.; Van Wagner, E.; Freeman, B. D.; Toy, L. G.; Gupta, R. P., Plasticization-enhanced hydrogen purification using polymeric membranes. *Science (Washington, DC, U. S.)* **2006,** 311, (Copyright (C) 2014 American Chemical Society (ACS). All Rights Reserved.), 639-642.
19. Figueroa, J. D.; Fout, T.; Plasynski, S.; McIlvried, H.; Srivastava, R. D., Advances in CO2 capture technology. The U.S. Department of Energy's Carbon Sequestration Program. *Int. J. Greenhouse Gas Control* **2008,** 2, (Copyright (C) 2014 American Chemical Society (ACS). All Rights Reserved.), 9-20.
20. Merkel, T. C.; Lin, H.; Wei, X.; Baker, R., Power plant post-combustion carbon dioxide capture: An opportunity for membranes. *J. Membr. Sci.* **2010,** 359, (Copyright (C) 2014 American Chemical Society (ACS). All Rights Reserved.), 126-139.
21. Bondar, V. I.; Freeman, B. D.; Pinnau, I., Gas sorption and characterization of poly(ether-b-amide) segmented block copolymers. *J. Polym. Sci., Part B: Polym. Phys.* **1999,** 37, (Copyright (C) 2014 American Chemical Society (ACS). All Rights Reserved.), 2463-2475.
22. Teo, L.-S.; Kuo, J.-F.; Chen, C.-Y., Permeation and sorption of CO2 through amine-contained polyurethane and poly(urea–urethane) membranes. *Journal of Applied Polymer Science* **1996,** 59, (10), 1627-1638.
23. Comer, A. C.; Kalika, D. S.; Kusuma, V. A.; Freeman, B. D., Glass-transition and gas-transport characteristics of polymer nanocomposites based on crosslinked poly(ethylene oxide). *J. Appl. Polym. Sci.* **2010,** 117, (Copyright (C) 2014 American Chemical Society (ACS). All Rights Reserved.), 2395-2405.
24. Richards, J. J.; Danquah, M. K.; Kalakkunnath, S.; Kalika, D. S.; Kusuma, V. A.; Matteucci, S. T.; Freeman, B. D., Relation between structure and gas transport properties of polyethylene oxide networks based on crosslinked bisphenol A ethoxylate diacrylate. *Chem. Eng. Sci.* **2009,** 64, (Copyright (C) 2012 American Chemical Society (ACS). All Rights Reserved.), 4707-4718.
25. Lin, H.; Freeman, B. D., Materials selection guidelines for membranes that remove CO2 from gas mixtures. *J. Mol. Struct.* **2005,** 739, (Copyright (C) 2014 American Chemical Society (ACS). All Rights Reserved.), 57-74.
26. Cateto, C. A.; Barreiro, M. F.; Rodrigues, A. E.; Brochier-Salon, M. C.; Thielemans, W.; Belgacem, M. N., Lignins as macromonomers for polyurethane synthesis: a comparative study on hydroxyl group determination. *J. Appl. Polym. Sci.* **2008,** 109, (Copyright (C) 2014 American Chemical Society (ACS). All Rights Reserved.), 3008-3017.
27. Celebi, O.; Lee, C. H.; Lin, Y.; McGrath, J. E.; Riffle, J. S., Synthesis and characterization of polyoxazoline–polysulfone triblock copolymers. *Polymer* **2011,** 52, (21), 4718-4726.

28. Colonna, M.; Berti, C.; Fiorini, M., Chemical modification of bisphenol a polycarbonate by reactive blending with ethylene carbonate. *J. Appl. Polym. Sci.* **2014,** 131, (Copyright (C) 2014 American Chemical Society (ACS). All Rights Reserved.), 39820/1-39820/10.
29. Yoshino, T.; Inaba, S.; Ishido, Y., Synthetic studies by the use of carbonates. III. Condensation reactions of ethylene carbonate with a variety of phenols catalyzed by lithium hydride or tetraethylammonium halides. *Bull. Chem. Soc. Jap.* **1973,** 46, (Copyright (C) 2014 American Chemical Society (ACS). All Rights Reserved.), 553-6.
30. Ronda, J. C.; Serra, A.; Mantecón, A.; Cádiz, V., End-group analysis of poly(phenyl glycidyl ether), 2. Hydroxylic groups using 19F nuclear magnetic resonance. *Macromolecular Chemistry and Physics* **1994,** 195, (10), 3459-3468.
31. Szycher, M., *Szycher's handbook of polyurethanes*. CRC Press: Boca Raton, 1999.
32. Dodge, J., Polyurethanes and Polyureas. In *Synthetic Methods in Step-Growth Polymers*, John Wiley & Sons, Inc.: 2003; pp 197-263.
33. Mark, J. E., *Polymer data handbook*. Oxford University Press: New York, 1999.
34. Oh, H. J.; Freeman, B. D.; McGrath, J. E.; Ellison, C. J.; Mecham, S.; Lee, K.-S.; Paul, D. R., Rheological studies of disulfonated poly(arylene ether sulfone) plasticized with poly(ethylene glycol) for membrane formation. *Polymer* **2014,** 55, (6), 1574-1582.
35. Oh, H. J.; Freeman, B. D.; McGrath, J. E.; Lee, C. H.; Paul, D. R., Thermal analysis of disulfonated poly(arylene ether sulfone) plasticized with poly(ethylene glycol) for membrane formation. *Polymer* **2014,** 55, (1), 235-247.
36. Walsh, D. J.; Singh, V. B., The phase behaviour of a poly(ether sulfone) with poly(ethylene oxide). *Die Makromolekulare Chemie* **1984,** 185, (9), 1979-1989.

## 4. Polyurethanes Containing Disulfonated Poly(arylene ether sulfone) and Poly(ethylene oxide) Segments for Gas Separation Membranes

*Ali Nebipasagil,* [a] *Andrew T. Shaver,* [a] *Sue J. Mecham,* [a] *Judy S. Riffle,* [a] *and James E. McGrath* [a]

[a] Macromolecules and Interfaces Institute, Virginia Tech, Blacksburg, VA 24061, USA

**Keywords**: Disulfonated poly(arylene ether sulfone) copolymers; PEO polyurethane; Membranes

### 4.1. Abstract:

Disulfonated poly(arylene ether sulfone) and poly(ethylene oxide)-containing polyurethanes were synthesized for potential applications as gas separation membranes. Polymers containing 20 and 40 mole percent of disulfonated repeat units with controlled molecular weights were prepared with phenol end groups by nucleophilic aromatic substitution polymerization of 4,4`-dichlorodiphenyl sulfone, 3,3′-disulfonated-4,4′-dichlorodiphenyl sulfone and a molar excess of 4,4'-(propane-2,2-diyl) diphenol (bisphenol A). The precursors with phenolic end groups were subsequently reacted with ethylene carbonate to obtain aliphatic hydroxyethyl terminal functionality. Disulfonated hydroxyethyl-functional poly(arylene ether sulfone) polyols and α,ω-hydroxy-terminated poly(ethylene oxide) were reacted with 4,4'-methylene diphenyl diisocyanate (MDI) to obtain polyurethanes. Compositions with high poly(arylene ether sulfone) content relative to poly(ethylene oxide) segments were of particular interest due to their mechanical integrity. Size exclusion chromatograms confirmed that the polyurethanes had high molecular weights with unimodal molecular weight distributions. DMA showed that the polyurethanes had a single $T_g$ which indicated a phase-mixed complex morphology.

## 4.2. Introduction

Polymeric membrane gas separation technology has received attention due to remarkable advantages over conventional distillation methods such as energy efficiency, lower capital investment and smaller industrial footprint.[1,2] Excellent articles cover the progress in polymeric membrane gas separations over the past two decades.[3-8] The solution-diffusion mechanism is the widely accepted model to explain gas transport in dense polymeric membranes.[1,7] Permeability is an inherent property that is a measure of the quantity of gas that diffuses through a membrane at a given temperature and pressure. Membrane selectivity is another vital material parameter that is the measure of separation efficiency. The gas kinetic diameter,[9] polymer composition and morphology,[10,11], polymer chain rigidity,[12] and interactions between the polymer and the gas largely determine permeability and selectivity.[13,14] Ideal gas separation membranes have both high selectivity and high permeability. In general, polymer composition and structural modifications of the polymer backbone that increase selectivity also cause a decrease in permeability and vice versa.[6,8,13,15] This trade-off relationship has been studied for many gas pairs.[8,13,15] An empirical relationship called the "upper-bound" phenomenon has been developed that describes this trade-off relationship.[6,8] The selectivity-permeability relationship constrains the practical applications of membranes, and careful material and membrane design is required to enhance membrane performance beyond the "upper bound" line.

Poly(arylene ether sulfone)s are well-known engineering thermoplastics that display excellent thermal and mechanical stability, as well as high chemical resistance against oxidation and hydrolysis.[16-19] Poly(arylene ether sulfone) membranes are widely used in the gas separation industry.[5] Gas selectivity and permeability can be tuned via modifications such as sulfonation of the polymer backbone.[9,20-23] Unsulfonated and sulfonated polysulfone block copolymers of were

studied as potential candidates for gas separation membranes. Block copolymers with equal block molecular weights of 5000:5000, 10,000:10,000 and 15,000:15,000 grams per mole of each block were evaluated.[9] Phase separation was more pronounced in the copolymers with 10,000 and 15,000 g/mole blocks than in the polymer with the 5,000 g/mole blocks. Storage and loss moduli measured via DMA showed that the copolymer with the 5,000 g/mole blocks had only a single glass transition whereas those with the larger blocks displayed two distinct glass transition temperatures. Ion domain sizes of the block copolymers were evaluated via SAXS experiments. .[9] Domain size increased from 213 Å to 362 Å and SAXS peak width became narrower as block size increased from 5000 to 15,000 g/mol. It was reasoned that distribution and number of ionic scattering units decreased, longer block lengths having fewer more concentrated ionic domains and therefore a greater number of ionic units in small block lengths led to a phase mixing of unsulfonated and sulfonated blocks.[9] Block copolymers with long blocks had enhanced physical crosslinks. Enhanced ionic interactions decreased the fractional free volume, resulting in a reduction in gas permeability and in permeability selectivity of $He/O_2$, $H_2/O_2$ and $He/CO_2$ gas pairs.[9]

Park and others[20] studied metal counterion exchanged sulfonated polysulfone to investigate the influence of counterion on permeability and selectivity of sulfonated polysulfone membranes. In general, conversion from the acid to the salt form via metal ion ($Na^+$, $K^+$, $Mg^{2+}$, $Ca^{2+}$, $Ba^{2+}$ and $Al^{3+}$) exchange improved the overall selectivity of sulfonated membranes. Monovalent ($Na^+$, $K^+$) counterions in the membranes resulted in the highest permeabilities, and this was attributed to better ionic crosslinking with divalent and trivalent counterions.[20] The diffusion coefficients of all of the gases were higher for the copolymers with $Na^+$ or $K^+$ counterions than for those with $Mg^{2+}$, $Ca^{2+}$ or $Ba^{2+}$, while the copolymer with the $Al^{3+}$ salt had the lowest diffusion coefficients.

This outcome was attributed to a possible improvement in the chain packing due to enhanced ionic interactions.[20]

$CO_2$ is an impurity in natural gas that has to be separated from gas mixtures to meet natural gas pipeline specifications.[24-26] Diffusivity selective membranes are used for $CO_2$ separations[7,27] which yield low pressure product ($H_2$, $N_2$ or $O_2$,) due to better permeability of light gases compared to $CO_2$.[27,28] Poly(ethylene oxide) (PEO) has been extensively investigated as a promising membrane material to selectively permeate $CO_2$.[29-31] The presence of polar ether oxygens in the PEO backbone leads to interaction between PEO repeat units and $CO_2$ molecules. This interaction enhances solubility of $CO_2$ in light gas streams, thus causing solubility selectivity.[7,32,33] PEO-containing linear polymer designs include PEO-polysulfone random copolymers,[34] PEO-containing polyamides and segmented polyurethanes.[7] Crosslinked membrane designs consist of UV-crosslinked low molecular weight PEO acrylates and methacrylates that are particularly of interest.[25,27,29,33,35] Photo-crosslinked poly(ethylene oxide)-containing films were prepared from bisphenol A ethoxylate diacrylates with a variety of chain lengths and poly(ethylene oxide)-based mono and diacrylate comonomers.[33] This synthetic strategy yielded amorphous networks, and this was attributed to suppression of chain mobility. Gas permeabilities showed an inverse relationship with crosslink density which correlated closely with the network free volume fraction. Moreover designing membranes with monoacrylate comonomers resulted in networks with dangling flexible side chains which increased the free volume fraction and thus the permeability of the membranes.[33] Unexpectedly, membrane selectivity did not suffer from the increase in membrane permeability, resulting in an overall membrane performance either approaching or exceeding the upper bound for a number of $CO_2$-light gas pairs.[33]

In this work, we report the synthesis and characterization of polyurethanes containing disulfonated poly(arylene ether sulfone) and poly(ethylene oxide) for gas separation applications. Compositions with high disulfonated polysulfone content relative to the PEO segments were prepared to obtain membranes with enhanced mechanical integrity.

## 4.3. Experimental

### *4.3.1. Materials*

4,4'-(Propane-2,2-diyl)diphenol (bisphenol A) and 4,4'-dichlorodiphenylsulfone (DCDPS, 99%) were kindly provided by Solvay and recrystallized from toluene before use. 3,3'-Disulfonated-4,4'-dichlorodiphenylsulfone (SDCDPS, 98%) was purchased from Akron Polymer Systems (Akron, OH) where it was prepared according to the procedure reported previously.[36] Potassium carbonate ($K_2CO_3$, ACS reagent grade, 99%) was purchased from Sigma Aldrich and dried at 150 ºC under vacuum for at least 24 h. Ethylene carbonate (98%), trifluoroacetic anhydride (reagent plus grade, >99%) and 4Å molecular sieves were purchased from Sigma Aldrich and used as received. α,ω-Hydroxy-terminated poly(ethylene oxide) (PEO, $M_n$ 1050 g/mol) was purchased from Sigma Aldrich and dried at 80 ºC under vacuum for 24 h. The PEO oligomers were titrated by a method adapted from the literature.[37] Celite 545 was purchased from EMD chemicals. 4,4'-Methylene diphenyl diisocyanate (MDI, >99.5%) was graciously donated by Bayer Material Science. Calcium hydride (90-95%) was purchased from Alfa Aesar. *N,N*-Dimethylacetamide (DMAc, 99%) and *N*-methylpyrrolidone (NMP, 99%) was purchased from Acros Organics. DMAc and NMP were dried over $CaH_2$ and distilled under reduced pressure before use. Toluene, chloroform and isopropanol (IPA), were purchased from Fisher Scientific and used as received. The SEC mobile phase, NMP, was purchased from Fisher Scientific. It was

stirred with phosphorus pentoxide, then distilled under reduced pressure and filtered through a 0.2 μm PTFE filter before use.

### *4.3.2. Synthesis of an ~15,000 g/mol (Mn) phenol-endcapped disulfonated poly(arylene ether sulfone)copolymer (BisASXX, Figure 4.1)*

Disulfonated poly(arylene ether sulfone) copolymers (BisASXX, XX = mole % of disulfonated repeat units) with controlled molecular weights were synthesized via nucleophilic aromatic substitution. Bisphenol A and DCDPS were recrystallized from toluene to eliminate impurities. SDCDPS was dried at 160 ºC for 72 h to eliminate moisture. NaCl is a by-product of SDCDPS synthesis and remains as an inert impurity in SDCDPS. UV-VIS light spectroscopy was used to quantify the NaCl content[38] in SDCDPS (97% pure) before it was used in the polymer synthesis. Bisphenol A was charged in excess to prepare a product with phenol endgroups and a controlled molecular weight. The ratio of bisphenol A to DCDPS+SDCDPS was calculated according to the Carothers equation to obtain target molecular weights. Slight excess of SDCDPS was charged to account for NaCl impurity in the monomer. A representative reaction which yielded 14,300 g/mol, phenol terminated, oligomer with 20 mole % of the units disulfonated (BisAS20) was conducted as provided below. Bisphenol A (34.244 g, 150 mmol), DCDPS (33.765 g, 117.6 mmol), SDCDPS (14.443 g, 29.4 mmol), $K_2CO_3$ (35.440 g, 256 mmol) and NMP (200 mL) were charged into a three neck, 500-mL flask equipped with a condenser, Dean-Stark trap filled with toluene, thermometer, nitrogen inlet/outlet, and a mechanical stirrer. A thermocouple-regulated oil bath was used to control the reaction temperature. After the monomers dissolved, toluene (100 mL) was added into the flask. The oil bath temperature was raised to 155$^{o}$C to bring the reaction to reflux. The reaction was azeotropically dehydrated at 155 ºC for 6 h until the water condensation ceased. Subsequently, toluene in the Dean-Stark trap was

drained and toluene in the reaction flask was completely removed by slowly increasing the temperature to 175 ºC. After 48 h, the viscous reaction mixture was cooled to room temperature and diluted with 200 mL of NMP and filtered to remove the salt and then was precipitated into stirring IPA as a white solid. The polymer was filtered, washed with IPA and dried under vacuum at 100 ºC overnight. The polymer was re-dissolved in NMP, filtered twice through Celite, then precipitated in IPA. The product was dried at 150 ºC under vacuum for 24 h. (yield>90 %) BisAS40 was synthesized in a similar manner utilizing a different stoichiometry of monomers calculated with the Carothers equation.

### *4.3.3. Conversion of phenol-endcapped copolymers to hydroxyethyl-endcapped copolymers (BisASXX-hydroxyethyl, Figure 4.1)*

A representative reaction was conducted as follows. Phenol terminated BisAS20 (60.5 g, 4.03 mmol), ethylene carbonate (7.09 g, 80.60 mmol), $K_2CO_3$ (1.15 g, 8.06 mmol) were dissolved in NMP (300 mL) in a 500-mL flask equipped with a magnetic stir bar. The reaction flask was sealed with a rubber septum, flame dried and purged with $N_2$ to eliminate moisture. The flask was placed in an oil bath and the temperature was regulated with a thermocouple. The reaction flask was purged with nitrogen for 15 min, then the temperature was gradually increased to 125 ºC and the reaction was stirred for 24 h. The solution was cooled to room temperature and filtered to remove the salt. The polymer was precipitated in IPA, then was filtered and dried at 100 ºC overnight under vacuum. The polymer was re-dissolved in NMP, filtered twice through Celite, and then precipitated in IPA. The product was dried at 150 ºC under vacuum for 24 h. (yield>90 %)

### *4.3.4. Polyurethane containing disulfonated poly(arylene ether sulfone) and poly(ethylene oxide, Figure 4.4)*

A typical reaction to synthesize a polyurethane containing disulfonated poly(arylene ether sulfone) and poly(ethylene oxide) was conducted as follows. BisAS20-hydroxyethyl (0.200 mmol, 3.000 g) and PEO with a titrated $M_n$ of 920 g/mole (0.462 mmol, 0.425 g) were dissolved in DMAc (12 mL) in a 100-mL three-neck round bottom flask. The flask was equipped with a condenser, Dean-Stark trap filled with toluene, nitrogen inlet/outlet, and a mechanical stirrer. A thermocouple-regulated oil bath was used to control the reaction temperature. After the BisAS20-hydroxyethyl and PEO dissolved, toluene (6 mL) was added into the reaction flask. The solution was refluxed at 135 ºC for 4 h until all moisture was azeotropically removed with toluene. Subsequently toluene in the Dean-Stark trap was drained and toluene in the flask was completely removed. The reaction temperature was gradually reduced to 60 ºC. MDI (0.662 mmol, 0.172 g) was dissolved in 4 mL of anhydrous DMAc and added drop-wise into the stirring BisAS20-hydroxyEthyl/PEO mixture. The reaction was purged with dry $N_2$ to protect the reactants from ambient humidity. The reaction was allowed to proceed at 60 ºC for 6 h. The viscous polymer mixture was cooled to room temperature and diluted with 30 mL of DMAc. The solution was precipitated into stirring IPA as a white solid. The polymer was filtered, washed with IPA and dried under vacuum at 100 ºC for 24 h. (Yield>90 %) The acronym for each oligomer (BisASXX and PEO) followed by number average molecular weight and weight percent in the polyurethane was used to identify each sample. For example BisAS20 PEO1000(10) stands for a polyurethane containing a 20% disulfonated hydroxyethyl end-capped poly(arylene ether sulfone) with 10 % by weight of an ~1000 g/mol PEO.

### *4.3.5. Polymer Characterization*

*Nuclear magnetic resonance spectroscopy (NMR)*

$^{1}H$ and $^{19}F$ NMR analysis of the copolymers was performed on a Varian Inova spectrometer operating at 400 MHz. Sixty-four scans for each spectrum were collected at ambient temperature. The spectra of the polymers were obtained from a 0.25 g/mL 1-mL solution in $d_6$-DMSO.

*Size Exclusion Chromatography (SEC)*

The NMP SEC mobile phase was dehydrated. After distillation, a 0.05 M solution of lithium bromide (LiBr) in NMP was prepared. Three Agilent PL gel 10 μm Mixed BLS polystyrene-divinylbenzene columns 300x7.5 mm connected in series were used as the stationary phase. A system of multiple detectors connected in series was used for the analysis. A multi-angle laser light scattering (MALLS) detector (DAWN-HELEOS II, Wyatt Technology Corporation, USA), operating at a wavelength of 658 nm; a viscometer detector (Viscostar, Wyatt Technology Corporation), and a refractive index detector operating at a wavelength of 658 nm (Optilab T-rEX, Wyatt Technology Corporation) provided online results. The system was corrected for inter detector delay, band broadening, and the MALLS signals were normalized using a 21,720 g/mole polystyrene standard obtained from Agilent Technologies with each set of samples. Data acquisition and analysis was completed using Astra 6 software from Wyatt Technology Corporation. The samples were analyzed at a concentration of approximately 3 mg/mL in NMP + 0.05 M LiBr at a flow rate of 0.5 mL/min. The polyurethane chromatograms were analyzed via light scattering. The dn/dc was calculated using the Astra 6 software to calculate the $d_n/d_c$ by assuming 100% recovery of the sample.

*Thermogravimetric Analysis (TGA)*

Thermal stability of the polymers in the range of thermal analysis (DSC and DMA) temperatures was probed using a TA Instruments TGA Q500. The samples were heated to at least 150 °C, held isothermally for 10 min to remove any ambient water, and then heated to 500 °C at 10 °C/min under nitrogen atmosphere.

*Dynamic Mechanical Analysis (DMA)*

DMA was performed on a TA Instruments Q800 Dynamic Mechanical Analyzer in tension mode at a frequency of 1 Hz, an oscillatory amplitude of 15 μm, and a static force of 0.01 N. The temperature ramp was 2 °C/min.

*Differential Scanning Calorimetry (DSC)*

DSC was conducted on a TA Instruments Q2000, under nitrogen at a 10 ºC/min heating/cooling rate. A heat/cool/heat protocol was used. First, samples were equilibrated at -85 ºC, then heated up to 200 ºC and cooled back down to -85 ºC. In the last cycle, it was heated back up to 300 ºC. Second heat data is reported.

*Water Uptake*

Water uptake of each polyurethane was measured gravimetrically. Films were dried at 150 °C under vacuum overnight prior to water immersion to obtain the dry weight ($W_{dry}$). The films were immersed in DI water at ambient temperature for at least 48 h. The films were removed, quickly blotted to remove water droplets on the surface and weighed to obtain the wet weight ($W_{wet}$). Equation 4.1 shows the calculation used to determine the gravimetric percent water uptake.

$$\text{Water Uptake}(\%) = \frac{W_{wet} - W_{dry}}{W_{dry}} \times 100$$

**Equation 4.1**

## 4.4. Results and Discussion

### *4.4.1. Synthesis of phenol and hydroxyethyl terminated BisASXX copolymers (Figure 4.1)*

Disulfonated poly(arylene ether sulfone) (BisASXX) copolymers with phenol endgroups were synthesized via nucleophilic aromatic substitution (Figure 4.1) between 4,4'-(propane-2,2-diyl)diphenol (bisphenol A), 4,4'-dichlorodiphenylsulfone (DCDPS) and 3,3'-disulfonated-4,4'-dichlorodiphenylsulfone (SDCDPS). SDCDPS was incorporated into the oligomer via a direct copolymerization route as previously reported by McGrath *et al.*[39-41] Step-growth aromatic substitution polymerizations demand high (~99.9%) monomer purity and exact stoichiometric ratios to achieve targeted number average molecular weights with high monomer conversion. The targeted number average molecular weights were calculated utilizing the Carothers equation. The amount of excesses of bisphenol A relative to DCDPS+SDCDPS and the mole ratios of monomers were calculated to achieve oligomers with 15,000 g/mol $M_n$ and either 20 or 40 mol % of disulfonated repeat units.

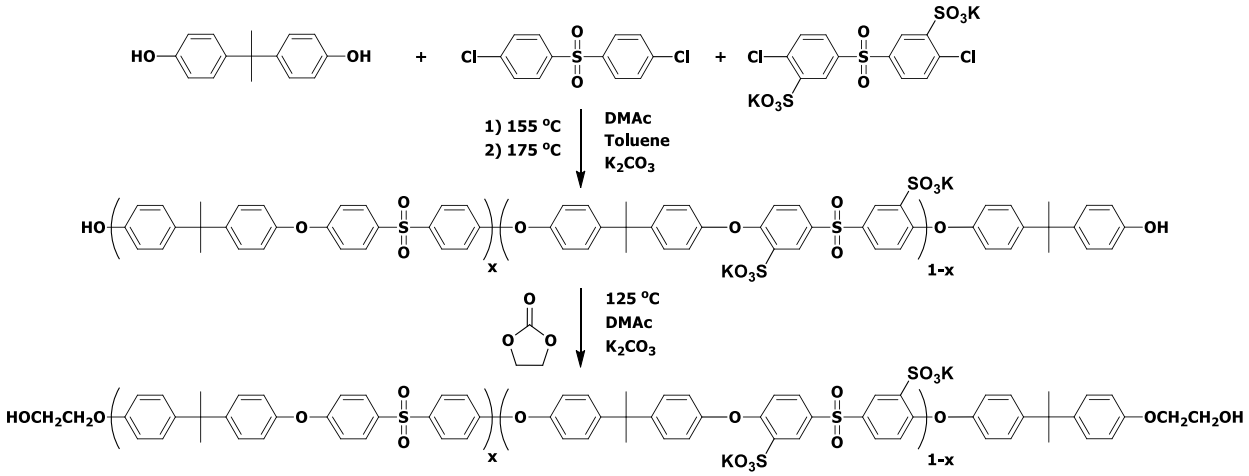


**Figure 4.1.** Synthesis of hydroxyethyl terminated partially disulfonated poly(arylene ether sulfone) (BisAS20 or 40-hydroxyethyl) copolymers with controlled molecular weight

Figure 4.2 presents a $^{1}H$ NMR spectrum of BisAS40 and validates the hydroxyethyl endgroup functionality of the copolymer. Hydroxyethyl endgroup protons resonate at 3.69 ppm (j) and 3.94 ppm (k). Backbone SDCDPS protons adjacent to sulfonyl groups (a) resonate at 8.28 and (b) 7.82 ppm. SDCDPS proton attached to the carbon next to the ether linkage (c) shows as a singlet at 6.91 ppm. Backbone DCDPS protons adjacent to the sulfonyl groups (g) resonate 7.90 ppm, and DCDPS protons adjacent to the ether linkage (f) resonate at 7.03 and 7.09 ppm. The doublet at 7.28 ppm and doublet at 6.99 ppm were assigned to the backbone aromatic bisphenol A peaks (d) and (e) respectively. Isopropylidene protons (h) of the bisphenol A resonate at 1.65 ppm. The number average molecular weights of the copolymers were calculated using endgroup peaks (k and j) and backbone peaks (a, b and g). This calculation assumes all polymer chains were quantitatively terminated with hydroxyethyl groups. The NMR endgroup analyses were in excellent agreement with the targeted number average molecular weights. The degrees of disulfonation of the copolymers were calculated using the peak integrations of the resonances labelled (a), (b) and (g).

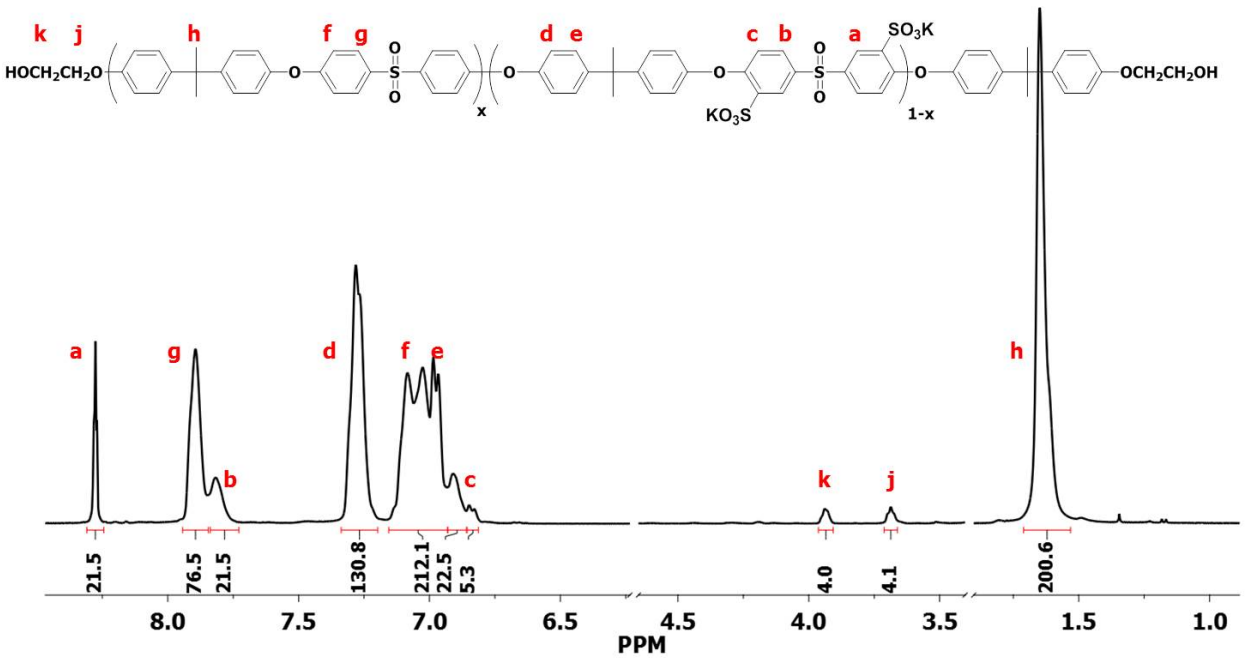


**Figure 4.2.** $^{1}$H NMR spectrum of a hydroxyethyl-endcapped 40 mole % disulfonated copolymer (BisAS40-hydroxyethyl)

Chemical modification to convert phenol groups into hydroxyethyl functionalities with ethylene carbonate is an efficient method.[42-44] BisAS20 and BisAS40 were modified with ethylene carbonate to yield oligomers with primary hydroxyl endgroups.[45] Bisphenol A terminated BisASXX oligomers were reacted with an excess of ethylene carbonate in the presence of the weak base $K_2CO_3$. This reaction converted phenolic endgroups of the BisASXX to aliphatic hydroxyethyl telechelic functionalities (Scheme 1). Nucleophilic attack of the phenoxide on either one of the alkyl carbons of the ethylene carbonate opens the ethylene carbonate ring with loss of $CO_2$ to yield the hydroxyethyl-functional polymer.[42] The $^{1}$H NMR spectrum in Figure 4.2 shows the aliphatic ethyl proton resonances at 3.69 and 3.94 ppm that confirms that this reaction produces hydroxyethyl functionality under the relatively mild conditions that were employed. The NMR peak integrals indicated that approximately one hydroxyethyl unit per phenol was present.

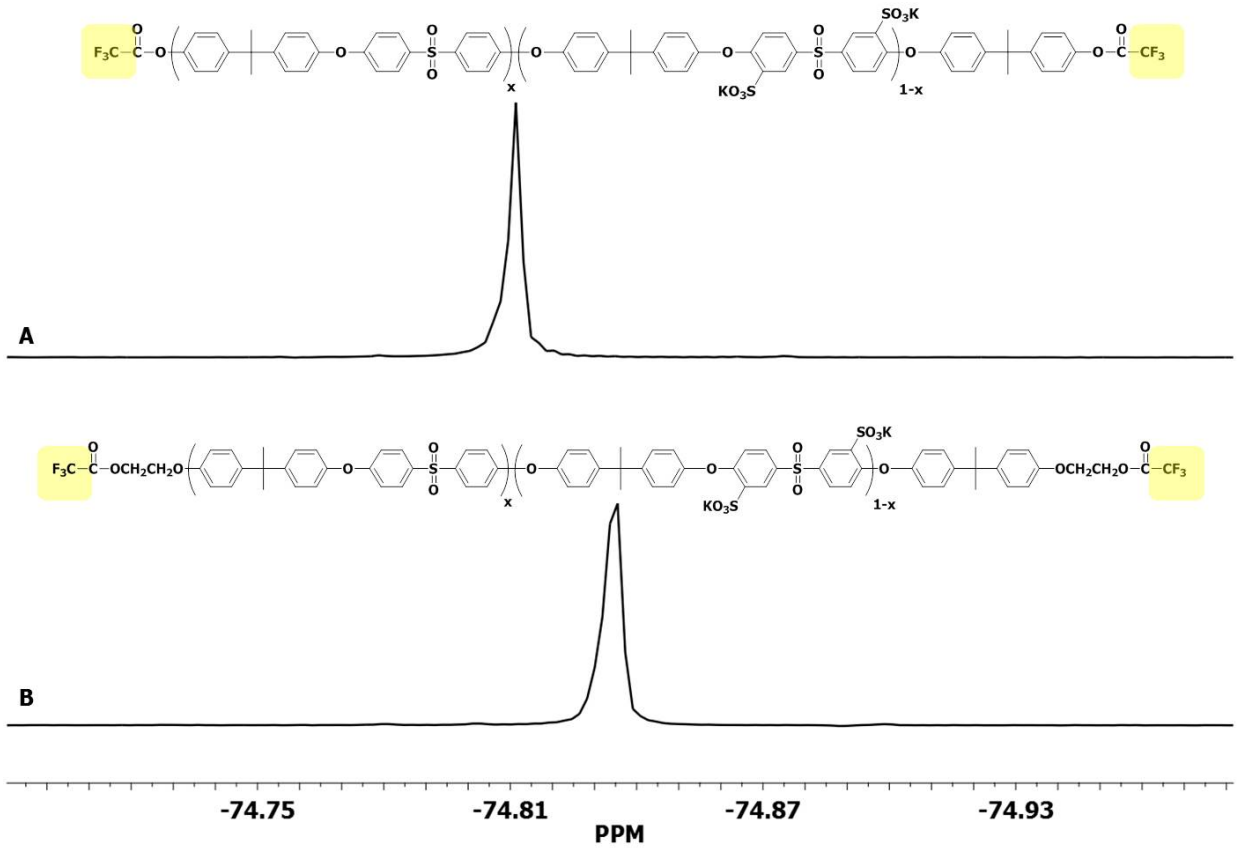


**Figure 4.3.** 19F NMR spectra of copolymers with the endgroups modified with trifluoroacetic anhydride: (A) BisAS20-phenol trifluoroacetate, and (B) BisAS20-hydroxyethyl trifluoroacetate

$^{19}$F NMR is a versatile method which can distinguish trifluoroacetate-modified hydroxylic endgroups.[46] Trifluoroacetic anhydride derivatization of phenol and hydroxyethyl terminated polymers have distinct $^{19}$F resonances due to different shielding effects of the ester products.[46] Figure 4.3 demonstrates that phenol endgroups were completely converted into hydroxyethyl functionalities. Fluorine atoms adjacent to phenolic esters resonate at -74.81 ppm whereas the ones next to hydroxyethyl groups resonate at -74.84 ppm.

### *4.4.2. Synthesis of polyurethanes containing poly(arylene ether sulfone) oligomers and poly(ethylene oxide) segments (Figure 4.4)*

Primary alcohols are more reactive towards isocyanates in comparison to phenols.[45,47] Moreover, the phenol-isocyanate reaction yields unstable polyurethanes compared to polyurethanes of aliphatic alcohols. The phenol-isocyanate reaction can be reversed at temperatures as low as 100 ºC.[45] Thus, bisphenol A terminated copolymers were modified with ethylene carbonate to yield oligomers with primary hydroxyl endgroups.[45] Hydroxyethyl derivatized BisASXX and the PEO oligomer (titration $M_n$ = 920 g/mol) were utilized as polyols for the synthesis of polyurethanes. The PEO endgroups were titrated via conventional methods by acetylating the hydroxyl groups with an excess of acetic anhydride, then the excess anhydride was hydrolyzed and the acetic acid content was back-titrated with potassium hydroxide.[37] Isocyanates are very susceptible to reaction with water. Therefore, BisASXX oligomer was dried at 150 ºC and the PEO was dried at 100 ºC overnight under vacuum to remove ambient water. Moreover, toluene was utilized in the synthesis as the azeotropic solvent with DMAc to ensure that the disulfonated poly(arylene ether sulfone) and PEO mixture were moisture-free prior to adding isocyanate. Scheme 2 shows the synthesis of a polyurethane containing the BisASXX and PEO.

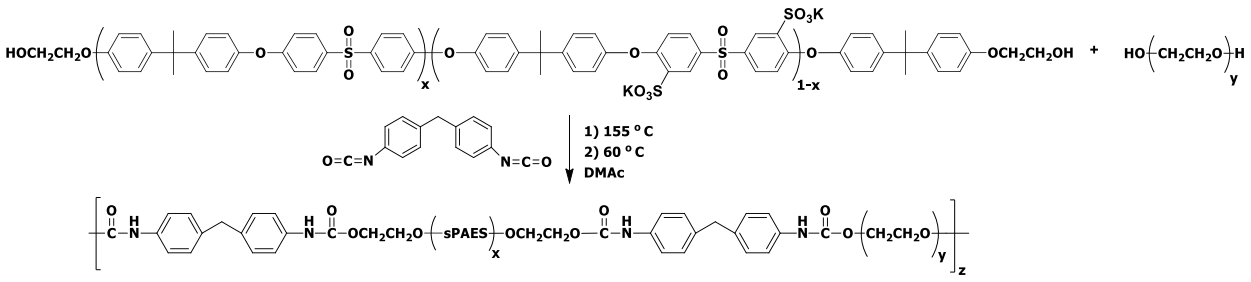


**Figure 4.4.**Synthesis of polyurethanes containing disulfonated poly(arylene ether sulfone) and poly(ethylene oxide)

SEC was utilized to determine the molecular weights of the polyurethanes. The SEC mobile phase was a 0.05 M LiBr solution in NMP. LiBr salt was added to reduce intermolecular polymer interactions. Figure 4.5 presents the comparison of SEC chromatograms of the BisAS20 precursor oligomer and the polyurethanes containing 0, 10 and 30 wt % of PEO. The chromatograms showed that the polymers yielded unimodal curves. The reaction of hydroxyethyl terminated disulfonated BisAS20 with MDI resulted in chain extension of BisAS20 which increased the molecular weight of the product. This increase was reflected as a shift to lower elution volumes in the chromatograms.

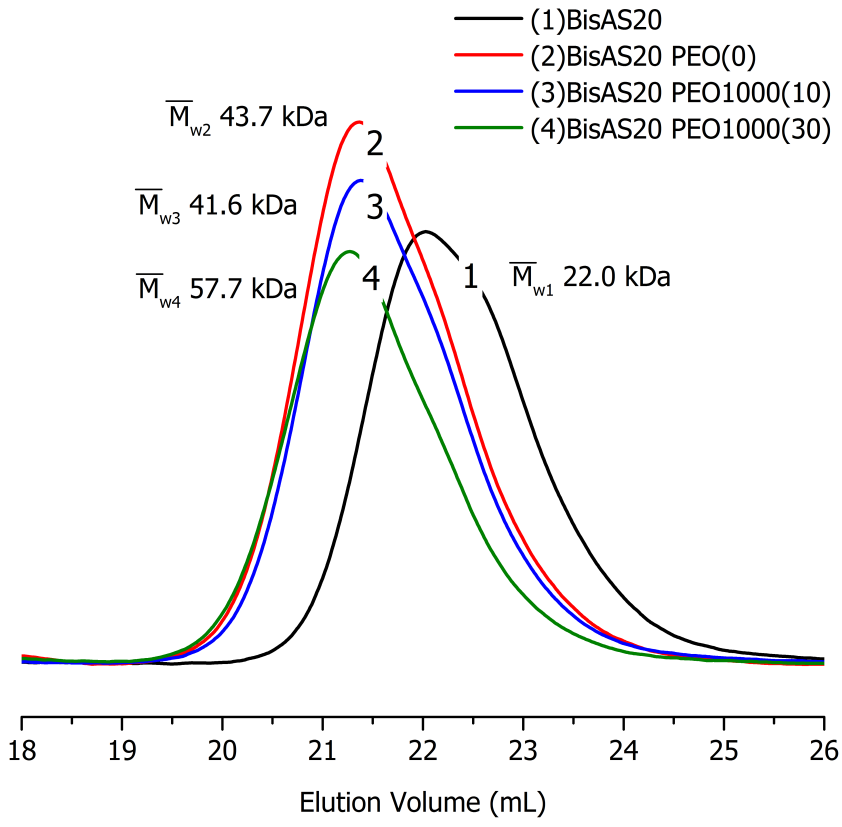


**Figure 4.5.** SEC chromatograms of (1) BisAS20-hydroxyethyl (2)BisAS20-hydroxyethyl that was chain extended with MDI, (3 and 4) the polyurethanes containing BisAS20-hydroxyethyl and 10wt.% and 30 wt.% PEO1000

Thermal degradation of membranes was studied to probe their thermal stabilities at elevated temperatures. Figure 4.6 presents the TGA thermograms of BisAS20-hydroxyethyl (1), BisAS20-hydroxyethyl chain extended with MDI (2), and BisAS20-hydroxyethyl PEO-containing polyurethanes. BisAS20-hydroxyethyl did not show a significant weight loss until 500 ºC (similar to disulfonated polysulfones), whereas polyurethanes start losing weight at lower temperatures as expected due to presence of ether and urethane bonds. The weight loss of polyurethanes at 300 ºC was attributed to the onset of thermal urethane degradation where the polyurethanes lost about three percent of their initial weight.

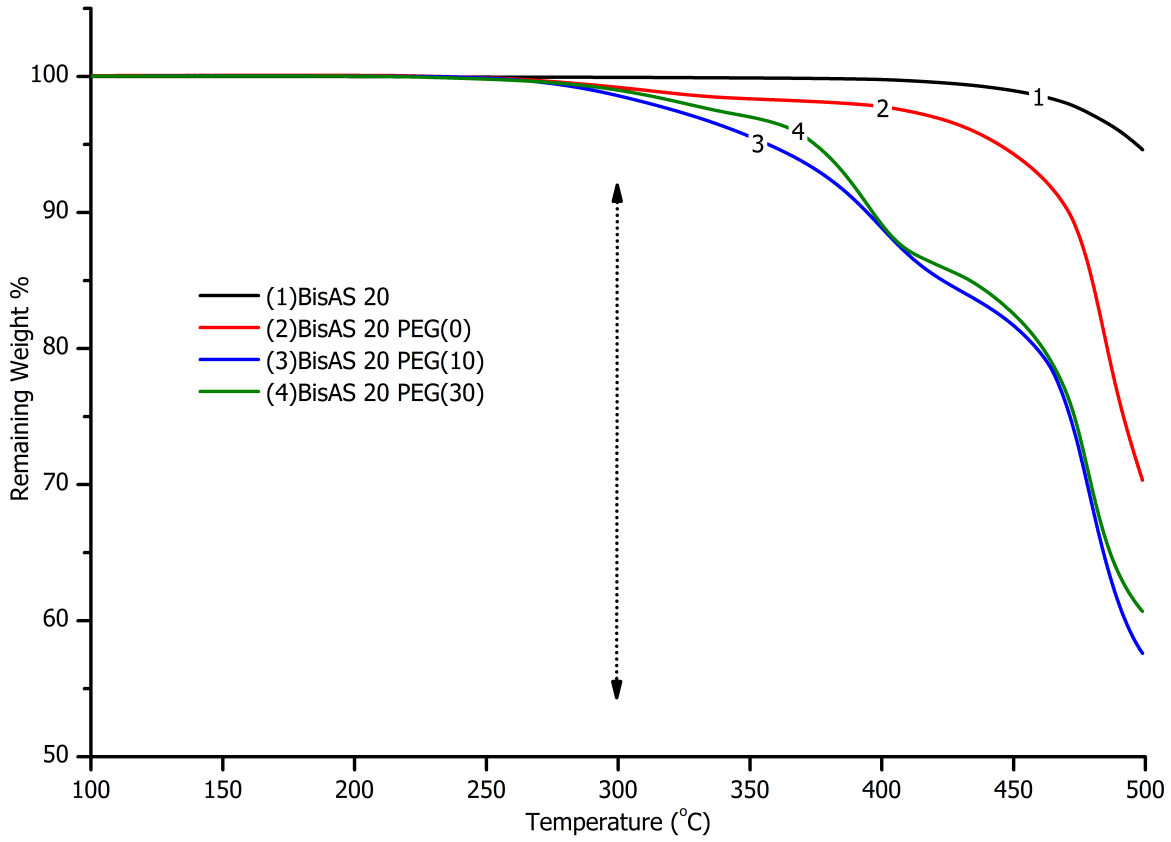


**Figure 4.6.** TGA thermograms of (1) BisAS20-hydroxyethyl (2)BisAS20-hydroxyethyl that was chain extended with MDI, (3 and 4) the polyurethanes containing BisAS20-hydroxyethyl and 10wt.% and 30 wt.% PEO1000

The solid state thermal properties of the polyurethanes were investigated to probe the phase structures of the hydrophilic membranes (Figure 4.7). DSC thermograms showed that the BisAS20-hydroxyethyl polymer that was chain extended with MDI (BisAS20 PEO(0)) (the control polyurethane) had a broad transition centered around 197 ºC. The DSC thermograms of the polyurethane with 10 wt % of PEO showed a single transition at 161 ºC, 36° lower than that of the control, whereas BisAS20 PEO1000 (30) showed two thermal transitions at 70 ºC and another thermal transition at 241 ºC.

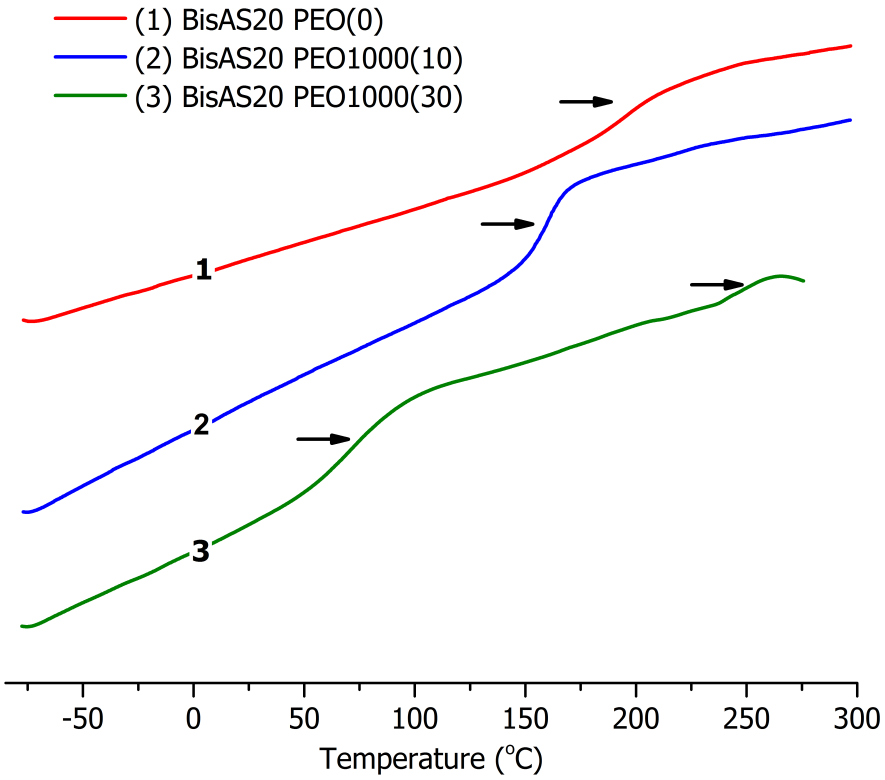


**Figure 4.7.** DSC thermograms (exo down) of polyurethanes (1) BisAS20-hydroxyethyl that was chain extended with MDI, (2 and 3) containing BisAS20-hydroxyethyl and 10 and 30 wt% PEO

The phase structures of these polyurethanes that contain both ionic and non-ionic polysulfone segments and PEO are complex. The experimental data shows clearly that there are at least two phases and we attribute this to phases that contain predominantly ionic and non-ionic segments. The data also suggests that the PEO partitions in some manner into both phases. The lower transitions of the BisAS20 PEO polyurethanes (197 ºC, 161 ºC and 70 ºC) were attributed to the glass transitions of phase-mixed non-ionic polysulfone and PEO segments. This transition decreased from 197 ºC for the control polyurethane without PEO to 161 ºC with 10 wt% PEO, and it decreased further to 70 ºC with 30 wt% PEO. The upper transitions corresponding to the

ionic phase were also depressed with addition of PEO. The $T_g$'s of BisAS 20 and BisAS 40 conrol polyurethanes without PEO were not visible up to 300 °C (the onset of thermal degradation). However, the copolymers containing BisAS20 and BisAS40 with 30 wt % of PEO showed a second high temperature transition at ~240 °C (Figure 4.8). The second transition at 240 ºC was the same for both the 20 and 40% disulfonated copolymers was attributed to the $T_g$ of ionic polysulfone segments that contained PEO. It was reasoned that phase mixing between the ionic domains and PEO segments plasticized this higher $T_g$ below 300 °C. This phenomenon occurs due to phase mixing of the PEO and BisASXX phases and plasticization of the disulfonated segments by short, flexible PEO segments.

Phase behavior of disulfonated polysulfone-PEO blends has been investigated and the compatibility of these blends has been previously established.[49-51] Due to their high $T_g$'s disulfonated polysulfones are susceptible to degradation during processing by melt extrusion. In disulfonated polysulfones $T_g$ increases and the degradation temperature generally decreases with increasing degree of sulfonation. Low molecular weight PEOs can depress the polysulfone $T_g$ to the 100 to 150 ºC range.[50] Moreover blends of disulfonated polysulfones and PEO show a single $T_g$,[50] which indicates miscibility between these two polymers, and these blends show shear thinning rheological behavior due to relaxation of entanglements.[49]

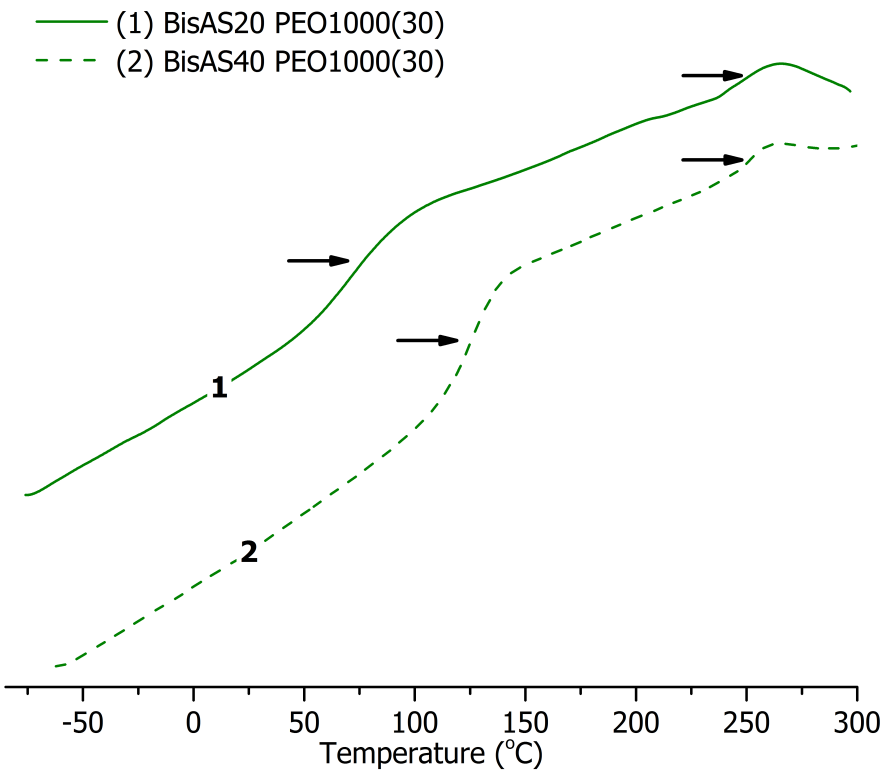


**Figure 4.8.** DSC thermograms (exo down) of polyurethanes (1) containing BisAS20-hydroxyethyl and 30 wt% PEO1000 (2) containing BisAS40-hydroxyethyl and 30 wt% PEO1000

The higher transitions of both the BisAS20 and BisAS40 polyurethanes were attributed to the glass transition temperature of ionic segments. Independent of the degree of disulfonation, DSC thermograms of both polyurethanes containing PEO had $T_g$'s around 240 ºC (Figure 4.8). Phase mixing between BisAS XX and PEO led to plasticization of the high $T_g$ of the BisASXX to below 300 ºC. This was not observed for the control polyurethanes or those with 10 wt% of PEO. Moreover, the polyurethanes containing PEO did not present a transition that could indicate the

presence of PEO-rich domains, and this further supports the phase-mixed morphology with the disulfonated polysulfone and neutral hydrophilic PEO segments.

DMA thermograms revealed more information about the thermal properties of the polyurethanes than DSC (Figure 4.9) indicating a complex phase structure. DMA of BisAS20 PEO (0) showed two separate thermal transitions: a transition onset at 190 ºC and an additional thermal transition undetected by DSC onset around 105 ºC. This signal has been attributed to the β relaxation of bisphenol A-containing polysulfone chains.[52] These two transitions cover a broad temperature range and this polymer displays a rubbery plateau as shown in the storage modulus plot in Figure 4.9. DMA thermograms of the polyurethanes containing 10 and 30 weight % of PEO exhibit the same thermal transition depression also observed in DSC. Consequently the relaxation due to disassociation of ionic domains starts to partially overlap with the β relaxation transition of the BisASXX-PEO polyurethanes. Due to this overlap, DMA thermograms of the PEO-containing polyurethanes don't exhibit a clear rubbery plateau but rather a broad range of thermal transition at temperatures starting right after the expected β relaxation. Moreover, the DMA thermograms of the PEO-containing polyurethanes did not exhibit the expected PEO $T_g$ around which indicated phase mixing between ionic and non-ionic PEO domains that are consistent with the DSC data.

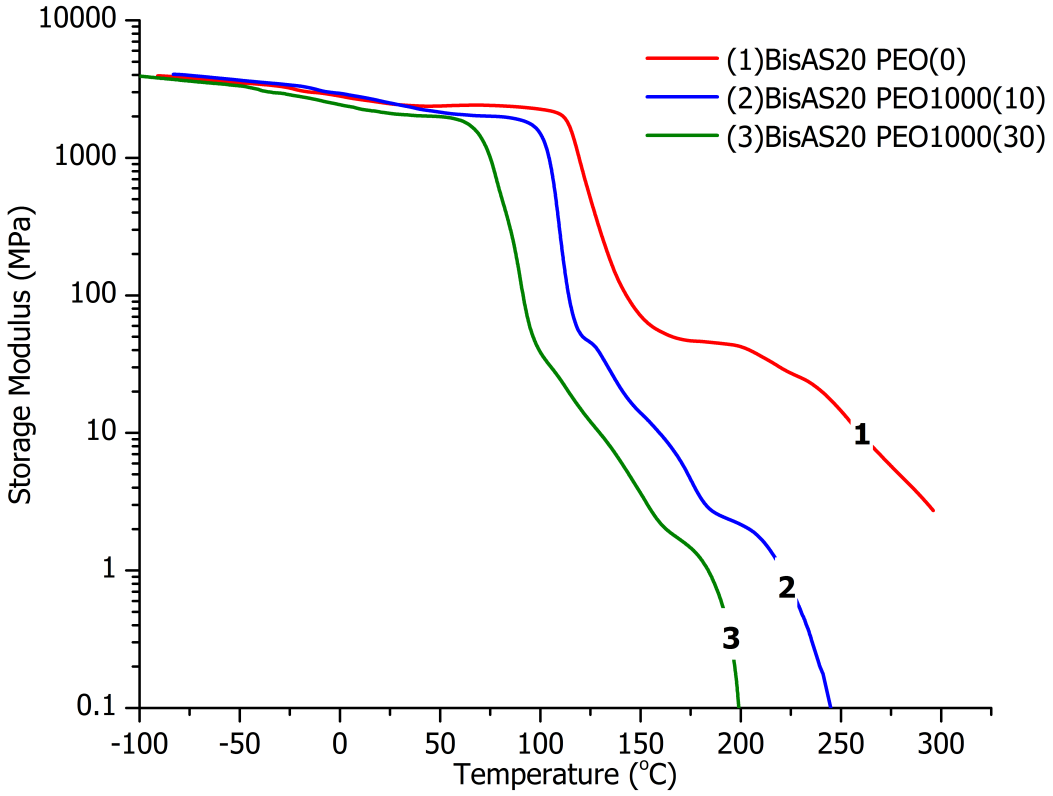


**Figure 4.9.** DMA thermograms of polyurethanes (1) BisAS20-hydroxyethyl that was chain extended with MDI, (2 and 3) containing BisAS20-hydroxyethyl and 10 and 30 wt% PEO

Copolymerization of PEO with ionic polysulfones introduced non-ionic hydrophilic segments into these membranes. Water uptake is often used to evaluate the hydrophilicity of a membrane and the degree of disulfonation and/or the weight percent of increasing PEO correlated with increased water uptake. Table 4.1 presents the water uptake data of BisASXX and PEO containing polyurethanes with different hydrophilic contents. Increasing the composition of PEO from 0 to 30 wt% in the BisAS20-containing copolymers led to an increase in the water uptake of between 9 and 18 %. The water uptake also showed an increase with the increasing ionic content from 20 to 40 mole%. However, even with the highest hydrophilic

content, gravimetric water uptake of BisAS40 PEO1000(30) polyurethane was a modest 25 % of its original weight. This very small increase in water uptake was attributed to the partial phase mixing between hydrophilic ionic and non-ionic PEO segments of these polyurethanes. The water uptakes followed a logical upwards trend with increasing PEO and increasing ionic content as anticipated.

**Table 4.1.** Water uptake of polyurethane films

| Sample | % Water Uptake |
|---|---|
| BisAS20 PEO (0) | 9 ± 1 |
| BisAS20 PEO1000(10) | 10 ± 1 |
| BisAS20 PEO1000(30) | 18 ± 1 |
| BisAS40 PEO (0) | 16 ± 1 |
| BisAS40 PEO1000(10) | 20 ± 1 |
| BisAS40 PEO1000(30) | 24 ± 1 |

### 4.5. Conclusions

In this work, the synthesis of novel segmented polyurethanes that contain both a glassy high $T_g$ disulfonated poly(arylene ether sulfone) and a flexible low $T_g$ poly(ethylene oxide) segment were described. These polyurethanes were prepared for gas separation membrane applications. Solid state thermal characterizations of these membranes revealed that PEO segments were at least partially phase-mixed. Thermo-mechanical analysis of polyurethane membranes displayed a decrease in the $T_g$ which corroborated with solid-state thermal analysis results. Membranes that contain 30% by weight of PEO displayed two-distinct thermal transitions which were attributed to low-$T_g$ non-ionic poly(arylene ether sulfone) domains and plasticized $T_g$ of the disulfonated poly(arylene ether sulfone) segment. These polyurethanes showed limited water uptake which was due to at least partial phase mixing between ionic and non-ionic hydrophilic domains of these polyurethanes.

### 4.6. References:


1. Baker, R. W., *Membrane technology and applications*. J. Wiley: Chichester; New York, 2004.
2. Stern, S. A., Polymers for gas separations: the next decade. *J. Membr. Sci.* **1994,** 94, (Copyright (C) 2012 American Chemical Society (ACS). All Rights Reserved.), 1-65.
3. Pandey, P.; Chauhan, R. S., Membranes for gas separation. *Prog. Polym. Sci.* **2001,** 26, (Copyright (C) 2014 American Chemical Society (ACS). All Rights Reserved.), 853-893.
4. Baker, R. W., Future Directions of Membrane Gas Separation Technology. *Ind. Eng. Chem. Res.* **2002,** 41, (Copyright (C) 2014 American Chemical Society (ACS). All Rights Reserved.), 1393-1411.
5. Bernardo, P.; Drioli, E.; Golemme, G., Membrane Gas Separation: A Review/State of the Art. *Ind. Eng. Chem. Res.* **2009,** 48, (Copyright (C) 2014 American Chemical Society (ACS). All Rights Reserved.), 4638-4663.
6. Robeson, L. M.; Burgoyne, W. F.; Langsam, M.; Savoca, A. C.; Tien, C. F., High performance polymers for membrane separation. *Polymer* **1994,** 35, (Copyright (C) 2012 American Chemical Society (ACS). All Rights Reserved.), 4970-8.
7. Liu, S. L.; Shao, L.; Chua, M. L.; Lau, C. H.; Wang, H.; Quan, S., Recent progress in the design of advanced PEO-containing membranes for CO2 removal. *Prog. Polym. Sci.* **2013,** 38, (Copyright (C) 2014 American Chemical Society (ACS). All Rights Reserved.), 1089-1120.
8. Robeson, L. M., The upper bound revisited. *J. Membr. Sci.* **2008,** 320, (Copyright (C) 2012 American Chemical Society (ACS). All Rights Reserved.), 390-400.
9. Fan, Y.; Cornelius, C. J.; Lee, H.-S.; McGrath, J. E.; Zhang, M.; Moore, R.; Staiger, C. L., The effect of block length upon structure, physical properties, and transport within a series of sulfonated poly(arylene ether sulfone)s. *Journal of Membrane Science* **2013,** 430, (0), 106-112.
10. McHattie, J. S.; Koros, W. J.; Paul, D. R., Gas transport properties of polysulphones: 1. Role of symmetry of methyl group placement on bisphenol rings. *Polymer* **1991,** 32, (5), 840-850.
11. McHattie, J. S.; Koros, W. J.; Paul, D. R., Gas transport properties of polysulphones: 2. Effect of bisphenol connector groups. *Polymer* **1991,** 32, (Copyright (C) 2012 American Chemical Society (ACS). All Rights Reserved.), 2618-25.
12. Pixton, M. R.; Paul, D. R., Gas transport properties of adamantane-based polysulfones. *Polymer* **1995,** 36, (16), 3165-3172.
13. Robeson, L. M., 8.13 - Polymer Membranes. In *Polymer Science: A Comprehensive Reference*, Matyjaszewski, K.; Möller, M., Eds. Elsevier: Amsterdam, 2012; pp 325-347.
14. Freeman, B. D., *Polymer membranes for gas and vapor separation : chemistry and materials science*. American Chemical Society: 1999.
15. Robeson, L. M., Correlation of separation factor versus permeability for polymeric membranes. *J. Membr. Sci.* **1991,** 62, (Copyright (C) 2014 American Chemical Society (ACS). All Rights Reserved.), 165-85.
16. Rose, J. B., Preparation and properties of poly(arylene ether sulphones). *Polymer* **1974,** 15, (7), 456-465.
17. Jennings, B. E.; Jones, M. E. B.; Rose, J. B., Synthesis of poly(arylene sulfones) and poly(arylene ketones) by reactions involving substitution at aromatic nuclei. *J. Polym.*

*Sci., Polym. Symp.* **1967,** 16, (Copyright (C) 2012 American Chemical Society (ACS). All Rights Reserved.), 715-24.
18. Johnson, R. N.; Farnham, A. G.; Clendinning, R. A.; Hale, W. F.; Merriam, C. N., Poly(aryl ethers) by nucleophilic aromatic substitution. I. Synthesis and properties. *Journal of Polymer Science Part A-1: Polymer Chemistry* **1967,** 5, (9), 2375-2398.
19. Robeson, L. M.; Farnham, A. G.; McGrath, J. E., Dynamic mechanical characteristics of polysulfone and other poly(arylethers). *Midl. Macromol. Monogr.* **1978,** 4, (Copyright (C) 2012 American Chemical Society (ACS). All Rights Reserved.), 405-25.
20. Bum Park, H.; Yong Nam, S.; Won Rhim, J.; Min Lee, J.; Kim, S. E.; Ran Kim, J.; Moo Lee, Y., Gas-transport properties through cation-exchanged sulfonated polysulfone membranes. *Journal of Applied Polymer Science* **2002,** 86, (10), 2611-2617.
21. Li, Y.; Chung, T. S., Highly selective sulfonated polyethersulfone (SPES)-based membranes with transition metal counterions for hydrogen recovery and natural gas separation. *Journal of Membrane Science* **2008,** 308, (1–2), 128-135.
22. Khan, A. L.; Li, X.; Vankelecom, I. F. J., SPEEK/Matrimid blend membranes for CO2 separation. *Journal of Membrane Science* **2011,** 380, (1–2), 55-62.
23. Khan, A. L.; Li, X.; Vankelecom, I. F. J., Mixed-gas CO2/CH4 and CO2/N2 separation with sulfonated PEEK membranes. *Journal of Membrane Science* **2011,** 372, (1–2), 87-96.
24. Kelman, S.; Lin, H.; Sanders, E. S.; Freeman, B. D., CO2/C2H6 separation using solubility selective membranes. *J. Membr. Sci.* **2007,** 305, (Copyright (C) 2014 American Chemical Society (ACS). All Rights Reserved.), 57-68.
25. Ribeiro, C. P., Jr.; Freeman, B. D.; Paul, D. R., Pure- and mixed-gas carbon dioxide/ethane permeability and diffusivity in a cross-linked poly(ethylene oxide) copolymer. *J. Membr. Sci.* **2011,** 377, (Copyright (C) 2014 American Chemical Society (ACS). All Rights Reserved.), 110-123.
26. Freeman, B. D.; Pinnau, I., Polymeric Materials for Gas Separations. In *Polymer Membranes for Gas and Vapor Separation*, American Chemical Society: 1999; Vol. 733, pp 1-27.
27. Reijerkerk, S. R.; Nijmeijer, K.; Ribeiro, C. P., Jr.; Freeman, B. D.; Wessling, M., On the effects of plasticization in CO2/light gas separation using polymeric solubility selective membranes. *J. Membr. Sci.* **2011,** 367, (Copyright (C) 2014 American Chemical Society (ACS). All Rights Reserved.), 33-44.
28. Kusuma, V. A.; Gunawan, G.; Smith, Z. P.; Freeman, B. D., Gas permeability of cross-linked poly(ethylene-oxide) based on poly(ethylene glycol) dimethacrylate and a miscible siloxane co-monomer. *Polymer* **2010,** 51, (Copyright (C) 2014 American Chemical Society (ACS). All Rights Reserved.), 5734-5743.
29. Lin, H.; Van Wagner, E.; Freeman, B. D.; Toy, L. G.; Gupta, R. P., Plasticization-enhanced hydrogen purification using polymeric membranes. *Science (Washington, DC, U. S.)* **2006,** 311, (Copyright (C) 2014 American Chemical Society (ACS). All Rights Reserved.), 639-642.
30. Lin, H.; Van Wagner, E.; Swinnea, J. S.; Freeman, B. D.; Pas, S. J.; Hill, A. J.; Kalakkunnath, S.; Kalika, D. S., Transport and structural characteristics of crosslinked poly(ethylene oxide) rubbers. *J. Membr. Sci.* **2006,** 276, (Copyright (C) 2014 American Chemical Society (ACS). All Rights Reserved.), 145-161.

31. Bondar, V. I.; Freeman, B. D.; Pinnau, I., Gas sorption and characterization of poly(ether-b-amide) segmented block copolymers. *J. Polym. Sci., Part B: Polym. Phys.* **1999,** 37, (Copyright (C) 2014 American Chemical Society (ACS). All Rights Reserved.), 2463-2475.
32. Lin, H.; Freeman, B. D., Materials selection guidelines for membranes that remove CO2 from gas mixtures. *J. Mol. Struct.* **2005,** 739, (Copyright (C) 2014 American Chemical Society (ACS). All Rights Reserved.), 57-74.
33. Richards, J. J.; Danquah, M. K.; Kalakkunnath, S.; Kalika, D. S.; Kusuma, V. A.; Matteucci, S. T.; Freeman, B. D., Relation between structure and gas transport properties of polyethylene oxide networks based on crosslinked bisphenol A ethoxylate diacrylate. *Chem. Eng. Sci.* **2009,** 64, (Copyright (C) 2012 American Chemical Society (ACS). All Rights Reserved.), 4707-4718.
34. Kim, H. W.; Park, H. B., Gas diffusivity, solubility and permeability in polysulfone–poly(ethylene oxide) random copolymer membranes. *Journal of Membrane Science* **2011,** 372, (1–2), 116-124.
35. Comer, A. C.; Kalika, D. S.; Kusuma, V. A.; Freeman, B. D., Glass-transition and gas-transport characteristics of polymer nanocomposites based on crosslinked poly(ethylene oxide). *J. Appl. Polym. Sci.* **2010,** 117, (Copyright (C) 2014 American Chemical Society (ACS). All Rights Reserved.), 2395-2405.
36. Sankir, M.; Bhanu, V. A.; Harrison, W. L.; Ghassemi, H.; Wiles, K. B.; Glass, T. E.; Brink, A. E.; Brink, M. H.; McGrath, J. E., Synthesis and characterization of 3,3'-disulfonated-4,4'-dichlorodiphenyl sulfone (SDCDPS) monomer for proton exchange membranes (PEM) in fuel cell applications. *J. Appl. Polym. Sci.* **2006,** 100, (Copyright (C) 2012 American Chemical Society (ACS). All Rights Reserved.), 4595-4602.
37. Cateto, C. A.; Barreiro, M. F.; Rodrigues, A. E.; Brochier-Salon, M. C.; Thielemans, W.; Belgacem, M. N., Lignins as macromonomers for polyurethane synthesis: a comparative study on hydroxyl group determination. *J. Appl. Polym. Sci.* **2008,** 109, (Copyright (C) 2014 American Chemical Society (ACS). All Rights Reserved.), 3008-3017.
38. Li, Y.; VanHouten, R. A.; Brink, A. E.; McGrath, J. E., Purity characterization of 3,3′-disulfonated-4,4′-dichlorodiphenyl sulfone (SDCDPS) monomer by UV–vis spectroscopy. *Polymer* **2008,** 49, (13–14), 3014-3019.
39. Harrison, W. L.; Hickner, M. A.; Kim, Y. S.; McGrath, J. E., Poly(arylene ether sulfone) copolymers and related systems from disulfonated monomer building blocks: synthesis, characterization, and performance - a topical review. *Fuel Cells (Weinheim, Ger.)* **2005,** 5, (Copyright (C) 2012 American Chemical Society (ACS). All Rights Reserved.), 201-212.
40. Wang, F.; Hickner, M.; Kim, Y. S.; Zawodzinski, T. A.; McGrath, J. E., Direct polymerization of sulfonated poly(arylene ether sulfone) random (statistical) copolymers: candidates for new proton exchange membranes. *J. Membr. Sci.* **2002,** 197, (Copyright (C) 2012 American Chemical Society (ACS). All Rights Reserved.), 231-242.
41. Wang, F.; Kim, Y.; Hickner, M.; Zawodzinski, T. A.; McGrath, J. E., Synthesis of polyarylene ether block copolymers containing sulfonate groups. *Polym. Mater. Sci. Eng.* **2001,** 85, (Copyright (C) 2012 American Chemical Society (ACS). All Rights Reserved.), 517-518.

42. Colonna, M.; Berti, C.; Fiorini, M., Chemical modification of bisphenol a polycarbonate by reactive blending with ethylene carbonate. *J. Appl. Polym. Sci.* **2014,** 131, (Copyright (C) 2014 American Chemical Society (ACS). All Rights Reserved.), 39820/1-39820/10.
43. Celebi, O.; Lee, C. H.; Lin, Y.; McGrath, J. E.; Riffle, J. S., Synthesis and characterization of polyoxazoline–polysulfone triblock copolymers. *Polymer* **2011,** 52, (21), 4718-4726.
44. Yoshino, T.; Inaba, S.; Ishido, Y., Synthetic studies by the use of carbonates. III. Condensation reactions of ethylene carbonate with a variety of phenols catalyzed by lithium hydride or tetraethylammonium halides. *Bull. Chem. Soc. Jap.* **1973,** 46, (Copyright (C) 2014 American Chemical Society (ACS). All Rights Reserved.), 553-6.
45. Szycher, M., *Szycher's handbook of polyurethanes*. CRC Press: Boca Raton, 1999.
46. Ronda, J. C.; Serra, A.; Mantecón, A.; Cádiz, V., End-group analysis of poly(phenyl glycidyl ether), 2. Hydroxylic groups using 19F nuclear magnetic resonance. *Macromolecular Chemistry and Physics* **1994,** 195, (10), 3459-3468.
47. Dodge, J., Polyurethanes and Polyureas. In *Synthetic Methods in Step-Growth Polymers*, John Wiley & Sons, Inc.: 2003; pp 197-263.
48. Hiemenz, P. C.; Lodge, T., *Polymer chemistry*. CRC Press: Boca Raton, 2007.
49. Oh, H. J.; Freeman, B. D.; McGrath, J. E.; Ellison, C. J.; Mecham, S.; Lee, K.-S.; Paul, D. R., Rheological studies of disulfonated poly(arylene ether sulfone) plasticized with poly(ethylene glycol) for membrane formation. *Polymer* **2014,** 55, (6), 1574-1582.
50. Oh, H. J.; Freeman, B. D.; McGrath, J. E.; Lee, C. H.; Paul, D. R., Thermal analysis of disulfonated poly(arylene ether sulfone) plasticized with poly(ethylene glycol) for membrane formation. *Polymer* **2014,** 55, (1), 235-247.
51. Walsh, D. J.; Singh, V. B., The phase behaviour of a poly(ether sulfone) with poly(ethylene oxide). *Die Makromolekulare Chemie* **1984,** 185, (9), 1979-1989.
52. Mark, J. E., *Polymer data handbook*. Oxford University Press: New York, 1999.

## 5. Conclusions

This dissertation have defined structure-property-performance relationships of poly(arylene ether sulfone and poly(ethylene oxide)-containing copolymers for water desalination and gas separation membranes. Polymers containing both ionic and non-ionic segments were investigated. Primary focus of this research was to identify the relationship between polymer compositions, thermal and mechanical properties of the polymers and transport properties.

Our research on water desalination membranes focused on the synthesis of novel UV crosslinkable oligomers and preparation of TFC's utilizing an aqueous based UV curing procedure. Novel UV crosslinkable oligomers were synthesized and characterized for use as water purification membranes. The UV crosslinking reaction conditions, reactant ratios, and concentrations were evaluated. For the first time, UV crosslinking of partially or fully sulfonated poly (arylene ether sulfone)s with telechelic functionality is demonstrated from methanol-water and aqueous solutions, thereby enabling application as thin film composites. UV crosslinking produced free-standing films with up to 98% gel fraction. Preparation of thin film composite membranes was demonstrated utilizing a rapid casting/crosslinking procedure under UV radiation. Surface characterization demonstrated that the composite membranes exhibited two orders of magnitude lower surface roughness compared to conventional commercial composite membranes. SEM cross-sectional micrographs displayed the presence of a top selective layer with a thickness of ~600 nm.

The synthesis of novel segmented polyurethanes that contain both a glassy high $T_g$ poly(arylene ether sulfone) and a flexible low $T_g$ poly(ethylene oxide) segment as potential gas separation membranes were described. Solid state thermal characterizations of these membranes revealed that at 10 weight % PEO-content, PAES and PEO segments were at least partially

phase-mixed. $T_g$ plasticization was revealed by thermo-mechanical analysis of polyurethane membranes which corroborated with solid-state thermal analysis results. Polyurethanes that contain PEO more than 10% by weight displayed two-distinct glass transition temperatures which indicated a phase separated morphology. Tensile properties showed that incorporation of flexible PEO segments toughened these polyurethanes at 10% and enhanced strain at break, however at 30 weight%, PEO segments started to compromise tensile properties observed at lower PEO contents. Single gas transport experiments displayed a strong dependence between PEO weight percent and $CO_2/CH_4$ and $CO_2/N_2$ selectivity without a significant sacrifice in gas permeability.

Finally, the synthesis of novel polyurethanes that contain both a glassy high $T_g$ disulfonated poly(arylene ether sulfone) and a flexible low $T_g$ poly(ethylene oxide) segment were described. These polyurethanes were prepared for gas separation membrane applications. Solid state thermal characterizations of these membranes revealed that disulfonated poly(arylene ether sulfone) and PEO segments were at least partially phase-mixed. Thermo-mechanical analysis of polyurethane membranes displayed plasticization of the $T_g$ which corroborated with solid-state thermal analysis results. Membranes that contain 30% by weight of PEO displayed two-distinct thermal transitions which were attributed to non-ionic poly(arylene ether sulfone) and plasticized $T_g$ of the disulfonated poly(arylene ether sulfone) segment. These polyurethanes showed limited water uptake which was due to at least partial phase mixing between ionic and non-ionic hydrophilic domains of these polyurethanes.

## 6. Recommended Future Research

The results of this dissertation call for further investigation of similar chemistries for separation membranes. Water desalination membranes with excellent salt rejection (>99%) and water flux can be achieved with UV-crosslinkable disulfonated poly(arylene ether sulfone) oligomers. Water desalination membranes require high degrees of hydrophilicity and crosslinking. Utilizing small comonomers along with the disulfonated poly(arylene ether sulfone) oligomers can increase the crosslink density of the membranes. High crosslink density reduces the free volume of polymers that improves the tortuosity of the path of penetrants (salt ions $Na^+$, $Cl^-$ and water). Figure 6.1 shows some of the recommended comonomers that can be used in preparation of thin film composite reverse osmosis membranes from benign solvents such as methanol.

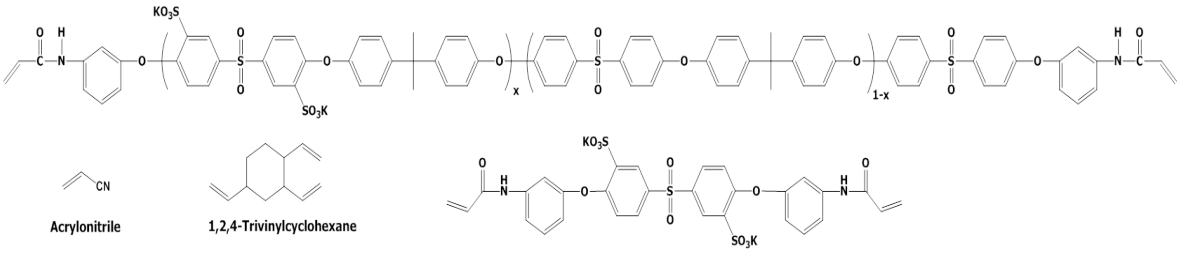


**Figure 6.1.** UV-crosslinkable monomers

Pendent reactive groups on the polymer backbone offer an alternative to telechelic crosslinking. Pendent groups can be reacted with a crosslinking agent to achieve branching and crosslink points along the backbone of the polymer. Bis(4-fluorophenyl)phenylphosphine oxide can be modified via a labile nitration/reduction procedure to obtain bis(4-fluorophenyl)-3-aminophenylphosphine oxide monomer. Direct copolymerization of this monomer can incorporate pendent amine functionalities along the backbone of the polymer.[1] Pendent amine-containing poly(arylene ether sulfone)s (Figure 6.2) can be crosslinked via interfacial polymerization using an acyl chloride such as trimesoyl chloride. In the presence of a

diisocyanate or a polyisocyanate, pendent amine-containing polymers could produce a densely crosslinked membrane. Moreover these pendent amine groups can be chemically modified into acrylamide functionalities to utilize such monomers in UV-crosslinking reactions. Such membranes could produce the highest possible crosslink density, resembling the structure of state of the art crosslinked polyamide reverse osmosis membranes.

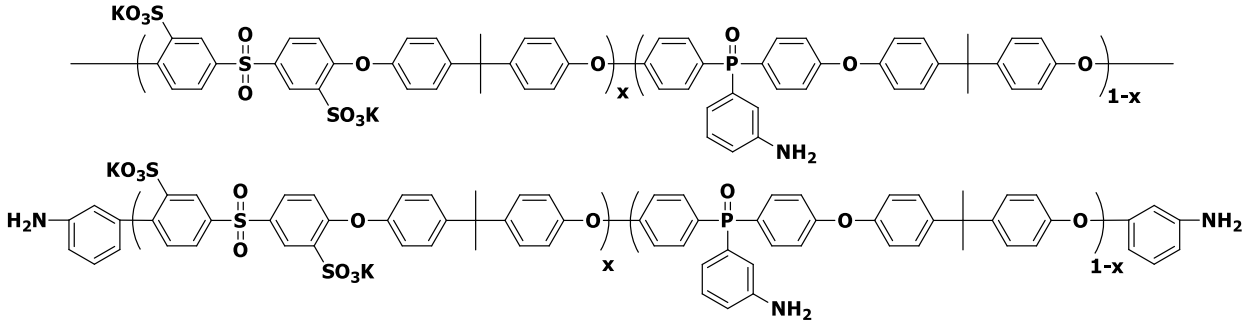


**Figure 6.2.** Pendent amine containing poly(arylene ether sulfone)s

High degrees of crosslinking can be achieved via poly(ether ketone) type polymers. Poly(arylene ether ketone)s that contain benzylic methyl groups can crosslink upon exposure to UV radiation. Crosslinking of such polymers depends on concentration of both ketone and benzylic methyl groups. Incorporation of a disulfonated monomer during the synthesis produces disulfonated poly(arylene ether ketone)s (Figure 6.3). Hydrophilicity of such polymers can be tuned via the composition of the disulfonated monomer feed.

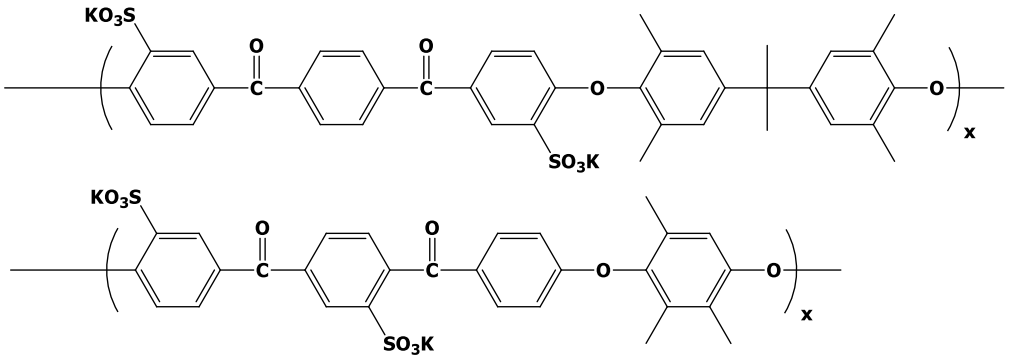


**Figure 6.3.** UV-Crosslinkable poly(arylene ether ketone)s

### 6.1. Reference:

1. Pak, S. J.; Lyle, G. D.; Mercier, R.; McGrath, J. E., Synthesis and characterization of novel toughened thermosets derived from pendent amines on the backbone of poly(arylene ether sulphone)s. *Polymer* **1993,** 34, (4), 885-895.